

DOCUMENT CONTROL DATA - R & D

(Security classification of title, body of abstract and indexing annotation must be entered when the overall report is classified)

1. ORIGINATING ACTIVITY (Corporate author)		2a. REPORT SECURITY CLASSIFICATION	
Naval Research Laboratory Washington, D.C. 20390		UNCLASSIFIED	
		2b. GROUP	
3. REPORT TITLE			
THE ROLE OF FRACTURE TOUGHNESS IN LOW-CYCLE FATIGUE CRACK PROPAGATION FOR HIGH-STRENGTH ALLOYS			
4. DESCRIPTIVE NOTES (Type of report and inclusive dates)			
A final report on one phase of the problem; work is continuing on other aspects.			
5. AUTHOR(S) (First name, middle initial, last name)			
Thomas W. Crooker			
6. REPORT DATE		7a. TOTAL NO. OF PAGES	7b. NO. OF REFS
June 20, 1972		16	24
8a. CONTRACT OR GRANT NO.		9a. ORIGINATOR'S REPORT NUMBER(S)	
NRL Problem No. M01-25		NRL Report 7422	
b. PROJECT NO.		9b. OTHER REPORT NO(S) (Any other numbers that may be assigned this report)	
Project RR 022-01-46-5432			
c.			
d.			
10. DISTRIBUTION STATEMENT			
Approved for public release; distribution unlimited.			
11. SUPPLEMENTARY NOTES		12. SPONSORING MILITARY ACTIVITY	
		Department of the Navy (Office of Naval Research) Arlington, Virginia 22217	
13. ABSTRACT			
<p>The trend toward broader application of high-strength structural alloys has increased the potential for failure by low-cycle fatigue crack propagation. There is a significant probability that complex structures will contain undetected cracks remaining from fabrication or that cracks will readily initiate from less severe fabrication defects. Under the repeated application of high stresses imposed on high-strength alloys, such cracks will rapidly grow in low-cycle fatigue. The guard against disastrous failures caused by cracks propagating to terminal fracture, high-strength structural alloys which also possess high levels of fracture resistance have been developed in recent years. This report describes the principal fatigue crack propagation characteristics derived from high fracture toughness and discusses the potential benefits available through the use of high-toughness alloys in cyclically loaded structures.</p>			

14. KEY WORDS	LINK A		LINK B		LINK C	
	ROLE	WT	ROLE	WT	ROLE	WT
Low-cycle fatigue Crack propagation Fracture resistance High-strength alloys Structural fatigue						

CONTENTS

Abstract	ii
Problem Status.....	ii
Authorization.....	ii
INTRODUCTION	1
NEW DEVELOPMENTS IN THE FRACTURE TOUGHNESS CHARACTERISTICS OF HIGH-STRENGTH ALLOYS	2
FATIGUE CRACK PROPAGATION CHARACTERISTICS OF HIGH-STRENGTH ALLOYS.....	5
CONCLUSION.....	8
ACKNOWLEDGMENTS	9
REFERENCES.....	9

ABSTRACT

The trend toward broader application of high-strength structural alloys has increased the potential for failure by low-cycle fatigue crack propagation. There is a significant probability that complex structures will contain undetected cracks remaining from fabrication or that cracks will readily initiate from less severe fabrication defects. Under the repeated application of high stresses imposed on high-strength alloys, such cracks will rapidly grow in low-cycle fatigue. To guard against disastrous failures caused by cracks propagating to terminal fracture, high-strength structural alloys which also possess high levels of fracture resistance have been developed in recent years. This report describes the principal fatigue crack propagation characteristics derived from high fracture toughness and discusses the potential benefits available through the use of high-toughness alloys in cyclically loaded structures.

PROBLEM STATUS

This report completes one phase of the problem; work on other aspects of the problem is continuing.

AUTHORIZATION

NRL Problem M01-25
Project RR 022-01-46-5432

Manuscript submitted April 11, 1972.

THE ROLE OF FRACTURE TOUGHNESS IN LOW-CYCLE FATIGUE CRACK PROPAGATION FOR HIGH-STRENGTH ALLOYS

INTRODUCTION

Low-cycle fatigue (i.e., high-stress fatigue which causes failures within 100,000 cycles of repeated load) has been recognized and studied as a structural failure mechanism for several decades. Early studies of low-cycle fatigue focused on the phenomenon of macrocrack initiation in unflawed material, and the well-known Coffin-Manson relationship between cyclic strain and crack initiation resulted from these initial studies. However, the more recent development of weldable high-strength alloys has placed new emphasis on low-cycle fatigue and has focused attention on macrocrack propagation at nominally elastic stress levels as an important aspect of low-cycle fatigue in welded high-strength structures.

The principal reason that low-cycle fatigue is so closely interrelated with the structural application of high-strength alloys is that low-cycle fatigue resistance, either to crack initiation or crack propagation, is largely independent of monotonic strength properties (1-4). Yet, it is monotonic strength properties which frequently govern the alloy selection process. As a common result of this inconsistency in materials properties, high-strength structures become susceptible to low-cycle fatigue because the high-strength material has no inherent advantage in fatigue resistance but must still sustain higher design stresses which are based on monotonic strength. If this deficiency is recognized and anticipated, some compensation can be made through superior design and quality control of fabrication. However, in the case of complex welded structures it is exceedingly difficult to assure that fabrication flaws too small to be detected by nondestructive inspection will not be present in critical locations. Under repeated application of high stresses such fabrication flaws serve as sites for the initiation of macrocracks. Therefore, in the design of many high-strength welded structures conservative practices require that service intervals between inspection and assessment of fatigue damage found during inspection will depend on an analysis of low-cycle fatigue crack propagation.

The chief remedy utilized to combat this potentially serious fatigue situation has been to use high-strength alloys which also possess high fracture resistance for those critical applications where crack propagation to terminal fracture is possible and would have disastrous consequences. The use of high-toughness alloys permits large cracks to develop in service, thus enhancing the possibility of detection prior to ultimate failure. The development of both ferrous and nonferrous high-strength, high-toughness alloys has made rapid progress in recent years. A number of these premium alloys are under consideration for critical applications in advanced structures. This report discusses the role of fracture toughness in determining the fatigue crack propagation performance of these alloys under the high stress cycling associated with low-cycle fatigue.

NEW DEVELOPMENTS IN THE FRACTURE TOUGHNESS CHARACTERISTICS OF HIGH-STRENGTH ALLOYS

The past decade has seen great progress in raising the level of fracture resistance attainable in high-strength alloys. Structural designers now have available considerable choice in making yield strength/fracture toughness tradeoffs among competing alloys. The Naval Research Laboratory (NRL) Ratio Analysis Diagram (RAD) provides a graphical means of quantitatively illustrating these effects. Figures 1 through 3 show the RAD characteristics for steels, for titanium, and for aluminum alloys in 1-in.-thick section sizes (5). Since thickness has a powerful effect on fracture, certain details of these diagrams which are influenced by through-thickness restraint will vary for thicknesses greater or less than 1 in. (5). Nevertheless, the general features of the RAD and its application are adequately illustrated by these figures.

The RAD is a cumulative plot, by alloy family, of fracture toughness vs yield strength for the full spectrum of high and intermediate yield-strength levels. The upper portions of the diagram have been compiled from Dynamic Tear (DT) (6) tests, and the lower portions of the diagram from valid plane strain fracture toughness (K_{Ic}) tests. However, the diagram can be utilized by conducting two simple engineering tests, a DT test and an ordinary tensile test. For alloys of sufficiently low toughness-to-strength ratios, a correlation is available between DT energy and K_{Ic} (7-9), thus enabling the lower portions of the diagram to yield graphical fracture mechanics solutions for brittle fracture problems (5).

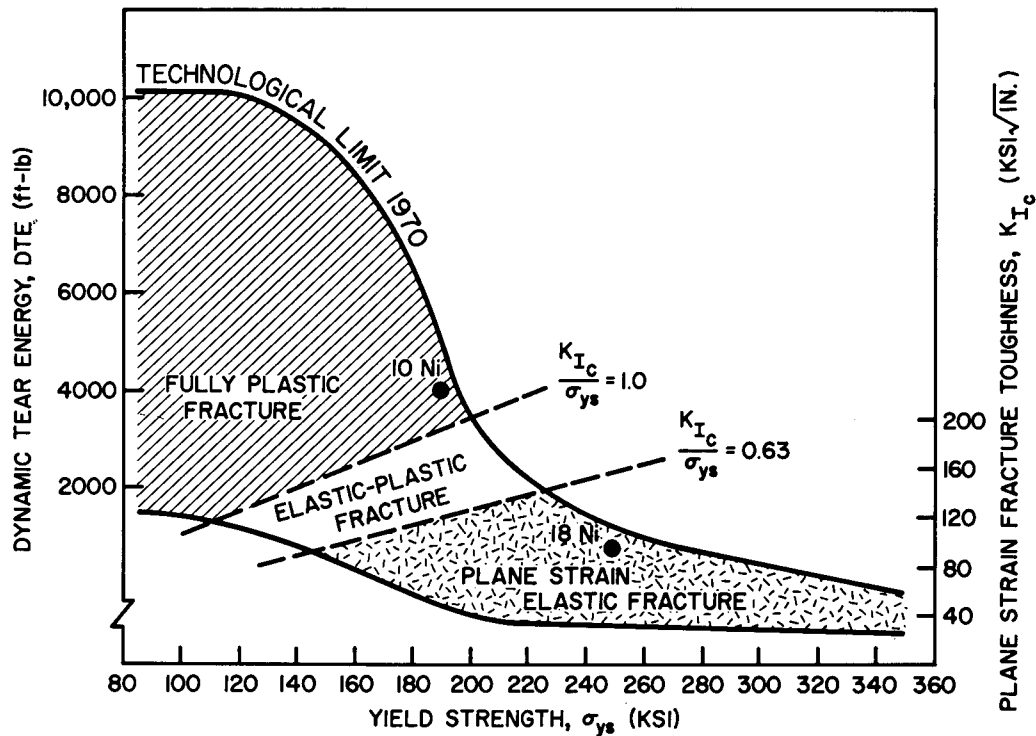


Fig. 1—Ratio Analysis Diagram showing the upper and lower limits of fracture toughness for 1-in.-thick steels over the yield-strength range from 80 to 360 ksi (5). The diagram is divided into subregions of fracture behavior as defined by significant K_{Ic}/σ_{ys} ratio lines. Data points are shown for a 10Ni steel ($\sigma_{ys} = 193$ ksi) and an 18Ni steel ($\sigma_{ys} = 248$ ksi).

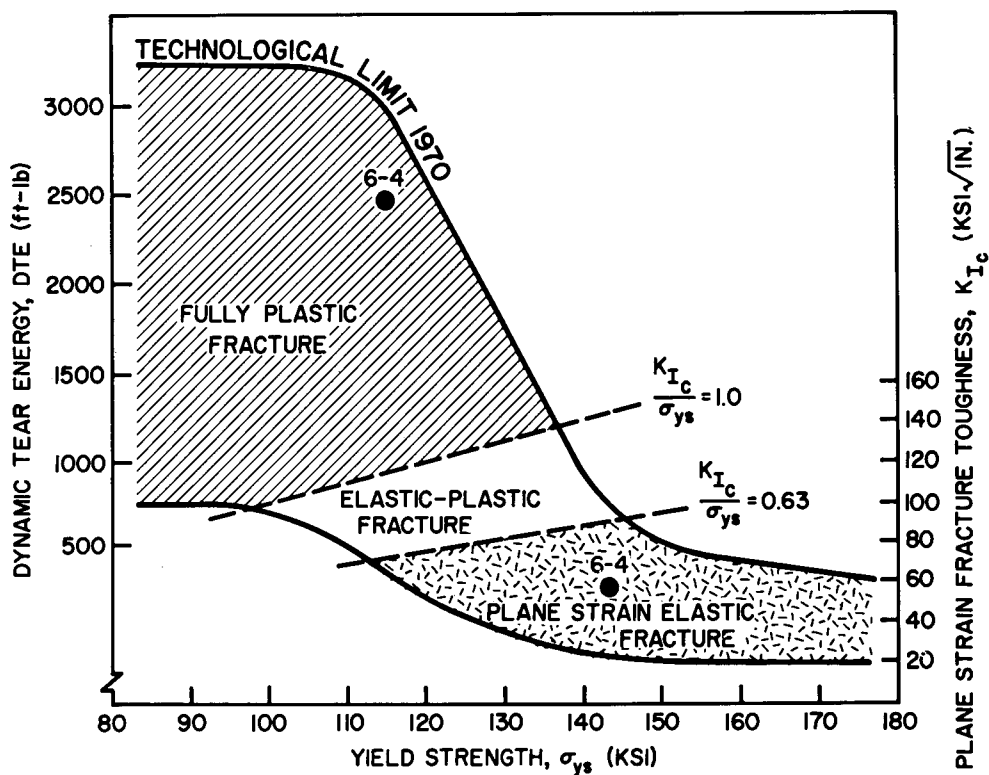


Fig. 2—Ratio Analysis Diagram for 1-in.-thick titanium alloys over the yield-strength range from 80 to 180 ksi (5) showing data points for two samples of Ti-6Al-4V ($\sigma_{ys} = 115$ and 143 ksi, respectively)

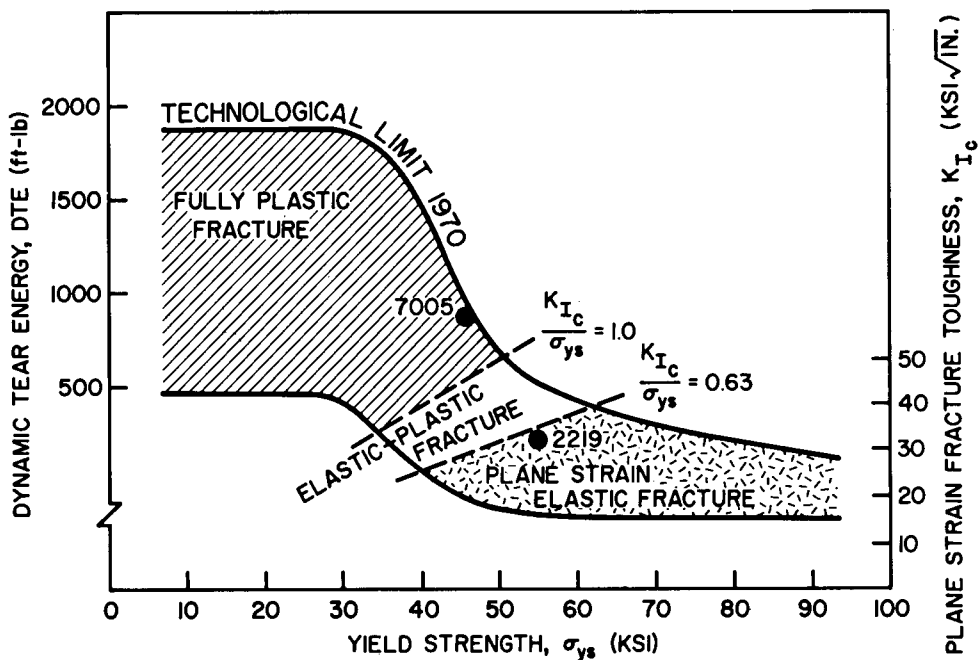


Fig. 3—Ratio Analysis Diagram for 1-in.-thick aluminum alloys over the yield-strength range from 10 to 90 ksi (5) showing data points for 7005-T63 ($\sigma_{ys} = 47$ ksi) and 2219-T87 ($\sigma_{ys} = 55$ ksi)

Limiting values for the upper and lower extremes of fracture toughness are indicated on the RAD, and within this overall region of observed fracture behavior further subregions are categorized on the basis of significant plane strain fracture toughness-to-yield strength (K_{Ic}/σ_{ys}) ratios. The fracture toughness characteristics of a given alloy, as defined by its location with respect to these K_{Ic}/σ_{ys} ratio subregions, has a vital bearing on its structural fracture performance.

For 1-in.-thick alloys, the two significant ratio lines are $K_{Ic}/\sigma_{ys} = 0.63$ and 1.0. The ratio value of 0.63 is derived from the thickness requirement for plane strain fracture toughness measurements (10) as given in Eq. (1) below;

$$B \geq 2.5(K_{Ic}/\sigma_{ys})^2 \quad (1)$$

Alloys which possess fracture toughness characteristics within the subregion bounded below the 0.63 ratio line are susceptible to plane strain elastic instability fracture. The precise objective of high-strength alloy development over the past decade has been to produce high yield-strength alloys which are sufficiently tough, in plate thickness, to remain significantly above this region of highly brittle fracture.

The ratio value of 1.0 has evolved as a reasonable estimate of a sufficient level of toughness to attain fracture over the yield stress for 1.0-in.-thick plates containing a through-thickness flaw several inches in length (5). Alloys possessing fracture toughness characteristics above this ratio can be expected to be immune from brittle elastic fracture and will require some degree of gross plastic deformation before fracture will occur. It must be emphasized that these limiting criteria for plane strain fracture ($K_{Ic}/\sigma_{ys} = 0.63$) and for fracture above the yield stress ($K_{Ic}/\sigma_{ys} = 1.0$) are arbitrary but appear to be well justified on the basis of present knowledge. The subregion between these two significant ratio lines is termed elastic-plastic fracture. Alloys which have fracture toughness characteristics between ratios 0.63 and 1.0 require some degree of large-scale localized plastic deformation in the vicinity of the crack before fracturing, even though net section stresses away from the crack remain below yield. However, the degree of localized deformation involved is sufficient to render a plane strain fracture mechanics analysis invalid. The net effect of this localized deformation is to relieve constraint around crack tips and thus permit substantially larger flaws to develop in service than would be predicted from a plane strain analysis. Therefore, truly analytical techniques of plane strain linear-elastic fracture mechanics can only be applied with more than approximate accuracy to 1-in.-thick alloys possessing K_{Ic}/σ_{ys} ratios less than 0.63.

One of the most important functions of the RAD is to illustrate the yield strength/fracture tradeoffs which can be made over a given yield strength range or the increases in fracture toughness available at a specific strength level through improvement of metal quality and thus guide the materials selection process out of the hazardous domain of plane strain brittle fracture. The metallurgical aspects of achieving this goal are beyond the scope of this paper. Generally speaking, high levels of fracture toughness are achieved through special metallurgical processing which removes undesirable constituents from the alloy composition (11,12). Nevertheless, several principles which control the fracture optimization aspects of the materials selection process are illustrated in Figs. 1 through 3. Basically, the tradeoffs frequently involve some sacrifice in yield strength in order to gain a substantial increase in fracture toughness. Nevertheless, overall structural performance is not necessarily reduced significantly because a smaller factor of safety can then be applied to stresses once fracture-safe design is insured through adequate fracture toughness. The

remainder of this paper will be devoted to examining the effects of such yield-strength/fracture-toughness/metal-quality tradeoffs on the high-amplitude fatigue crack propagation characteristics of high-strength alloys. Six alloys which serve to illustrate such tradeoffs have been selected and are shown in pairs on Figs. 1 through 3.

FATIGUE CRACK PROPAGATION CHARACTERISTICS OF HIGH-STRENGTH ALLOYS

The most broadly accepted criterion for establishing the fatigue crack propagation characteristics of high-strength alloys is to empirically determine crack growth rates (da/dN) as a function of the fracture mechanics stress-intensity factor range (ΔK). The functional relationship between these two variables is commonly of the power-law form

$$\frac{da}{dN} = C(\Delta K)^m, \quad (2)$$

which results in a rectilinear data plot on logarithmic coordinates (13).

An example of data presented in this form is shown in Fig. 4, which shows the scatterband limits for a broad sample of high-strength steels (4). This band illustrates several aspects central to the problem of fatigue crack propagation in high-strength alloys. First, several investigators (4,14-16) have noted that there are two regimes of crack propagation behavior, as indicated by the inflection in the scatterband. This observation is supported by fractographic evidence which shows that the predominant mode of metal separation is different for the two regimes (17,18). Low-amplitude fatigue crack propagation occurs primarily by striation formation, whereas high-amplitude crack propagation occurs by dimple formation. In any event, the upper regime indicates a condition to be avoided in structural service because it represents very rapidly increasing crack growth rates. Second, in the lower regime of crack propagation behavior, alloys possessing widely different mechanical properties can display very similar characteristics. Low-amplitude fatigue crack growth rates are largely unaffected by variations in yield strength and fracture toughness. This has been found to occur within steel, titanium, and aluminum alloy families (4,16,19). Finally, an examination of the crack size and stress level conditions relevant to the problem of low-cycle fatigue crack propagation in heavy-section high-strength structures reveals that the transition to the upper regime is critical to this problem. The respective ΔK values corresponding to a 0.25-in.-deep semicircular flaw cycled from 0 to 75 percent of yield-strength stress for HY-80 ($\sigma_{ys} = 80$ ksi), HY-130 ($\sigma_{ys} = 130$ ksi), and 10Ni ($\sigma_{ys} = 190$ ksi) steels are indicated on Fig. 4. This arbitrary flaw size and stress level combination is well within anticipated service requirements for these high-toughness materials. It can be seen that increasing the yield strength of structural alloys has a very serious potential for aggravating fatigue problems involving crack propagation. It also focuses attention on the upper regime of crack propagation where fracture toughness will play a role in determining the low-cycle fatigue behavior of structures.

To illustrate this role of fracture toughness in high-amplitude fatigue crack propagation, da/dN vs ΔK data plots for the six alloys noted in pairs on Figs. 1 through 3 are shown in Figs. 5 through 7. These six alloys include 10Ni and 18Ni steels, two samples of Ti-6Al-4V, and 7005-T63 and 2219-T87 aluminum alloys. Each of these pairs was chosen because their fracture toughness and yield-strength characteristics represent the tradeoffs that can be made from plane strain elastic fracture behavior to fully plastic fracture behavior over a reasonably modest yield-strength range. It is of interest to note, from Figs.

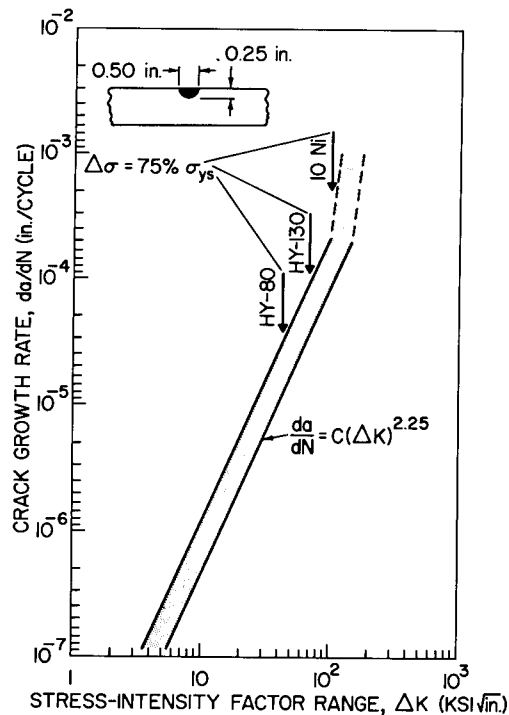


Fig. 4—Log-log plot of fatigue crack growth rate (da/dN) vs stress-intensity factor range (ΔK) showing the scatterband limits for a broad sample of high-strength steels (4). The bold arrows indicate the respective rates of crack propagation that would occur in each of three steels (HY-80, HY-130, and 10Ni) for a stress-level/flaw-size condition of a 0.25-in.-deep, semicircular, embedded surface flaw cycled at 0 to 75 percent of the yield-strength stress

5 through 7, what comparative changes in fatigue crack propagation characteristics might accompany such significant gains in fracture toughness.

The general conclusion apparent from an examination of the data in Figs. 5 through 7 is that fatigue crack propagation resistance at high ΔK levels is only marginally improved in the high-toughness alloys as a result of large increases in fracture resistance. However, this margin of improvement is highly significant to structural integrity. All of the alloys studied exhibited a transition to accelerated crack growth rates, regardless of toughness. However, there were distinct differences among the behavior of these materials at ΔK levels beyond the point of transition, depending upon alloy toughness. In each case, test specimens of the low-toughness alloys failed from elastic fracture in this region of accelerated crack propagation behavior, whereas the tougher alloys remained intact in this region. Nevertheless, high fracture toughness, per se, does not prevent a transition to accelerated fatigue crack growth.

For brittle alloys this point of transition is generally related to impending fracture and can be reasonably estimated as occurring at a ΔK value somewhat below the fracture toughness of the alloy, generally near 80% of K_{Ic} as seen on Figs. 5 through 7 and also

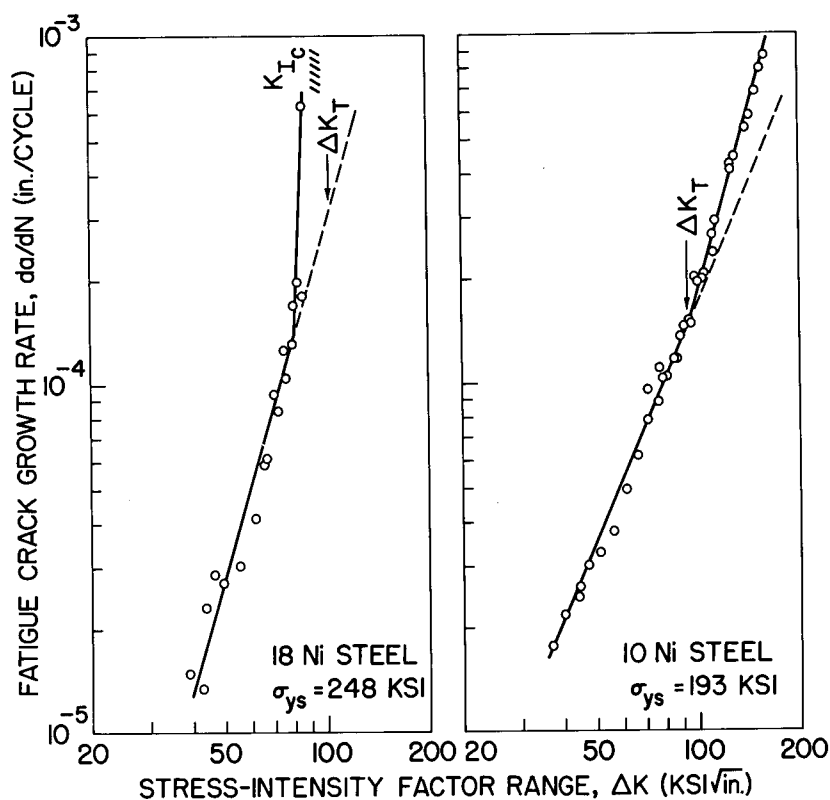


Fig. 5—Logarithmic plots of da/dN vs ΔK for the 10Ni and 18Ni steels shown on Fig. 1. Note that both alloys undergo a transition to accelerated crack growth rates beyond $da/dN = 10^{-4}$ in./cycle. However in the lower toughness 18Ni steel, brittle fracture occurs just beyond the point of slope transition, as indicated by the K_{Ic} level of the material (~ 95 ksi $\sqrt{in.}$). In the higher toughness 10Ni steel, the point of slope transition is accurately predicted by the parameter ΔK_T .

noted in Ref. 20. For ductile alloys, it can be reasonably estimated that the transition to accelerated crack growth rates will occur in the vicinity of $da/dN = 10^{-4}$ in./cycle (15). A more accurate estimate based on a critical crack-opening-displacement (COD) concept has been proposed (21) and has been shown to be valid for a wide range of steels and titanium and aluminum alloys (4,16,21-24). The COD concept is based on an empirical correlation which shows that the point of slope transition in the $da/dN - \Delta K$ logarithmic plot will occur near a constant value of COD for all alloys of sufficient toughness to be well below fracture conditions at these ΔK levels. This correlation reduces to the following equation (16) for estimating the ΔK level beyond which accelerated crack growth rates can be anticipated (ΔK_T);

$$\Delta K_T = \sqrt{0.0016E\sigma_{ys}} \quad (3)$$

where E is Young's modulus and σ_{ys} is the 0.2% yield-strength stress. The respective values for ΔK_T are indicated for each alloy in Figs. 5 through 7. It can be seen that this parameter provides an accurate estimate of the point of slope transition for the high-toughness alloys. Since this equation does not contain any fracture toughness parameter and is dependent on yield strength to the one-half power, it is apparent that the phenomenon of accelerated fatigue crack growth in ductile alloys is not amenable to elimination through

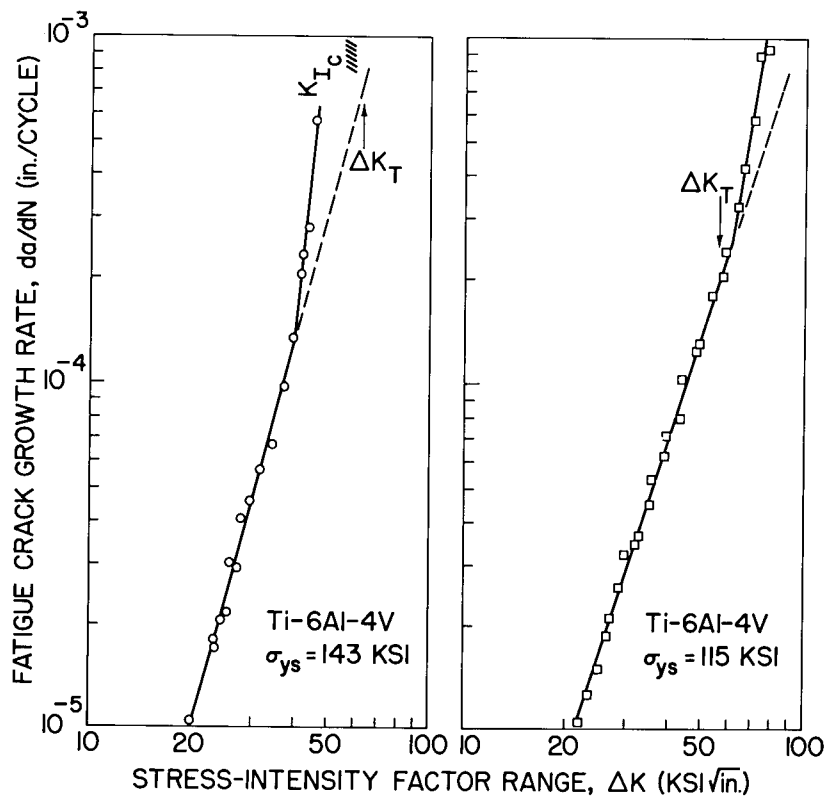


Fig. 6—Logarithmic plots of da/dN vs ΔK for the Ti-6Al-4V alloys shown on Fig. 2. The slope transition behavior is similar to that exhibited by the steels in Fig. 5.

strength/toughness tradeoffs in materials selection. Thus, the high levels of fracture toughness which can be attained in the newer high-strength alloys are not a reliable index to the high-amplitude fatigue crack propagation resistance of these materials.

CONCLUSION

Conditions involving very rapid rates of fatigue crack propagation in high-toughness, high-strength alloys have not been the subject of serious study because so few cycles of fatigue life can be endured under such high-amplitude cycling. Nevertheless, this is where the margin of safety lies in the application of high-toughness alloys in critical structures. It is this ability to endure limited repeated loading in the region beyond the fracture level of low-toughness counterparts that distinguishes the high-toughness alloys for critical applications. Herein lies the role of fracture toughness in designing against failure by low-cycle fatigue crack propagation. When all other preventive measures of fatigue design and nondestructive inspection have failed, fracture toughness alone can stave off terminal failure. For the situation of the undetected large flaw and/or the situation of intermittent severe loading, high fracture toughness can permit high-strength alloys to endure limited high-amplitude cycling. However, designers should be aware that such high-amplitude cycling is not a simple extrapolation of low-amplitude fatigue crack propagation. Both the metallurgical failure processes and the form of the $da/dN - \Delta K$ data curves change under high-amplitude cycling. Efforts to determine fatigue life under high-amplitude

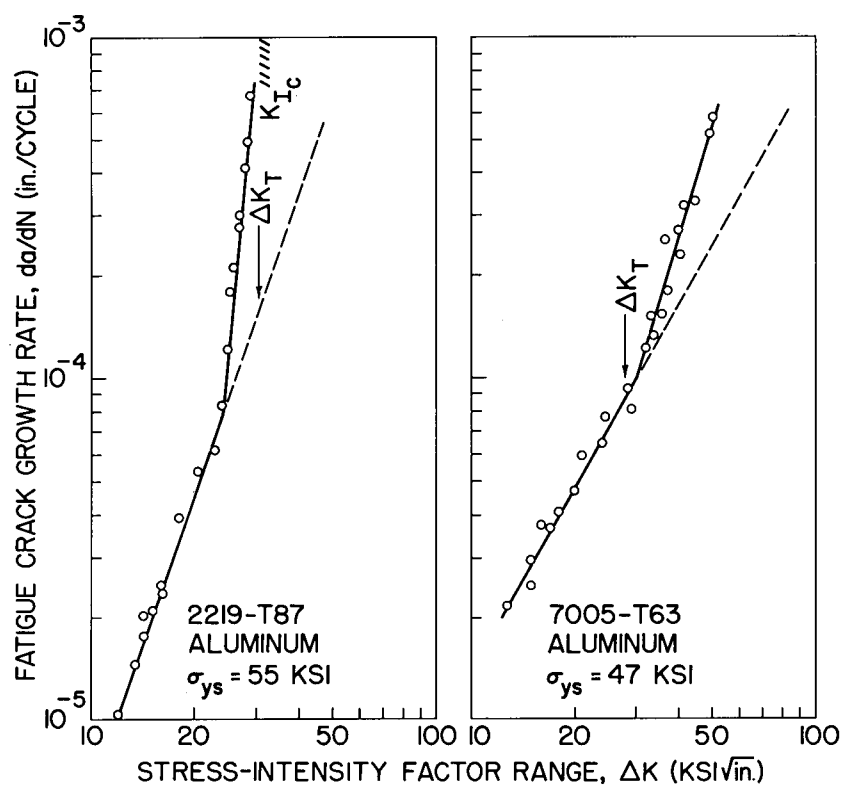


Fig. 7—Logarithmic plots of da/dN vs ΔK for the 2219-T87 and 7005-T63 aluminum alloys shown on Fig. 3. The slope transition behavior is similar to that exhibited by the steels and Ti-6Al-4V alloys in Figs. 5 and 6.

cycling by extrapolation of low-amplitude crack propagation data to end points based upon high levels of fracture toughness are likely to result in nonconservative estimates.

ACKNOWLEDGMENTS

The author wishes to acknowledge the contributions of R. J. Hicks and M. L. Cigledy, who conducted the fatigue testing, and the Office of Naval Research for their financial support of this work.

REFERENCES

1. A. M. Freudenthal, "Fatigue Mechanisms, Fatigue Performance and Structural Integrity," in *Proceedings, Air Force Conference on Fatigue and Fracture of Aircraft Structures and Materials*, Miami Beach, Fla., Dec. 15-18, 1969, Air Force Flight Dynamics Laboratory Technical Report 70-144 (published 1971), p. 9.
2. M. R. Gross, "Low-Cycle Fatigue of Materials for Submarine Construction," *Naval Eng. J.* 75, 783 (1963).
3. T. W. Crooker and E. A. Lange, "Low-Cycle Fatigue Crack Propagation Resistance of Materials for Large Welded Structures," in *Fatigue Crack Propagation*, ASTM STP 415, Am. Soc. for Testing and Materials, 1967, p. 94.

4. J. M. Barsom, E. J. Imhof, and S. T. Rolfe, "Fatigue-Crack Propagation in High Yield-Strength Steels," *Eng. Fracture Mech.* 2, 301 (1971).
5. W. S. Pellini, "Criteria for Fracture Control Plans," NRL Report 7406.
6. P. P. Puzak and E. A. Lange, "Standard Method for the 1-Inch Dynamic Tear Test," NRL Report 6851, Feb. 13, 1969.
7. C. N. Freed and R. J. Goode, "A Correlation Between Fracture Toughness Test Procedures for Ferrous Alloys," in *Pressure Vessel Technology, Part II, Materials and Fabrication*, ASME, 1969, p. 723.
8. C. N. Freed, "A Comparison of Fracture Toughness Parameters for Titanium Alloys," *Eng. Fracture Mech.* 1, 175 (1968).
9. C. N. Freed, R. J. Goode, and R. W. Judy, Jr., "Comparison of Fracture Toughness Test Procedures for Aluminum Alloys," *Eng. Fracture Mech.* 2, 359 (1971).
10. W. F. Brown, Jr., and J. E. Srawley, *Plane Strain Crack Toughness Testing of High Strength Metallic Materials*, ASTM STP 410, Am. Soc. for Testing and Materials, 1966.
11. P. P. Puzak and E. A. Lange, "Fracture Toughness of 180 to 210 ksi Yield Strength Steels," *Metals Eng. Quart.* 10, p 6 (1970).
12. R. J. Goode and R. W. Judy, Jr., "Fracture-Safe Design of Aluminum and Titanium Alloy Structures," NRL Report 7281, Feb. 14, 1972.
13. P. Paris and F. Erdogan, "A Critical Analysis of Crack Propagation Laws," *ASME Trans., J. Basic Eng.* 85D, p 528 (1963).
14. G. T. Hahn, M. Sarrate, and A. R. Rosenfield, "Experiments on the Nature of the Fatigue Crack Plastic Zone," in *Proceedings, Air Force Conference on Fatigue and Fracture of Aircraft Structures and Materials*, Miami Beach, Fla., Dec. 15-18, 1969, Air Force Flight Dynamics Laboratory Technical Report 70-144, p. 425 (1971).
15. R. J. Donahue, H. McL. Clark, P. Atanmo, R. Kumble, and A. J. McEvily, "Crack Opening Displacement and the Rate of Fatigue Crack Growth," University of Connecticut Institute of Materials Science Report (to be published).
16. T. W. Crooker, "Crack Propagation in Aluminum Alloys Under High-Amplitude Cyclic Load," NRL Report 7286, July 12, 1971.
17. W. G. Clark, Jr., and E. T. Wessel, "Interpretation of the Fracture Behavior of 5456-H321 Aluminum with WOL Toughness Specimens," Westinghouse Research Laboratories Scientific Paper 67-106-BTLFR-P4, Sept. 8, 1967.
18. T. W. Crooker, L. A. Cooley, E. A. Lange, and C. N. Freed, "Fatigue Crack Propagation and Plane Strain Fracture Toughness Characteristics of a 9Ni-4Co-0.25C Steel," *ASM Trans.* 61, 568 (1968).
19. T. W. Crooker and D. J. Krause, "Fatigue Crack Growth Rates in Ti-6Al-4V Alloys at Various Yield Strength and Fracture Toughness Levels," Report of NRL Progress, Jan. 1972, p 18.
20. C. M. Carman and J. M. Katlin, "Low Cycle Fatigue Crack Propagation Characteristics of High Strength Steels," *ASME Trans., J. Basic Eng.* 88D, 792 (1966).
21. J. M. Barsom, "The Dependence of Fatigue-Crack Propagation on Strain-Energy Release Rate and on Crack-Opening Displacement," in *Damage Tolerance in Aircraft Structures*, ASTM STP 486, Am. Soc. for Testing and Materials, p. 1 (1971).

22. J. M. Barsom, "Fatigue-Crack Propagation in Steels of Various Yield Strengths," ASME Paper No. 71-PVP-12.
23. T. W. Crooker, "Slope Transition Behavior of Fatigue Crack Growth Rate Curves," Report of NRL Progress, Dec. 1970, p. 25.
24. T. W. Crooker, "Fatigue Crack Growth Rates in Ti-6Al-4V Alloys at Various Yield Strength and Fracture Toughness Levels," Report of NRL Progress, June 1971, p. 32.

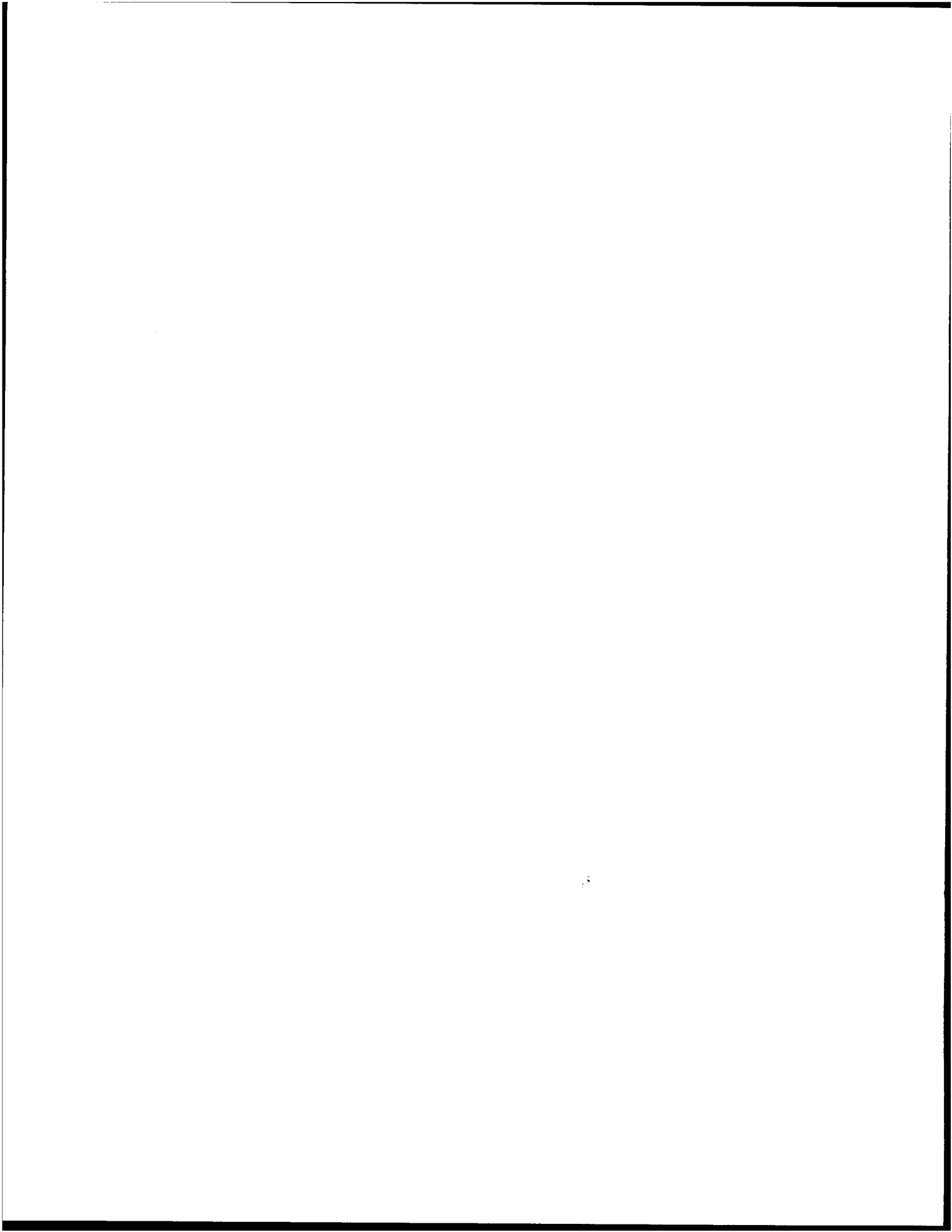
• .

.





NRL7284



DOCUMENT CONTROL DATA - R & D

(Security classification of title, body of abstract and indexing annotation must be entered when the overall report is classified)

1. ORIGINATING ACTIVITY (Corporate author) Naval Research Laboratory Washington, D.C. 20390		2a. REPORT SECURITY CLASSIFICATION Unclassified	
		2b. GROUP	
3. REPORT TITLE A COMPUTER PROGRAM FOR EVALUATING RADAR PERFORMANCE IN A HIGH-ALTITUDE NUCLEAR ENVIRONMENT			
4. DESCRIPTIVE NOTES (Type of report and inclusive dates) An interim report on one phase of a continuing problem.			
5. AUTHOR(S) (First name, middle initial, last name) James B. Mead and Leonard S. Wagner			
6. REPORT DATE September 10, 1971		7a. TOTAL NO. OF PAGES 118	7b. NO. OF REFS 10
8a. CONTRACT OR GRANT NO. NRL Problem H02-27		9a. ORIGINATOR'S REPORT NUMBER(S) NRL Report 7284	
b. PROJECT NO. HC04001		9b. OTHER REPORT NO(S) (Any other numbers that may be assigned this report)	
c.			
d.			
10. DISTRIBUTION STATEMENT Distribution limited to U.S. Government Agencies only; test and evaluation; September 1971. Other requests for this document must be referred to the Director, Naval Re- search Laboratory, Washington, D.C. 20390.			
11. SUPPLEMENTARY NOTES		12. SPONSORING MILITARY ACTIVITY Department of Defense (Defense Atomic Support Agency) Washington, D.C. 20305	
13. ABSTRACT This report documents work completed on the development of a computer program to predict radar performance following a high-altitude nuclear detonation. The program has been designed to carry out calculations of radar propagation quantities such as absorption, refraction, and apparent sky temperature. For a description of the propagation medium, the program depends upon explosion phenomenology tapes generated at NRL. It differs from other programs directed at predicting radar performance under similar conditions in that no attempt is made within the program to calculate phenomenology parameters. Thus, lengthy phenomenology calculations need not be duplicated if it is desired to rerun the program with a different geometry or a different set of radar characteristics. A brief discussion is given of the general features and limitations of the program as well as a description of its operation. Fortran listings and flowcharts for the more important routines are not included. A summary and discussion of the prop- agation equations employed is also presented. Some preliminary results for runs carried out using the NRL CDC-3800 computer are given, using as input an artificial nuclear environment contrived for test purposes.			

CONTENTS

Abstract	ii
Problem Status	ii
Authorization	ii
INTRODUCTION	1
GENERAL FEATURES AND LIMITATIONS OF PROGRAM	2
Limitations on Accuracy	3
Propagation-Related Quantities	3
Input Parameters	5
PROGRAM DESCRIPTION	5
Main Program and Ray-Tracing Procedure	5
Outputs and Display Format	10
Propagation Expressions	10
Description of Subroutines	15
Subroutine BEND	15
Subroutine COLLF	16
Subroutine DGROUP	18
Subroutine GEOM	21
Subroutine PRELDA (Entry PRELP)	21
Subroutine REFRAC	22
Subroutine RFRAC2	22
Subroutine TEST	24
Subroutine TRANS	24
Subroutine TROPAT	27
Subroutines XCOORD, BACOR, XDRCOS	27
Miscellaneous Subroutines	30
Subroutine CONTR	30
Subroutine INIT	30
Subroutine INTERP	31
Subroutine MODATM	31
Subroutine POSIT	31
Subroutine SHDRAY	31
Subroutine SUMARY	31
Program Structure	31
TEST RUNS AND PRELIMINARY RESULTS	33
Description of Burst-Region Model	33
Studies of the Granularity Criteria	33
Test Results	38
Two-Way Absorption (Path Loss) Sky Map	39
Refraction Sky Map (REFRAY)	39
ACKNOWLEDGMENTS	40
REFERENCES	40
APPENDIX A - Collision Frequencies	51
APPENDIX B - Model Atmosphere	58
APPENDIX C - Fortran Program Listings	59
APPENDIX D - User Instructions	111

ABSTRACT

This report documents work completed on the development of a computer program to predict radar performance following a high-altitude nuclear detonation. The program has been designed to carry out calculations of radar propagation quantities such as absorption, refraction, and apparent sky temperature. For a description of the propagation medium, the program depends upon explosion phenomenology tapes generated at NRL. It differs from other programs directed at predicting radar performance under similar conditions in that no attempt is made within the program to calculate phenomenology parameters. Thus, lengthy phenomenology calculations need not be duplicated if it is desired to rerun the program with a different geometry or a different set of radar characteristics.

A brief discussion is given of the general features and limitations of the program as well as a description of its operation. Fortran listings and flowcharts for the more important routines are not included. A summary and discussion of the propagation equations employed is also presented. Some preliminary results for runs carried out using the NRL CDC-3800 computer are given, using as input an artificial nuclear environment contrived for test purposes.

PROBLEM STATUS

This is an interim report on one phase of the problem.

AUTHORIZATION

NRL Problem H02-27
Project HC04001

Manuscript submitted April 1, 1971.

A COMPUTER PROGRAM FOR EVALUATING RADAR PERFORMANCE IN A HIGH-ALTITUDE NUCLEAR ENVIRONMENT

INTRODUCTION

In early 1969, the Radar Geophysics Branch of the NRL Radar Division was assigned the problem of developing a computer program to predict the effects of a high-altitude nuclear explosion on radar detection. The objective of this report is to summarize work done to date and to document the computer program in its present stage.

It is well known that the ionization produced by a nuclear explosion causes numerous radar propagation effects, most of them detrimental. Among the effects produced are (a) target-position location errors due to refraction and to reduction of group velocity, (b) reduction of the signal strength due to wave absorption, (c) an increase in the received thermal noise level, and (d) production of clutter echoes by reflection from ionized regions. Experimental data on some of these effects were obtained in the atmospheric tests conducted prior to the nuclear test ban treaty. Computer programs to predict the effects of nuclear explosions at low altitudes, based largely on the data of these tests, have been developed by the General Electric Tempo organization (1,2). Unfortunately, however, the data of the tests are deficient in many respects, and of course there is no longer a possibility of remedying these defects by further atmospheric experiments. In particular, the data are inadequate in the high-altitude regions (above 100 km) which are of primary interest in modern weapon-system technology.

The NRL Plasma Physics Division has undertaken a program of theoretical prediction, via computer calculation, of the high-altitude nuclear effects* for which experimental data are lacking. The Radar Division effort is supplementary to this work. The objective is to produce a computer program for the radar propagation effects which will utilize the outputs of the Plasma Physics Division computer programs for a description of the disturbed high-altitude physical environment. Among the quantities needed as inputs for the propagation calculations are electron density and its gradient, temperature, and neutral species concentrations as functions of space and time.

The initial phase of the Radar Division effort consisted of a review of the pre-test-ban atmospheric experiments and of the computer programs known as the RANC Code (Radar Absorption, Noise, and Clutter) developed by General Electric Tempo, and other activities of an educational nature. These included a visit to the U.S. Army Safeguard System offices and meetings with Plasma Physics Division personnel to become familiar with their approach to the problem and to establish the necessary coordination between their computer programs and ours. During this period, Radar Division personnel attended numerous meetings at which the physicists concerned with the explosion phenomenology discussed their work.

During this initial phase it was recognized that most of the effects to be calculated depended upon position in space along the propagation path. Therefore, concurrently with these investigations of previous work and other educational activities, work was begun on

*In the remainder of this report, these effects will be referred to as phenomenology, a term used to refer to the gross atmospheric motion following a nuclear detonation and to detailed predictions of changes in atmospheric electron density and temperature.

a computer routine to calculate, in some detail, the propagation path. The resulting three-dimensional ray-tracing routine is thus basic to the calculation of all propagation parameters.

Included in this report is a description of the general features and limitations of the program. The operation of the main program and, in particular, of the ray-tracing procedure is explained. A section is devoted to the outputs and display formats. Another section contains a description of the propagation expressions employed. The operation of nontrivial subroutines is described in a brief manner, and flowcharts are provided for those routines where the logic is more involved. There are four appendixes devoted to the treatment of collision frequencies (Appendix A), the model atmosphere (Appendix B), Fortran program listings (Appendix C), and user instructions and program options (Appendix D). A section has been included to cover preliminary results of test runs carried out using the NRL CDC-3800 computer. For these tests an artificial phenomenology model described by analytical expressions was used.

GENERAL FEATURES AND LIMITATIONS OF PROGRAM

The purpose of the computer program to be described in the following sections is the prediction of specific aspects of radar performance to be expected during the detection and tracking of targets (reentry vehicles) in a high-altitude nuclear environment. The calculations carried out are those involving radar propagation. By-products of separating the phenomenology and propagation calculations are improved flexibility and savings in computer operating time and memory. Results of phenomenology calculations for a specific nuclear yield and altitude may be stored on magnetic disc or tape. These results are then available for a number of propagation calculations at diverse radar frequencies or at various locations relative to ground zero, without the necessity for repeating the phenomenology calculations for each analysis of radar effects.

Primary emphasis has been placed upon obtaining answers as free from approximations and avoidable error as is reasonably possible; considerations relating to computer running time or memory allocation have been secondary. This policy is intended to provide results that can serve as a basis for evaluating approximation techniques used in faster-running codes and for analyzing the effects of changes in phenomenology calculations on radar propagation quantities.

An attempt has been made to present the output data in a form which facilitates a quick-look analysis but yet which embodies as complete a display as possible for the quantities of interest. Where feasible, quantities have been presented as "sky maps," for example, one form of output is a line-printer plot of apparent sky noise temperature on an elevation-azimuth grid. This format represents essentially what the viewer "sees" when looking out from the radar location.

The radar frequency range for the program is 100 MHz to 10 GHz. The classical Appleton-Hartree expression for refractive index is assumed valid within the ionosphere with certain modifications and assumptions. Tropospheric effects on propagation are handled in a manner described by Blake (3). An important approximation pertaining to ionospheric propagation is that magnetic field effects can be ignored, i.e., $\omega \gg \omega_b$, where ω is the radar angular frequency (in megaradians per second) and ω_b is the electron gyroresonance frequency. For frequencies greater than 100 MHz this approximation is justified. A more detailed discussion of this approximation is given in a later section.

Limitations on Accuracy

The propagation calculations are limited in accuracy by two classes of errors—those attributable to the phenomenology predictions and passed to the propagation code through input quantities such as electron density and electron temperature (extrinsic errors), and those arising from the propagation program itself (intrinsic errors).

Extrinsic sources of error could possibly arise as a result of incompleteness in the high-altitude physics or from inaccuracies in transport coefficients or rates of chemical processes. Another important source of extrinsic error is related to the granularity of calculated quantities arising from the spatial zoning which is necessary for solving hydrodynamic differential equations by the finite-difference method. Interpolation between points in space is essential and is employed. Some granularity may be expected to survive such a smoothing process.

Among the expected sources of intrinsic error are those arising from representing the propagation medium by a series of strata and slabs.* Such errors will depend on the spatial gradients of both input and calculated quantities and may be minimized by choosing sufficiently small strata and slabs during ray tracing. Inaccuracies related to the granularity of the medium are difficult to evaluate analytically because of the interaction of many effects; however, it is possible to obtain some estimate of their magnitude by running a series of test calculations differing only in the sizes of the strata and the slabs used in ray tracing. A discussion of these limitations is given in the section covering test runs and preliminary results.

Propagation-Related Quantities

Absorption (blackout) and refraction in a high-altitude nuclear environment are well-known limitations on the performance of antiballistic missile tracking radars. The calculation of these quantities requires a knowledge of the macroscopic space-time dependence of electron density and temperature in the disturbed region.

A diagram showing the geometry involved in the radar tracking of an incoming target is given in Fig. 1. The pointing direction of the radar is given by the vector OA' . The curved line OB represents the path of the actual (refracted) ray whose end point defines the actual position of a target generating a radar return. A number of useful quantities are available once the end point of the ray has been determined. Among these are radar range error, radar pointing-angle error, and radar miss distance.

Radar range is inferred from measurements of signal delay made at the radar assuming that the signal velocity is the free-space value c . In ionized regions, because of a reduced group velocity and because of the curvature of the ray path, the signal delay is increased and therefore the radar overestimates the target range. The apparent target location, as deduced by the radar, is at the position A' , whereas the actual target position is at the point B . The target-location errors referred to in the preceding paragraph are illustrated in Fig. 1. The program designations of range error, angle error, and miss distance are RERROR, AERROR and DISMIS, respectively.

The absorption in decibels (or path loss referred to 1 m) along the ray path is calculated by numerical integration. As a by-product of this calculation, the apparent sky temperature in the direction of initial pointing of the ray is also derived. Results of apparent sky temperature are presented on a conventional "sky map" with an elevation-azimuth grid.

*The slab representation is convenient for a simple Snell's law formulation of refraction and also is consistent with the discrete nature of machine computation. The differences between strata and slabs will be elaborated on in a later section.

calculations is that all targets to be tracked will lie above most of the troposphere; i.e., the troposphere is completely penetrated by the radar beam. A set of tabular values for tropospheric absorption based on Blake's results has been used in the program for these calculations. The tropospheric refractive index is assumed to decrease exponentially with altitude, and is calculated from a simple analytical expression (see section on Subroutine RFRAC2) involving the atmospheric scale height below 30 km (3).

Input Parameters

The Fortran identifiers of inputs required from phenomenology calculations and other input parameters are as follows:

WPE - electron plasma angular frequency in megaradians per second.

TEP - electron temperature in electron volts.

N1, N2, N3 - direction cosines of the electron-density gradient (or of plasma frequency gradient).

R - (km) a selection of 10 reference ranges for which propagation quantities are to be tested against their allowable limits.

ABSL - two-way absorption limit in decibels.

PATHL - two-way path-loss limit in decibels.

RFCRL - angle error limit in degrees.

GRPL - radar range error limit in kilometers.

DEVL - ray deviation limit in degrees.

COLATI - the colatitude of the radar in degrees.

THETA - the azimuth of ground zero in degrees.

RANGE - ground range, in kilometers, from radar to ground zero.

FR - the radar frequency in megahertz.

ELMAX, ELMIN - the elevation angle scan limits in degrees.

THETMX, THETMN - azimuth angle scan limits in degrees.

INC - the angular resolution for both azimuth and elevation scanning.

AZERO - the central azimuth (degrees) for the sky-map displays.

ELEO, THETAO - elevation and azimuth angles, respectively, of the target engagement direction.

RTRGET - the target range in kilometers, for the engagement option.

TSKY - the average temperature of the background sky in degrees Kelvin.

RAMAX - limiting distance in kilometers to which any ray will be traced.

PROGRAM DESCRIPTION

Main Program and Ray-Tracing Procedure

The program is built around an incremental ray-tracing routine in which the radar ray path is approximated by a series of straight-line segments. Sector coverage and angular resolution of the ray trace calculation are defined by card-controlled variables.

Several important quantities, such as cumulative absorption, group path delay, and apparent sky-noise temperature, are calculated along each ray.

To facilitate the ray-tracing procedure, the propagation medium is subdivided into a series of slabs and strata (subslabs). The faces of a stratum are aligned perpendicular to the local gradient of electron density. A slab is composed of one or more contiguous strata. The strata and the slabs are geometrically identical, and in a spatially varying medium, are actually wedges rather than plane-parallel-sided figures as the term slab connotes. If the slab (stratum) thickness is small compared with the scale for the change of electron density, the two sides of the wedge are approximately parallel and the terms slab and stratum are justified.

The size of a stratum is determined by the step size of the ray-tracing procedure. The step size is variable within the program and the width of a stratum is, therefore, also variable. Within a stratum, the imaginary part of the phase refractive index and the group refractive index are assumed constant. Within a slab, the real part of the phase refractive index is assumed constant. The stratum, therefore, defines the granularity structure for the absorption and for the radar range calculations, whereas the slab defines the granularity structure for the refraction calculation. The thicknesses of strata and slabs are controlled by program parameters which will be elaborated upon. In what follows, the terms step and step size will refer to the advance of the ray in stratum-size increments.

Within a slab the real part of the refractive index of the medium is assumed equal to the actual value at the leading edge, and the ray path is approximated by a straight-line segment. At the interface between adjacent slabs, a refractive bend, based on Snell's law, is executed. The slab thickness of any given section of the medium is chosen so that the refractive-index change between slabs is small enough to produce a piecewise-linear ray path that satisfactorily approximates the actual ray path in the medium. In the program as presently constituted, the limit on the change of refractive index between adjacent slabs has been set at 1%. This limit is determined by the Fortran variable, LMU. The value assigned to LMU is controlled by an input data card and may be changed at the discretion of the operator. The effect on the calculations of a change in the granularity limit is discussed later in this report.

Each straight-line segment of the ray path is constructed from a series of collinear steps. Incremental absorption is evaluated at each step. Step size is controlled so that the incremental absorption may not exceed a prescribed granularity limit. This limit is determined by the Fortran variable LABS which is controlled by an input data card. The value assigned to LABS can be changed at the discretion of the operator. A limit of 0.1 dB per step has been used in preliminary calculations.

The sizes of the steps are discretely adjustable. The procedure is to start by taking the largest step size permitted. After each step the cumulative fractional change in refractive index within the slab and the incremental absorption are checked against the granularity limits. When either of these limits is exceeded, the ray is forced to step back and to advance subsequently in steps a factor of 10 smaller in size. The calculation continues with the new step size until either one of the granularity criteria is again exceeded, whereupon the step refinement procedure is repeated. A minimum step size, controlled by the Fortran variables DEL and ITER, is defined such that if either of the granularity criteria is exceeded at this step size, slab synthesis is terminated and the ray is forced to bend (i.e., a refraction calculation is made). The ray in the next slab proceeds in the direction of the refracted ray and the step size is reset so that slab construction again starts at the largest allowable step size.

Step size DL in constructing a straight-line segment of a ray path, is controlled by the expression

$$DL = DEL / 10^{(L3 - 1)}. \quad (1)$$

The parameters controlling the size of a step are the variables DEL and L3. L3 is an index which starts at a value of unity at the start of each ray segment (slab). It is increased by one each time the absorption or refraction granularity criteria are exceeded.

The largest step size permitted is equal to DEL kilometers since $DL = DEL$ when $L3 = 1$. DEL therefore controls the granularity of the medium for calculating absorption and radar (group path) range and, hence, is usually chosen to be small compared with the expected scale for change in the medium. DEL is allowed to take one of two possible values denoted by the Fortran variables DEL1 and DEL2 which are defined by data card input. DEL1 defines a course step size for ray tracing in an essentially unperturbed environment. DEL2 defines a finer step size for ray tracing through a disturbed medium. In regions of space which are nonabsorbing and nonrefracting, DEL is usually assigned a value of $DEL1 = 10$ km, which permits rapid completion of those portions of a ray that are negligibly affected by the propagation medium. In perturbed regions of space DEL has been set to $DEL2 = 1$ km, but this value will probably have to be changed in accordance with the requirements of specific propagation conditions.

In the construction of a straight-line section of the ray path, the index L3 is allowed to attain a maximum value given by the program parameter denoted ITER. The value assigned to ITER determines the smallest allowable step size. From Eq. (1) it is evident that the smallest step size allowed is given by

$$DL_{min} = DEL / 10^{(ITER - 1)}. \quad (2)$$

Thus, once DEL is chosen so as to establish a maximum step size, ITER determines the minimum length of a straight-line section of ray path. In regions where the medium is only moderately perturbed, ITER has a negligible effect on the granularity of the calculation. In severely disturbed regions of space the granularity limits are often exceeded in a single step of the smallest size. Under these circumstances, the granularity of the calculations is controlled by the minimum step size and hence by the variable ITER. ITER is usually chosen to be 4 in regions of space which are nonrefracting and nonabsorbing. The very fine step size that this permits is used for accurately locating the boundaries of a perturbed region of space. Within a perturbed region ITER is usually reset to 2. $ITER = 2$, in conjunction with $DEL2 = 1$ km, permits a minimum step size of 100 m, which is deemed acceptable from the standpoint of being small compared with the scale for change in the medium while still allowing relatively rapid execution. It is emphasized that the choices for DEL and ITER can be readily altered at the discretion of the operator.

A wave normally incident on a stratified plasma whose density is increasing in the direction of propagation is ultimately reflected at a point at which the wave frequency equals the plasma frequency of the medium. Waves obliquely incident on the same medium are also reflected but at a lesser penetration distance. For oblique incidence, the reflection process can be treated as a refraction process. Alternatively, the reflection process can be described in terms of a wave formulation which provides for coupling between ingoing and outgoing waves. For a discrete medium, the analog of the wave formulation in a continuous medium is the phenomenon of total reflection, and this is the approach used in the present program.

Theoretically the results of the total-reflection method approach those of the full-wave treatment as the granularity of the medium goes to zero. Total reflection of an obliquely incident ray introduces a discontinuity in the direction of the ray path which does not occur in a continuous medium. Since the critical angle for total reflection is governed by the change in refractive index at the slab interface, its value depends upon the slab thickness. The true reflection (or refraction) process can be closely approximated by making the slab thickness so small that total reflection does not occur until the grazing angle of the ray is nearly parallel to the slab. The slab width at the time of reflection is always equal to the smallest allowable step size.

The critical angle is defined in terms of the ratio of the refractive indexes between slabs. The total reflection region is sensed in the following manner. Each step in the construction of a slab requires that the refractive index be evaluated at the ray tip. The ratio of this refractive index to that assigned to the slab is used for evaluating a critical angle which is then compared with the angle of incidence of the ray. At the first step wherein the critical angle is exceeded, the ray is forced to step back a single step and a refractive bend is executed at that point. Thereafter, the slab thickness is made equal to the length of a single step with a resulting increase in the critical angle. Each subsequent time that the critical angle is exceeded the last step is retracted and the step size is reduced. When the critical angle is exceeded at the smallest step size, a reflection is executed. If, at any step size, more than 20 steps are taken without exceeding the critical angle, then the program assumes that the total-reflection region has been traversed and it reverts to the normal stepping procedure.

The granularity limit on the cumulative fractional change in refractive index imposes a minimum value for the critical angle. For example, for a 1-% limitation on the change of refractive index between slabs, the minimum critical angle is 89.43° . Smaller refractive index changes result in the critical angle approaching still closer to 90° .

The program provides for an interruption of the ray-tracing procedure when the distance from the radar to the tip of the ray equals any of a set of reference ranges. At these ranges, various parameters relevant to the radar detection and location problem are calculated and used in the preparation of output displays. These parameters include cumulative absorption and path loss* to the reference range in question, ray deviation from the initial pointing direction, radar range and pointing angle errors, and radar miss-distance. Radar range error is defined as the difference between the group range and the actual (straight-line) range to the ray tip. Radar angle error is defined as the angle between the radar pointing direction and the straight line to the actual ray tip. Miss distance defines the spatial separation between the apparent position of the ray tip, as inferred from the radar range and radar direction, and the actual position of the ray tip.

The program incorporates a number of contingency features for terminating a given ray. These will be discussed individually.

1. Range Limitation. Ray tracing is not allowed to proceed beyond a given range denoted RAMAX. RAMAX is card-controllable by the operator and is usually set equal to the nominal detection range of the radar system. There is obviously no advantage in tracing a ray out beyond the range of the radar. Choice of RAMAX depends, of course, on a somewhat arbitrary assumption of expected target cross section. Ray termination at RAMAX results in a printed output statement to that effect.

2. Absorption (or Path Loss) Limitation. In a propagation environment wherein the medium is lossy, the effective range of the radar system can be seriously curtailed.

*Path loss includes the effect of absorption but in addition incorporates an R^{-4} power attenuation due to the divergence of the radar beam.

Because very weak signals are undetectable, some limit must be set on the allowable absorption (or path loss) beyond which the ray tracing should be discontinued. Clearly, these limits will depend on the sensitivity of the radar as well as on the expected target cross section. For this reason, ray termination occurs at the nearest subsequent reference range and is documented by a printed output statement and, where appropriate,* by a coded representation of the output displays.

3. Overdense Medium. An overdense medium is, by definition, opaque to the radar wave. Targets beyond the overdense boundary will not be illuminated by the wave. Termination occurs, therefore, at the point in the ray path at which the overdense boundary is encountered.

The exact behavior of the wave in the vicinity of an overdense medium depends very strongly on the effective electron collision frequency and on the magnitude of the gradient of electron density in the region. Total absorption, total reflection, or some combination of absorption and reflection, may occur. It is difficult (if not impossible) to calculate sufficiently detailed phenomenology in this region to obtain an accurate assessment of absorption and refraction. For this reason, the ray is terminated and, where appropriate, the output sky maps are marked to indicate this reason for termination. Noise background temperature in the direction of this ray is modified to incorporate a contribution of the overdense medium, based on the assumption that the ray is completely absorbed at that point.

4. Excessive Bending. In a highly refracting medium the ray may be so severely refracted as to make any radar data useless for purposes of target location. This has been deemed sufficient grounds for ray termination. When excessive bending occurs, the ray is terminated at the nearest subsequent reference range. Rays terminated in this manner are so designated, when appropriate, on the output sky maps. The ray deviation limit is arbitrary and can be adjusted at the discretion of the program user. If a clutter calculation were incorporated into the computer program, the arbitrary termination of a ray because of excessive bending would be discarded.

5. Ray Intersection with Ground. Ray intersection with the ground represents an obvious ray termination point. Except for its contribution to radar clutter, this occurrence is of little interest to the problem of the radar environment associated with a high-altitude nuclear burst.

6. All Direction Cosines are Zero. This result is indicative of a calculational error. It causes the immediate termination of a ray with an appropriate output diagnostic.

7. Too Many Bends. The number of bends executed in the course of constructing each ray is monitored. An excessive number of bends quite likely indicates that the ray has been trapped in an infinite loop. As a safeguard against this possibility, the program allows for a maximum number of bends (999) on any given ray. Rays terminated in this manner are documented by a printed output statement. Modification of the maximum allowable number of bends requires a program edit.

The program operation discussed in this section of the report is described in more detail by the flow diagram of Fig. 2. The flow diagram is representative of the actual order of the operations as they are performed in the computer. It is not meant, however, to describe the actual structure of the program and its division into subroutines; this will be done in a later section.

*If the radar parameter limit for a given output display has not been exceeded at the time of termination of the ray, then a coded mark is made on the display at the angular coordinates of the initial pointing of the ray, indicating the reason for termination.

Outputs and Display Format

The output displays take the form of line-printer-produced coded sky maps for each radar parameter. The map coordinates are azimuth and elevation and the coding defines ranges at which the radar parameter appropriate to the display first exceeds a prescribed limit. The coding is numerical and the limited number of single-symbol code words limits the number of ranges that can be displayed to a discrete set of reference ranges. The parameters described in terms of these maps are range error, angle error, miss distance, absorption or path loss, and ray deviation. The parameter limits that are documented by the sky maps are designated GRPL, RFRCL, MISL, ABSL OR PATHL, and DEVL, respectively, and their values are controllable by punched card input. Sky maps of this kind provide the radar specialist with a comprehensive and yet concise description of the radar environment. Information regarding localized effects of the nuclear blast environment are available in much greater detail on demand.

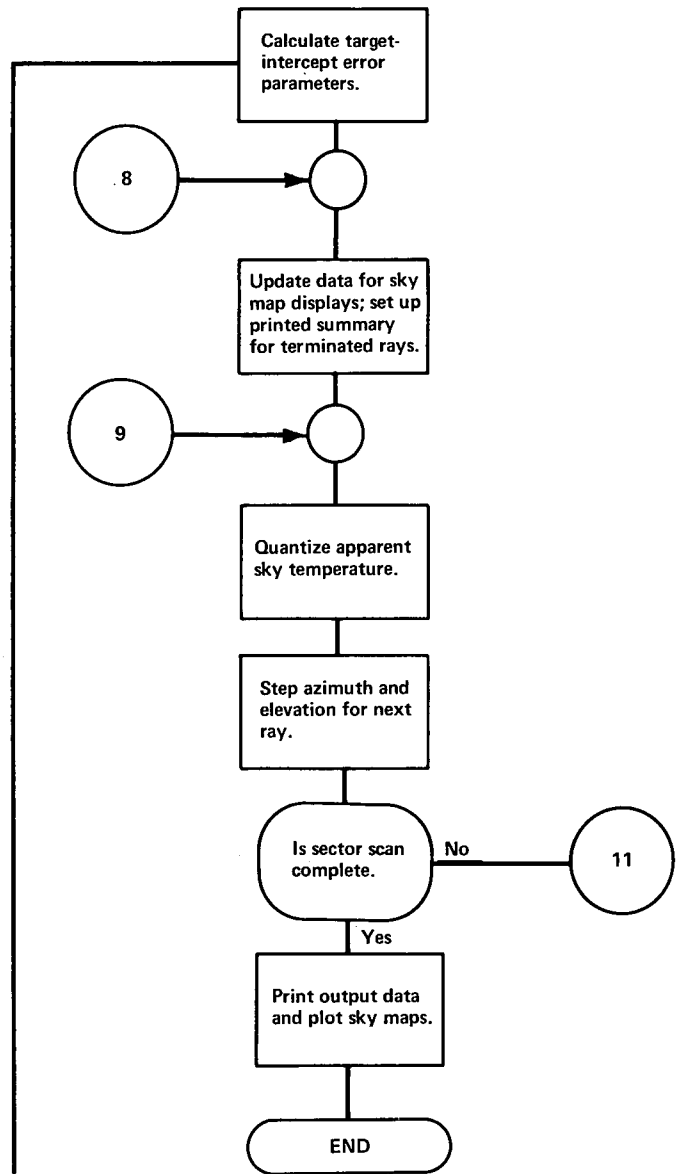
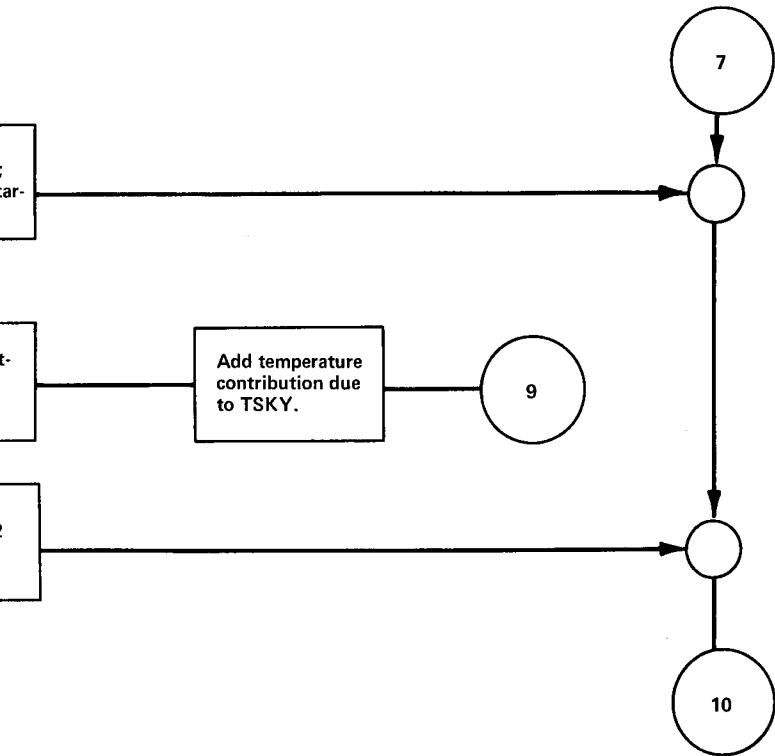
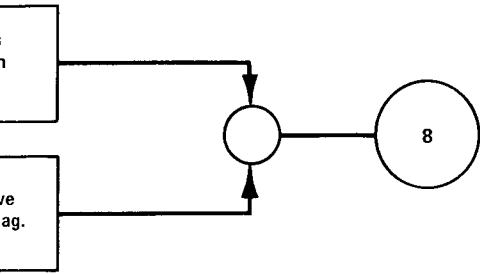
A sky map can be interpreted as defining a surface in space within which a detection or location parameter lies within specified limits. For example, if the quantity of interest is target location, then target miss distance is a suitable radar location variable. The interception problem can define a limit on miss distance MISL such that miss distances in excess of MISL result in failure of the mission. A sky map of miss distance based upon this limit will then result in a range surface which divides space into two regions. For ranges smaller than those defined by the range surface the mission has a chance of success, at least insofar as the interception problem is concerned. Ranges greater than those defined by the range surface define a region of space in which the interception problem is, by definition, hopeless.

Apparent sky temperature includes contributions from absorption effects in the propagation medium. Since range is not a relevant parameter in defining sky temperature, the output display simply consists of a numerical "shade plot" on an azimuth-elevation background coordinate system. Sky temperature is quantized and a numerically coded representation of temperature is printed on the azimuth-elevation map for each angular resolution element.

The program provides the option of a target-engagement calculation as well as general calculations for describing the total radar environment. The target-engagement calculation requires the target coordinates as inputs. For a ray whose initial pointing is in the target direction and at a true range to the ray tip which equals the target range, the ray-tracing procedure is interrupted and the radar parameters (absorption or path loss, range error, angle error, and miss distance) are calculated. These results are useful in the evaluation of radar performance for a specific radar-target and nuclear-blast geometry, and their calculation does not measurably lengthen the running time of the program.

Propagation Expressions

The classical Appleton-Hartree equation for refractive index is used for the calculation of propagation-related quantities in the ionosphere. A detailed treatment of the underlying theory may be found in Ref. 4 and some modifications for a realistic handling of collisions are given in Refs. 5 through 7.





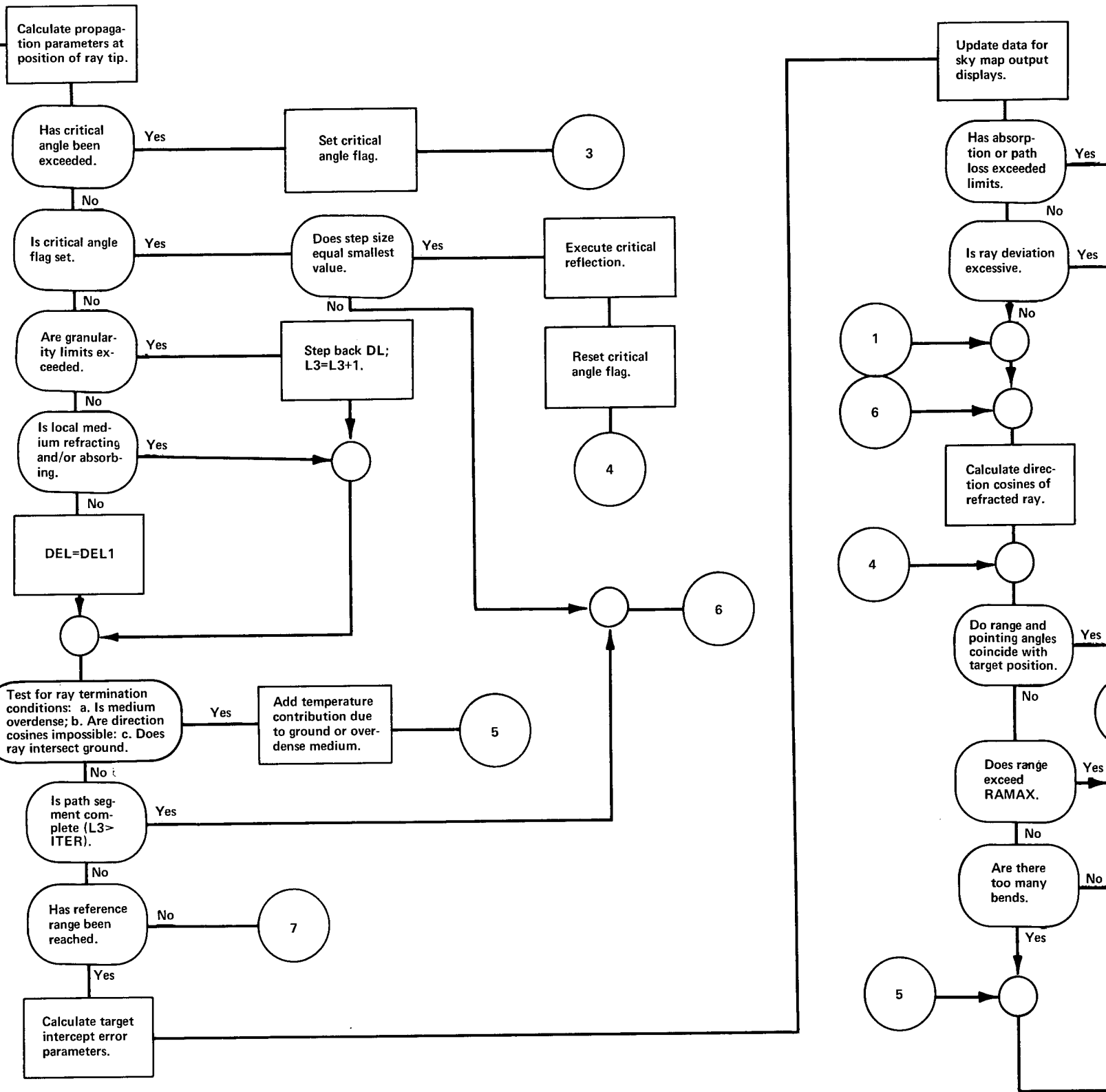
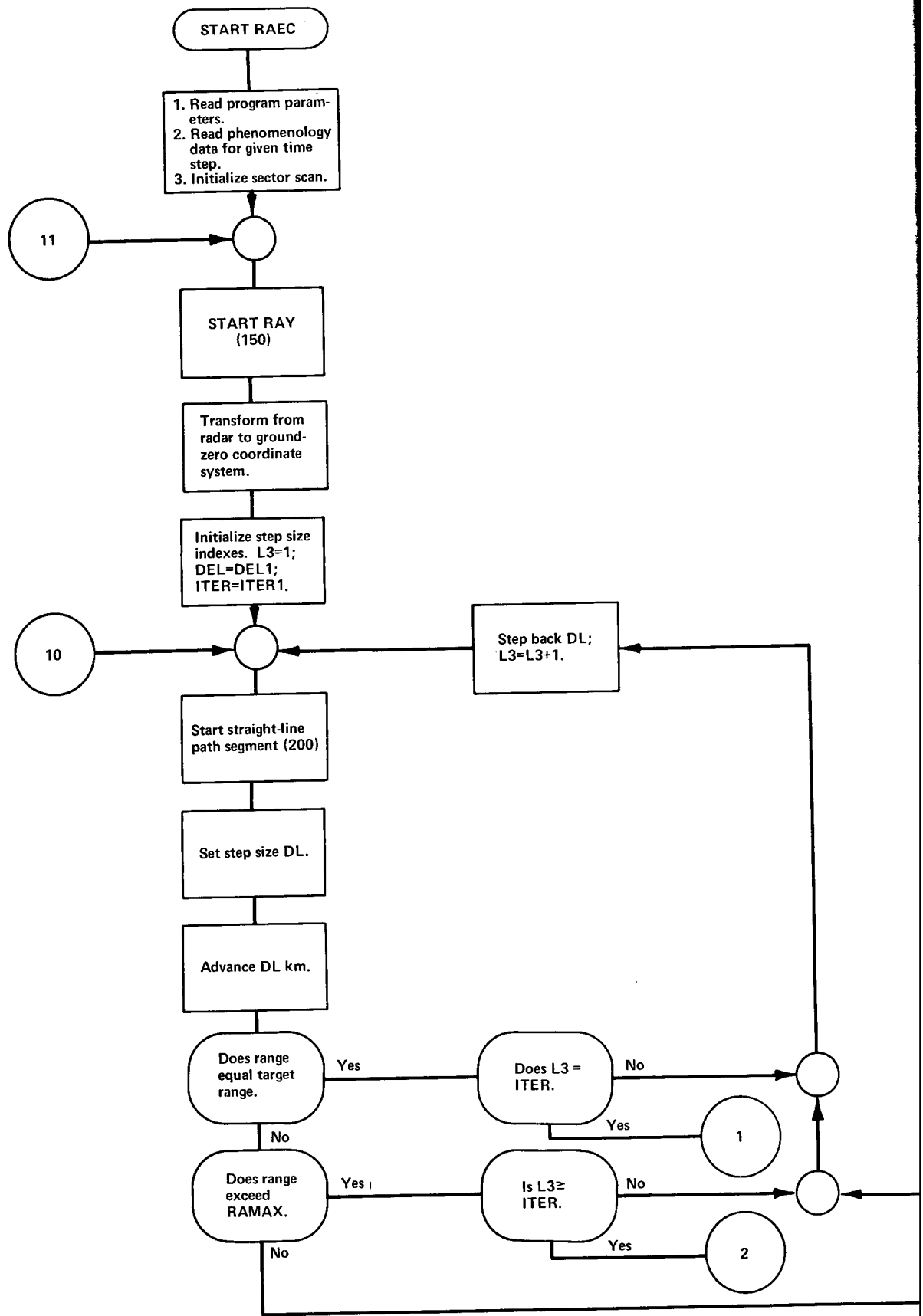
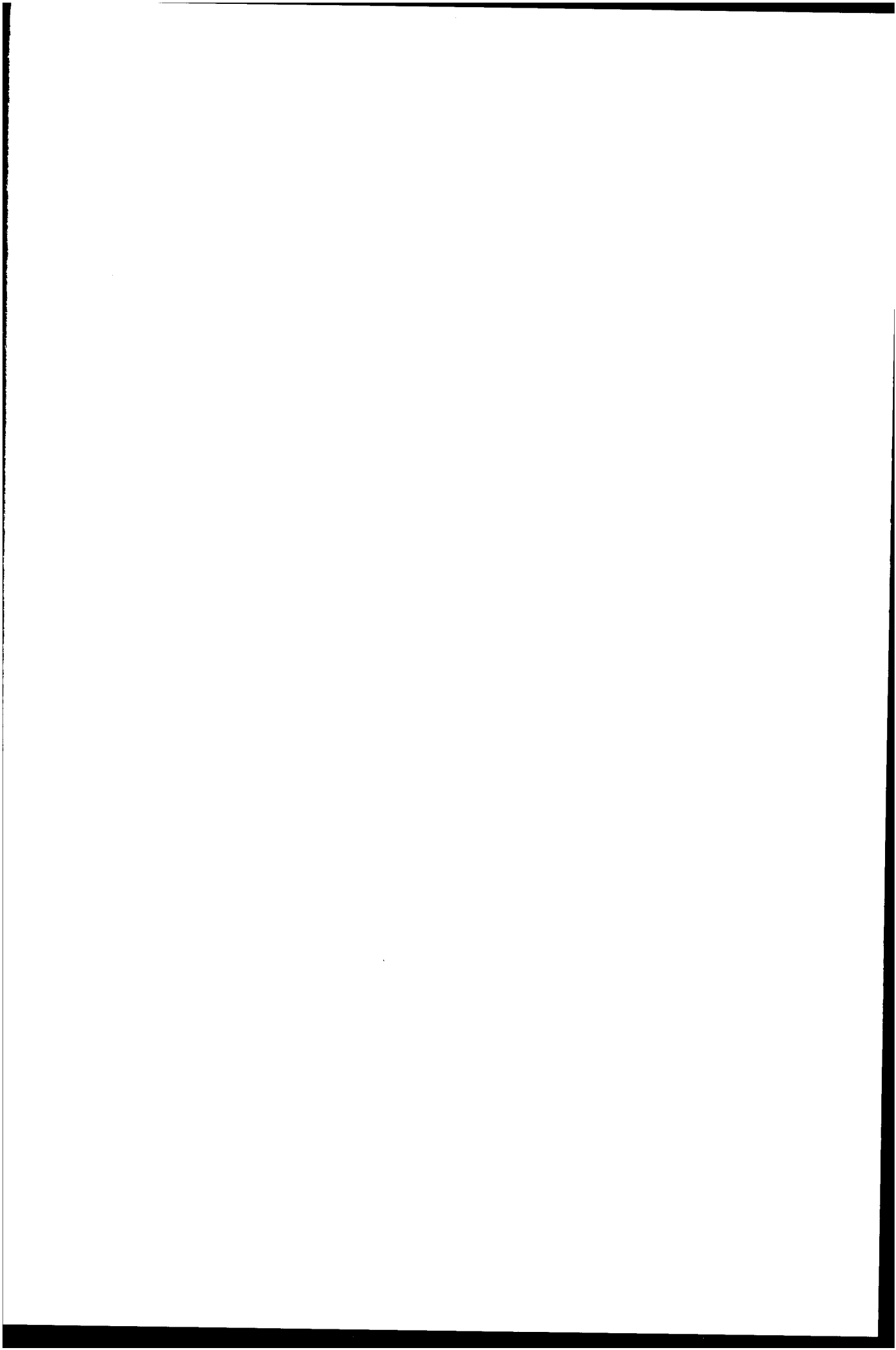


Fig. 1 - Logical flow diagram, RAEC







The Appleton-Hartree equation for the complex index of refraction η for a plane wave propagating within a magneto-ionic medium is

$$\eta^2 = 1 - \frac{X}{1 - iZ - \frac{Y_T^2}{2(1 - X - iZ)} \pm \sqrt{\frac{Y_T^4}{4(1 - X - iZ)^2} + Y_L^2}}, \quad (3)$$

where

$$X = (\omega_p/\omega)^2, \quad Y_L = \omega_{BL}/\omega, \quad Y_T = \omega_{BT}/\omega, \quad Z = \nu/\omega.$$

Here, ω_p is the electron plasma angular frequency, ω is the wave angular frequency, ν is the electron collision frequency for momentum transfer, and ω_{BT} and ω_{BL} are the electron gyroresonance angular frequencies associated, respectively, with the transverse and longitudinal components of the geomagnetic field.

For a geomagnetic field of typically 0.5 Gauss, the upper limit on ω_{BT} and ω_{BL} becomes about 10 mrad/sec and at radar frequencies above 100 MHz, one obtains $Y_L \ll 1$ and $Y_T \ll 1$. This means that an important simplifying approximation can be made, namely the neglect of magnetic effects. Even for magnetic field compressions as large as a factor of 10, an unlikely situation for times of interest, the approximation $\omega_B \ll \omega$ will still be valid.

With this simplification, the index of refraction reduces to

$$\eta^2 = 1 - \frac{X}{1 - iZ}, \quad (4)$$

where $\eta = \mu - i\chi$.

The real part of the refractive index μ , in conjunction with Snell's law, is used to calculate refraction. The complete expression for μ is

$$\mu^2 = \frac{1}{2(1 + Z^2)} \left\{ \left[(1 + Z^2 - X)^2 + (XZ)^2 \right]^{1/2} + 1 + Z^2 - X \right\}. \quad (5)$$

The absorption coefficient κ in nepers/km, is related to the imaginary part of the refractive index χ by

$$\kappa = \frac{\omega\chi}{c}.$$

χ can be expressed in terms of μ by

$$\chi = \frac{1}{2\mu} \frac{XZ}{1 + Z^2}, \quad (6)$$

and for two-way absorption,

$$\kappa = 1 \times 10^6 \frac{\omega X Z}{\mu c (1 + Z^2)} \text{ nepers/km}, \quad (7)$$

where

$$c = 3 \times 10^5 \text{ km/sec.}$$

To derive the group path as a function of refractive index, it is useful to express the group velocity V_g in its differential form

$$V_g = \frac{d\omega}{dK},$$

where K , the propagation constant $2\pi/\lambda$, is related to the real part of the refractive index μ by

$$K = \frac{\omega}{c} \mu.$$

Therefore, the group refractive index μ_g becomes

$$\mu_g = \frac{c}{V_g} = \frac{d}{d\omega} (\omega \mu) = \mu + \omega \frac{d\mu}{d\omega}. \quad (8)$$

The round-trip delay time measured for the radar pulse is given by

$$t = 2 \int_0^L \frac{ds}{V_g(s)},$$

where s is a position along the ray path and where V_g is assumed to vary along the path. As interpreted at the radar, the apparent target distance (or radar range) is calculated as

$$R' = \frac{ct}{2} = \int_0^L \mu_g(s) ds,$$

and for small path lengths δs the incremental radar range is given by

$$\delta R' = \mu_g \delta s.$$

After differentiating μ as given in Eq. (3) and rearranging terms, the derivative $d\mu/d\omega$ becomes

$$\frac{d\mu}{d\omega} = \frac{X}{(1+Z^2)^2} \cdot \frac{1}{4\mu A \omega} \left\{ 2(A+1) - X \left[Z^2 \left(1 + \frac{2}{1+Z^2} \right) + \frac{2}{1+Z^2} \right] \right\}, \quad (9)$$

where

$$A = \left\{ \left(\frac{XZ}{1+Z^2} \right)^2 + \left(1 - \frac{X}{1+Z^2} \right)^2 \right\}^{1/2}. \quad (10)$$

Apparent sky temperature at a particular frequency in a given direction is defined as the noise temperature sensed by a radio antenna of infinitesimal beamwidth looking in that direction. The apparent sky temperature is affected by all thermally radiating bodies in the field of view of the hypothetical antenna. This includes contributions from the atmosphere as well as from the background sky. The radiation from any given source is, of course, attenuated by absorption effects in the intervening medium. For frequencies of interest to radar, apparent source temperature is proportional (by the Rayleigh-Jeans law) to apparent source brightness, for which Kraus (8) gives an equation of transfer. Expressing the transfer equation in terms of temperature gives

$$dT(r) = -T(r) \alpha(r) dr + T_i(r) \alpha(r) dr, \quad (11)$$

where $T(r)$, $T_i(r)$, and $\alpha(r)$ are apparent sky temperature, propagation-medium temperature, and linear absorption coefficient, respectively, at position r . The solution is

$$T = T_{sky} \exp \left[- \int_0^\infty \alpha(r) dr \right] + \int_0^\infty \exp \left[- \int_0^r \alpha(r') dr' \right] T_i(r) \alpha(r) dr . \quad (12)$$

This is the form of equation utilized in the calculation of sky temperature with the exception that the linear absorption coefficient is expressed in terms of the voltage attenuation factor κ in nepers/km. The relationship is $\alpha = 2\kappa$.

The first term represents the contribution due to background sky T_{sky} , and the second term on the right-hand side of Eq. (10) represents the atmospheric contribution to apparent sky temperature. It should be emphasized that apparent sky temperature is not the same as the antenna temperature of any real antenna. For a real antenna, antenna temperature is the average of apparent sky temperature over its field of view with the antenna power pattern as the weighting function. Furthermore, antenna temperature usually includes contributions from the ground due to spillover of the illumination pattern onto the ground and due to ohmic losses in the antenna and feed structure. A treatment of the effects of ground radiation and sky temperature as a function of frequency may be found in Ref. 3, p. 48. The program assumes the background sky temperature to be spatially uniform. The value assigned to the variable T_{sky} is controlled by data card input.

Description of Subroutines

Subroutine BEND

Subroutine BEND calculates the direction cosines of the refracted (or reflected) ray. Eight quantities are needed for this calculation. These are the direction cosines of the incident ray: C1, C2, C3; the direction cosines of the electron density gradient: N1, N2, N3; and the indexes of refraction on either side of the slab boundary.

Figure 3 shows the geometry involved. The incident and refracted rays are defined by the unit vectors \bar{C} and \bar{R} , and the gradient by the unit vector \bar{N} . The vector representation of Snell's law is given by the expression

$$\frac{\bar{R} \times \bar{N}}{\bar{C} \times \bar{N}} = \frac{\text{INDEX 1}}{\text{INDEX 2}},$$

where the \times implies a vector cross product.

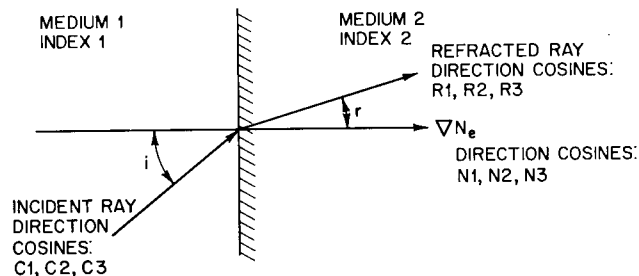


Fig. 3 - Geometry of the refraction calculation

Implicit in this expression is the coplanarity of the three unit vectors \bar{C} , \bar{R} , and \bar{N} . For convenience \bar{C}' is defined

$$\bar{C}' = \frac{\text{INDEX 1}}{\text{INDEX 2}} \bar{C}.$$

The first expression becomes

$$\bar{R} \times \bar{N} = \bar{C}' \times \bar{N}.$$

A solution for \bar{R} in terms of \bar{C} and \bar{N} may be obtained through the following vector manipulations:

$$\begin{aligned} \bar{N} \times (\bar{R} \times \bar{N}) &= \bar{N} \times (\bar{C}' \times \bar{N}) \\ \bar{R} (\bar{N} \cdot \bar{N}) - \bar{N} (\bar{N} \cdot \bar{R}) &= \bar{C}' (\bar{N} \cdot \bar{N}) - \bar{N} (\bar{N} \cdot \bar{C}') \\ \bar{R} &= \bar{C}' + \bar{N} (\bar{N} \cdot \bar{R}) - \bar{N} (\bar{N} \cdot \bar{C}') \\ \bar{R} &= \frac{\text{INDEX 1}}{\text{INDEX 2}} \bar{C} + \bar{N} \left[(\bar{N} \cdot \bar{R}) - \frac{\text{INDEX 1}}{\text{INDEX 2}} (\bar{N} \cdot \bar{C}) \right]. \end{aligned} \quad (13)$$

The incident angle i is defined by $\cos i = \bar{N} \cdot \bar{C} = \sum_{i=1}^3 N_i C_i$. It is calculated in Subroutine TEST as ARGIN and passed to BEND through the calling sequence. The reflected angle r ($\cos r = \bar{N} \cdot \bar{R}$) is related to i through the scalar form of Snell's law:

$$\sin r = \frac{\text{INDEX 1}}{\text{INDEX 2}} \sin i. \quad (14)$$

Equations (11) and (12), along with the calculated value for ARGIN ($\bar{N} \cdot \bar{C}$), are employed in the subroutine to calculate the components of \bar{R} , the refracted ray vector. In the case where $i = 0$, ARGIN = 1, and a bypass loop is provided to set the components of the "refracted" ray equal to those of the incident ray.

Also included in BEND are tests to sense the presence of an overdense medium ($WPE > WR$) and to sense the condition for total reflection. Where an overdense medium is encountered, a flag variable RKK is set equal to 25 and a diagnostic is printed. The total reflection calculation is accompanied by printer message which specifies the grazing angle of the incident ray on the reflecting boundary.

A flow diagram for Subroutine BEND is given in Fig. 4.

Subroutine COLLF

Values for the effective electron collision frequency for momentum transfer are derived from Subroutine COLLF and are subsequently used in the absorption calculation. Prior to the actual calculation, the plasma frequency and electron temperature from the phenomenology input are compared to values provided by the model atmosphere at the same altitude. The larger of these quantities is retained for the collision frequency calculation. The altitude RA of the point defined by the coordinates X, Y, Z is obtained through a call to the Subroutine TRANS. Also calculated by TRANS are the direction cosines of electron-density gradient for a vertically varying model atmosphere. The correct signs for the direction cosines are established in COLLF through two calls to the model atmosphere.

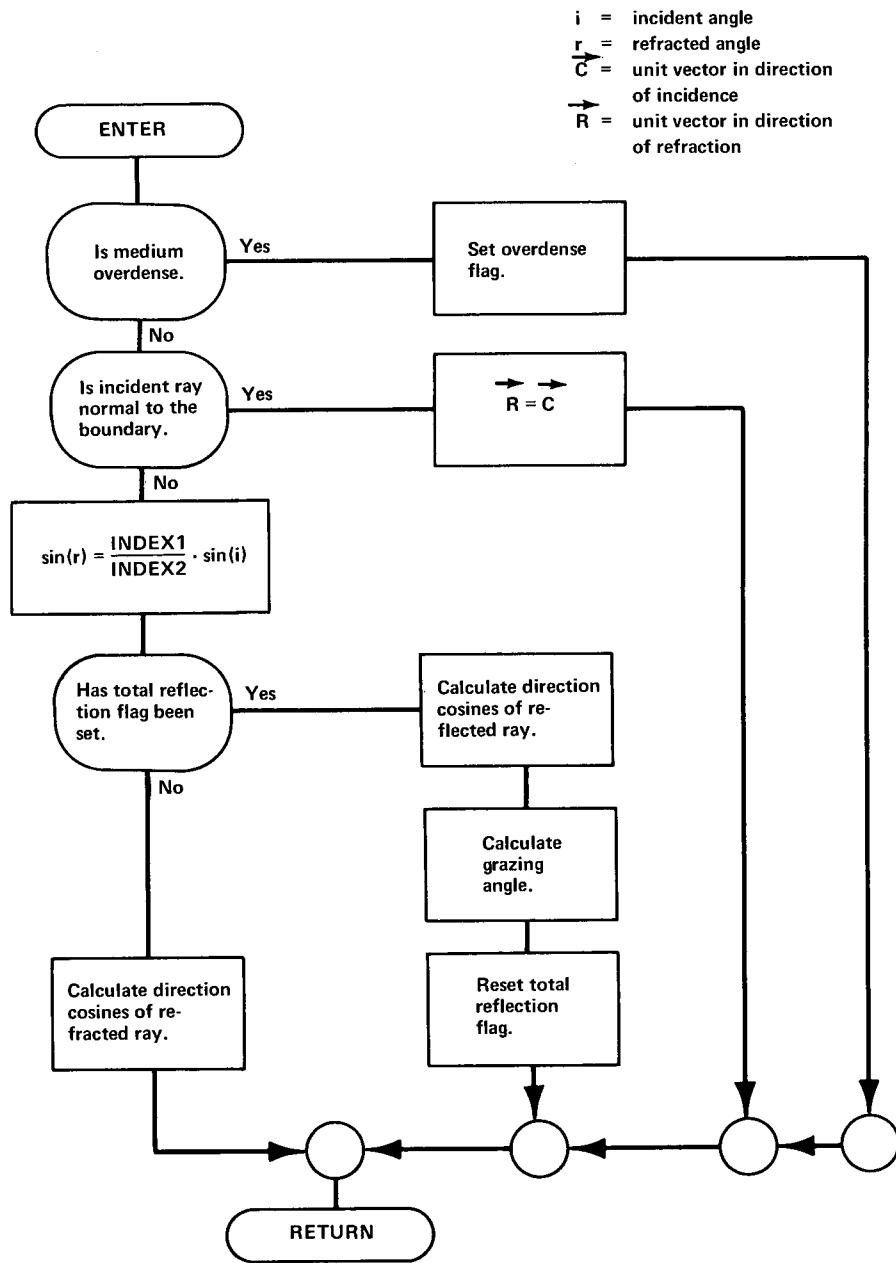


Fig. 4 - Subroutine BEND

Plasma frequencies supplied by the phenomenology input are transformed to electron densities. Input temperatures in electron volts are transformed to degrees Kelvin. These steps are taken before the comparison with equivalent values in the model atmosphere. The value of electron density selected is retransformed back to plasma frequency WPE, and it and the associated direction cosines are retained for later use in other parts of the program.

The electron-ion collision frequency is calculated from the electron density and temperature by using the analytical expression given by Shkarofsky (6). (See Appendix A.) Electron-neutral collision frequencies for N_2 , O_2 , and O are obtained from the results of numerical integrations by Hochstim (7,9) (see Appendix A) for temperatures between 200 and 2000°K. The corresponding values of $G(T)$ ($= \nu_{e-N_i}(T) \times 10^{-8}/N_i$) are included in the subroutine; interpolated values are obtained through a call to Subroutine INTERP. Beyond this temperature range, a simple power-law extrapolation is used. The effective collision frequency NUCOLL is the sum of the electron-ion component NUEI and an electron-neutral component NUEM. The collision frequency is returned through the calling sequence in units of mega-collisions per second.

A flow diagram illustrating the operation of Subroutine COLLF is given in Fig. 5.

Subroutine DGROUP

Subroutine DGROUP calculates the group refractive index for the propagation medium using the standard form (10)

$$\mu_g = \mu + \omega \frac{d\mu}{d\omega},$$

where μ_g = group refractive index

μ = phase refractive index

ω = radar angular frequency in radians per second.

The group refractive index is assumed to be unity throughout the troposphere, and in the ionosphere it is calculated by assuming that the phase refractive index is well represented by the Appleton-Hartree relation simplified to the case of negligible magnetic field effects. The expressions used for μ and $d\mu/d\omega$ are otherwise exact, incorporating no assumption of nondeviative absorption. The equations defining μ and $d\mu/d\omega$ are

$$\mu^2 = 1/2 \left(\frac{1 - X + Z^2}{1 + Z^2} \right) \left(\sqrt{\frac{X^2 Z^2}{1 - X + Z^2} + 1} - 1 \right),$$

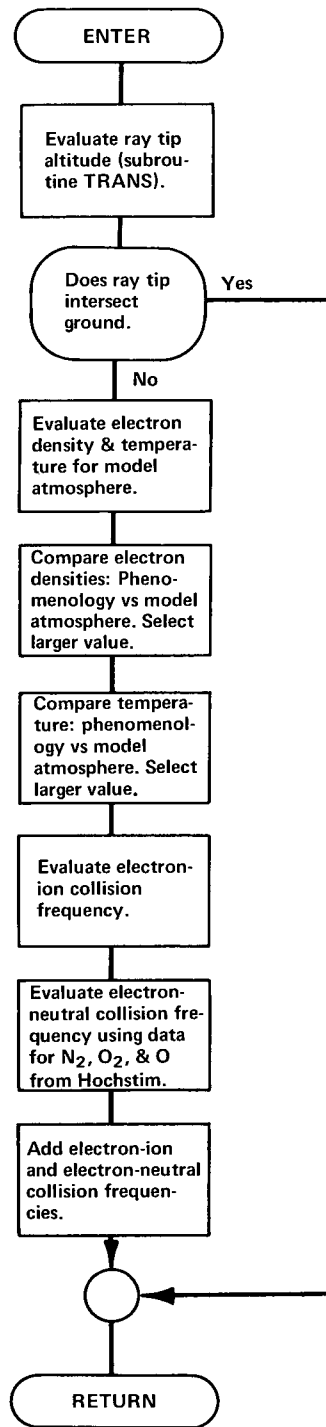
$$\frac{d\mu}{d\omega} = \frac{XF^2}{4\mu\omega A} [2(1 + A) - X(Z^2(1 + 2F) + 2F)],$$

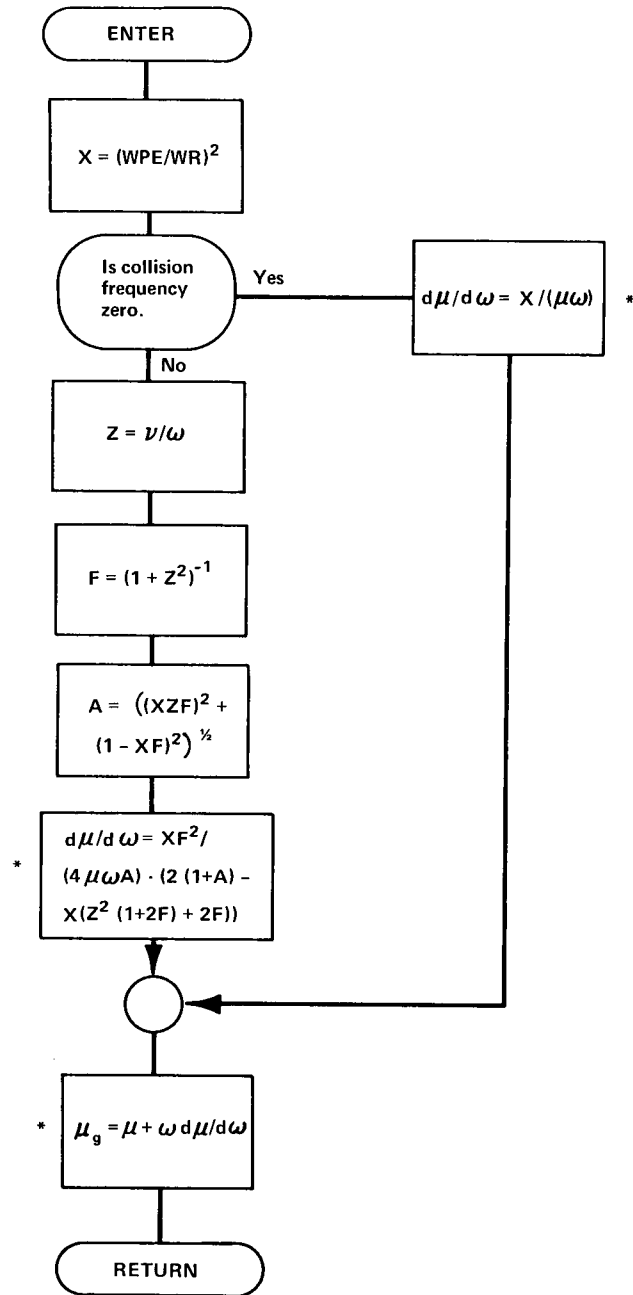
$$Z = \nu/\omega$$

$$F = 1/(1 + Z^2)$$

$$A = [(XZF)^2 + (1 - XF)^2]^{1/2},$$

Fig. 5 - Subroutine COLLF





* μ is available from a prior calculation in subroutine REFRAC and is passed to DGROUP.

Fig. 6 - Subroutine DGROUP

where ω_p = plasma frequency of the medium

ω = radar angular frequency

ν = effective collision frequency as defined by Shkarofsky (6)

$X = (\omega_p/\omega)^2$.

A flow diagram for the subroutine is shown in Fig. 6.

Subroutine GEOM

Subroutine GEOM performs a calculation of various geometric quantities which are pertinent to the target location problem. The relevant geometry is shown in Fig. 7. Quantities required for this calculation are the direction cosines of initial pointing of the ray path from radar to target (C10, C20, C30), the true position of the ray tip in the radar coordinate system (XB, YB, ZB), the true range to the ray tip (DIST1), and the radar range to the ray tip (RGRP). Quantities calculated are radar range error (RERROR), target miss distance (DISMIS), and radar angle error (AERROR). Equations used in the calculations are

$$RERROR = RGRP - DIST1,$$

$$DISMIS = (PRX - XB)^2 + (PRY - YB)^2 + (PRZ - ZB)^2,$$

$$AERROR = \cos^{-1} [(DIST1)^2 + (RGRP)^2 - (DISMIS)^2 \cdot (2 \cdot DIST1 \cdot RGRP)],$$

where

$$PRX = RGRP \cdot C10$$

$$PRY = RGRP \cdot C20$$

$$PRZ = RGRP \cdot C30.$$

The calculation presumes that the true target position is on the ray path, and that the antenna pointing direction correctly gives the initial ray direction. In other words, error due to finite antenna beamwidth or to boresighting error is not considered here. The quantities selected as error variables represent the errors entailed in specifying the position of a detected target. The subroutine is sufficiently straightforward that a flowchart is not considered necessary.

A proper treatment of the target engagement problem would require that the error quantities be calculated when the prescribed target position coincides with the ray tip. This is not the procedure which is followed because the true angle from the radar to the ray tip is not an input variable in the calculation. It is one of the output variables. The input variables corresponding to a specified true direction of the target (ray tip) can be found only by an iterative procedure, which is time consuming. Therefore, the radar location errors are calculated when the range to the ray tip (DIST1) equals the prescribed target range and when the initial pointing direction of the ray is in the true target direction. If the ray path to the target does not undergo severe refraction, location errors calculated in these two different ways will not be very different.

Subroutine PRELDA (Entry PRELP)

The initial version of Subroutine PRELDA was developed in the Plasma Physics Division. It provides the interface between the phenomenology codes and the radar propagation program. Data describing the spatial distribution of electron density and temperature, at a selected time step, are read from magnetic tapes in the form of arrays.

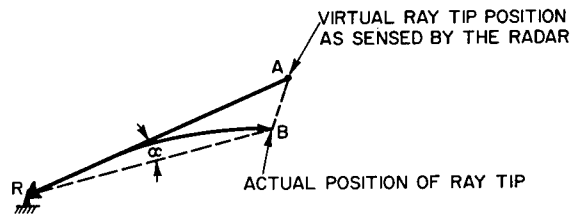


Fig. 7 - Geometry for target location

\overline{RA} ≡ "GROUP" RANGE TO THE RAY TIP ≡ RGRP
 \overline{RB} ≡ TRUE RANGE TO THE RAY TIP ≡ DIST 1
 \overline{AB} ≡ RADAR MISS DISTANCE ≡ DISMIS
 α ≡ RADAR POINTING ERROR ≡ AERROR

The array indexes correspond to spatial coordinates centered on ground zero, and the data are specified at discrete positions corresponding to the array lattice points.

A two-dimensional, third-order, Lagrangian interpolation is performed on the data arrays to yield values for the desired quantities and their gradients at the current position of the ray tip.* These quantities are used in the propagation program for calculation of the real and imaginary parts of the refractive index and for calculation of collision frequencies. The interpolation is done in PRELP, which is an entry point in Subroutine PRELDA.

The radar angular frequency WR is passed to PRELP through the calling sequence. A comparison between WR and WPE is made early in the routine. If an overdense condition prevails, WPE is set to -1 and control is immediately returned to the calling program, thus bypassing an unnecessary calculation of gradients and direction cosines.

The coordinate system used for phenomenology calculations is either spherical for one-dimensional (1-D) codes or cylindrical (2-D) codes. A coordinate transformation converts to the Cartesian coordinate system used in the propagation program.

Subroutine REFRAC

Subroutine REFRAC calculates the real and imaginary parts of the refractive index as specified by the Appleton-Hartree expression as well as the two-way absorption coefficient κ (see Eqs. 2 through 5 in the section on Propagation Expressions). A flowchart showing the program organization is given in Fig. 8.

Subroutine RFRAC2

The altitude dependence of the tropospheric refractive index is determined in this routine by a simple analytical expression† (3):

$$\eta = 1 + (N_s \times 10^{-6}) e^{-\gamma h}.$$

In this equation h is altitude and γ is a scale factor. N_s is the surface (zero-altitude) refractivity. The expression assumes a simple exponential atmosphere with inverse scale

*Since electron density changes by several orders of magnitude at the edge of the phenomenology region, it was found that interpolation errors could be quite severe. This was corrected by performing the interpolation on the logarithm of the electron density. This change does not appear in the listing for Subroutine PRELDA supplied with this report.

†CRPL exponential reference atmosphere.

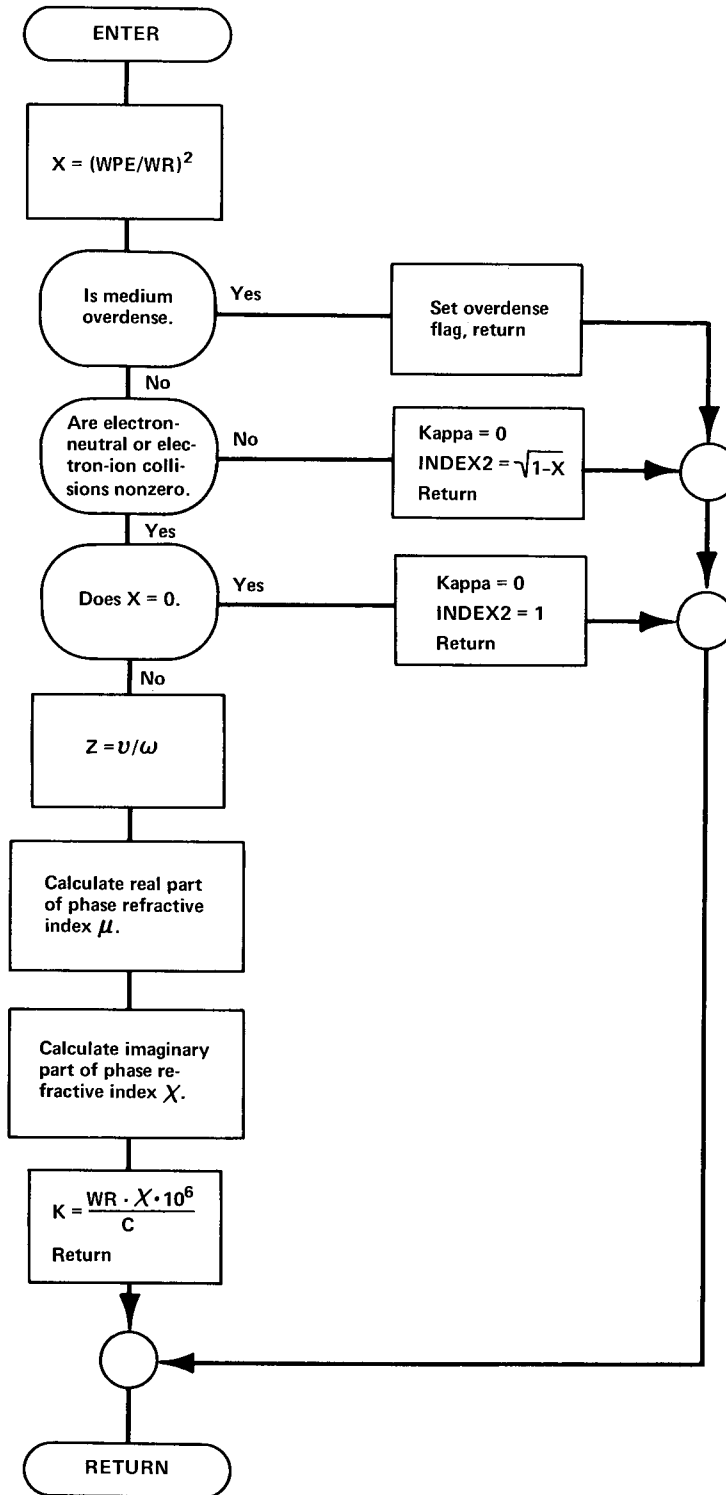


Fig. 8 - Subroutine REFRAC

height γ . Computations are carried out for a conventional value of 313 for N_s and a value for γ of 0.14386/km.

Subroutine TEST

Subroutine TEST plays a major role in controlling the details of the ray-tracing procedure. After each step in the construction of a straight-line segment of the ray path, TEST is called to investigate whether granularity limits have been exceeded and, if so, to select the subsequent step size.

On the basis of various criteria in TEST, flags are set which control the ray-tracing step size and, indirectly, the access to the refraction subroutine, BEND. Calculations made in TEST depend upon phenomenology data acquired via Subroutine PRELDA and the interpolation Subroutine PRELP. Additional data relating to the ambient atmosphere are obtained from other subroutines which define a model atmosphere.

In addition TEST performs several important sensing functions upon which the fate of the ray is dependent. Among these are

1. Intersection of ray with ground — results in ray termination.
2. Altitude less than 30 km — invokes tropospheric model for calculation of propagation factors.
3. Overdense region ($WPE > WR$) — terminates ray.
4. Critical reflection — sets a flag which initiates a modified stepping routine in the vicinity of the total reflection region.

TEST depends upon calls to Subroutines COLLF, REFRAC, DGROUP, RFRAC2, and TROPAT for the calculation of the necessary propagation variables. A flow diagram describing the logical flow of Subroutine TEST is shown in Fig. 9.

Subroutine TRANS

The TRANS Subroutine has two purposes. The first is to calculate the altitude above the earth for the point X, Y, Z in the phenomenology coordinate system. The second is to calculate the direction cosines of the electron-density gradient in a spherically stratified model atmosphere. The direction cosines are subsequently used in the refraction calculation if the model-atmosphere electron density is greater than the phenomenology-derived value.

Figure 10 shows the geometry involved. The point X, Y, Z is located at an altitude RA. The radius of the earth is given by RE. The horizontal distance R_0 is defined by the expression

$$R_0^2 = X^2 + Y^2.$$

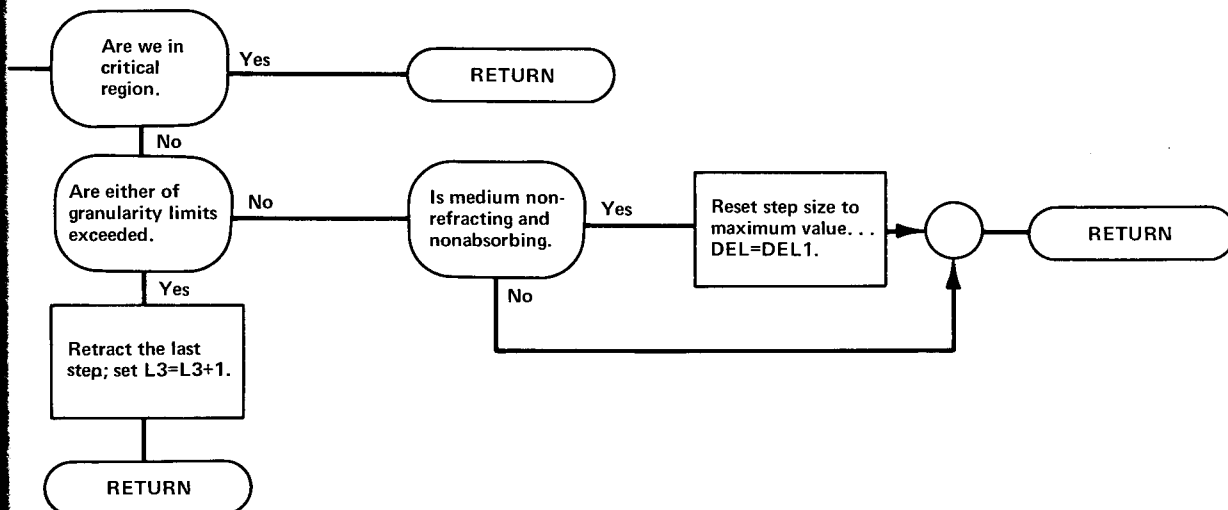
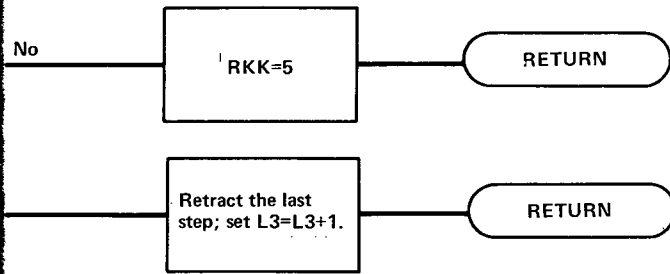
These quantities are related by the equation

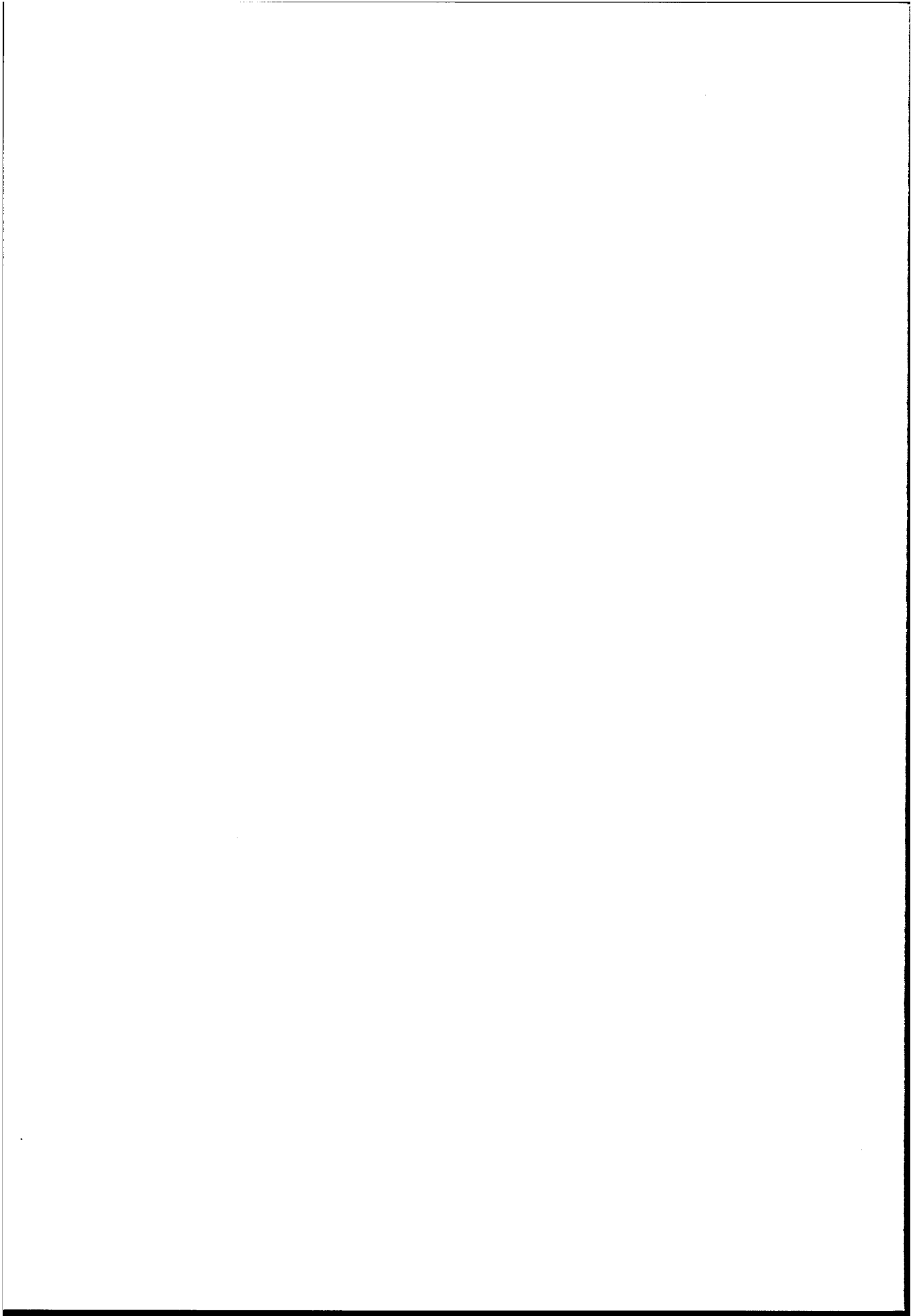
$$(RA + RE)^2 = R_0^2 + (RE + Z)^2.$$

Solving for the altitude gives

$$RA = [X^2 + Y^2 + (RE + Z)^2]^{1/2} - RE.$$

A value for RE of 6371.2 km has been adopted.





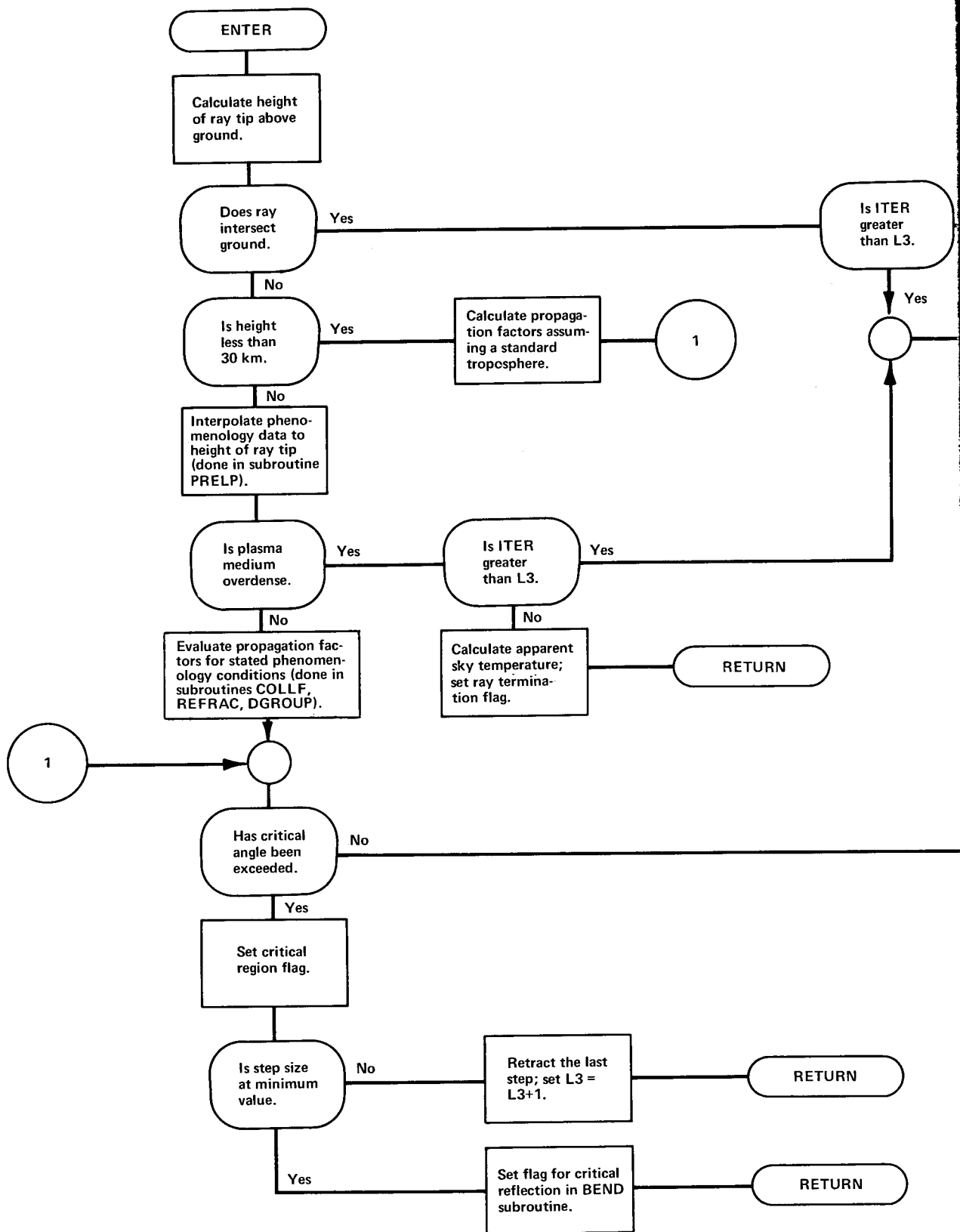
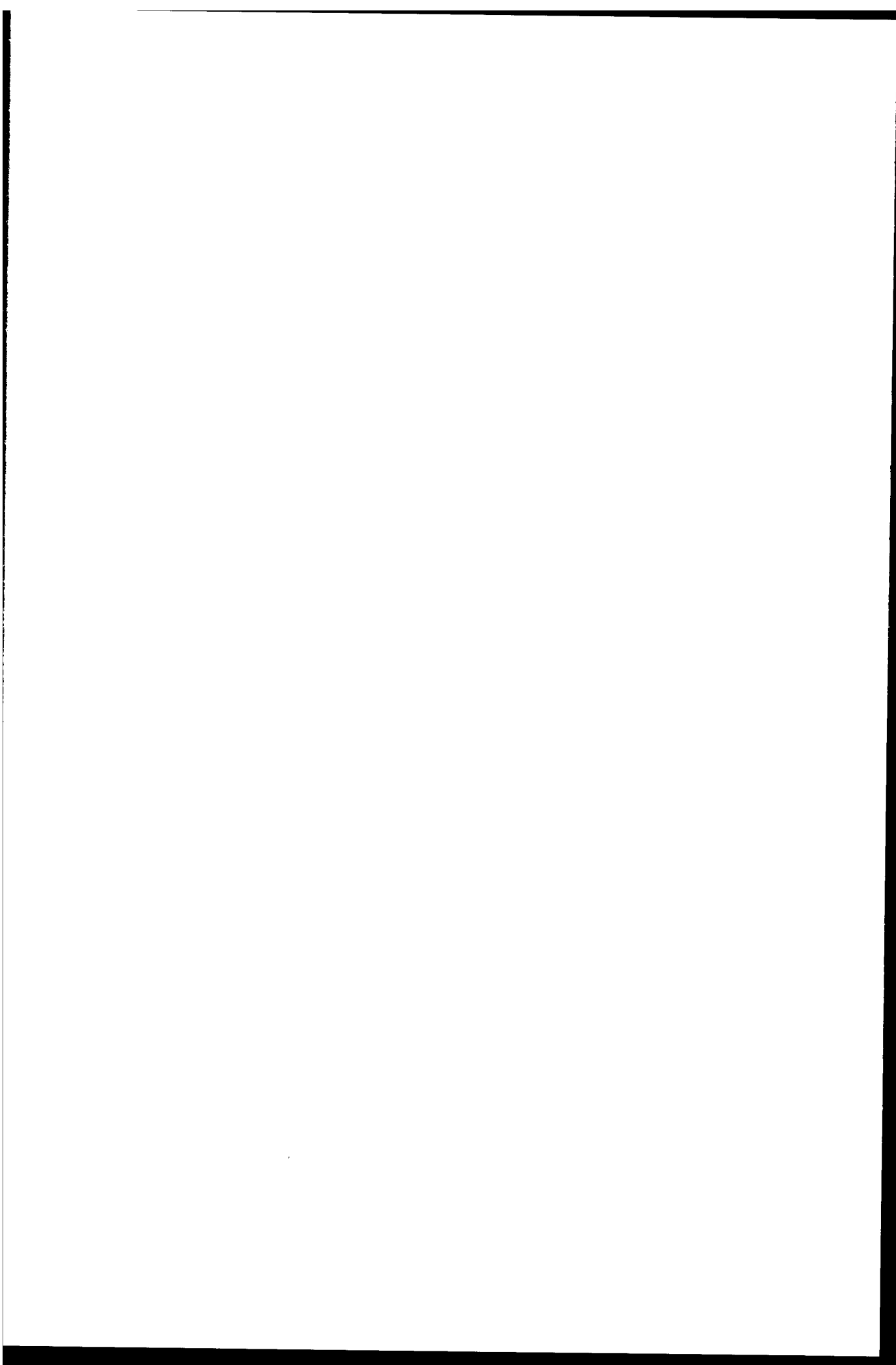


Fig. 9 - Subr



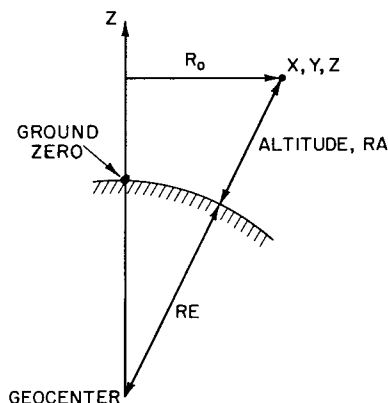


Fig. 10 - Spherical earth geometry

The direction cosines of the (vertical) electron-density gradient are identical to those of the vector from the geocenter to the point (X, Y, Z) . They are given by

$$N_1 = X/Q,$$

$$N_2 = Y/Q,$$

$$N_3 = Z/Q,$$

where

$$Q = [X^2 + Y^2 + (Z + RE)^2]^{1/2}.$$

Subroutine TROPAT

Subroutine TROPAT determines the two-way signal attenuation due to absorption within the troposphere. Results from a series of computations carried out by Blake (3) form the basis of the tropospheric absorption calculations. Selected values of signal attenuation have been included in the subroutine as a two-dimensional array with indexes depending on antenna elevation angle and frequency. The range in frequency is 100 MHz to 10 GHz. In elevation angle, the range is 0 to 10 deg. Above 10 deg the attenuation is assumed zero. (It is actually about 0.5 dB at 10 deg and 10 GHz, and less at higher angles and lower frequencies.)

A two-dimensional linear interpolation is used to derive the correct value for attenuation. The frequency interpolation is carried out once for the entire program. The elevation-angle interpolation is performed for each ray unless elevation is greater than 10 deg, whereupon ATTRO, the attenuation, is set to zero. Errors arising from tabular interpolation and in employing the data array are less than 0.5 dB.

Implicit in this treatment is the assumption that ionization effects and targets to be tracked lie outside the major portion of the troposphere. This is likely to be a valid assumption, since two scale heights for the troposphere correspond to only 15 km, an altitude below which detection and tracking of targets is not likely to be of interest.

Subroutines XCOORD, BACOR, XDRCOS

The purpose of Subroutine XCOORD is to transform points within a rectilinear coordinate system located at the radar to a similar coordinate system centered at ground zero. The ground-zero point is an essential reference point for all phenomenology

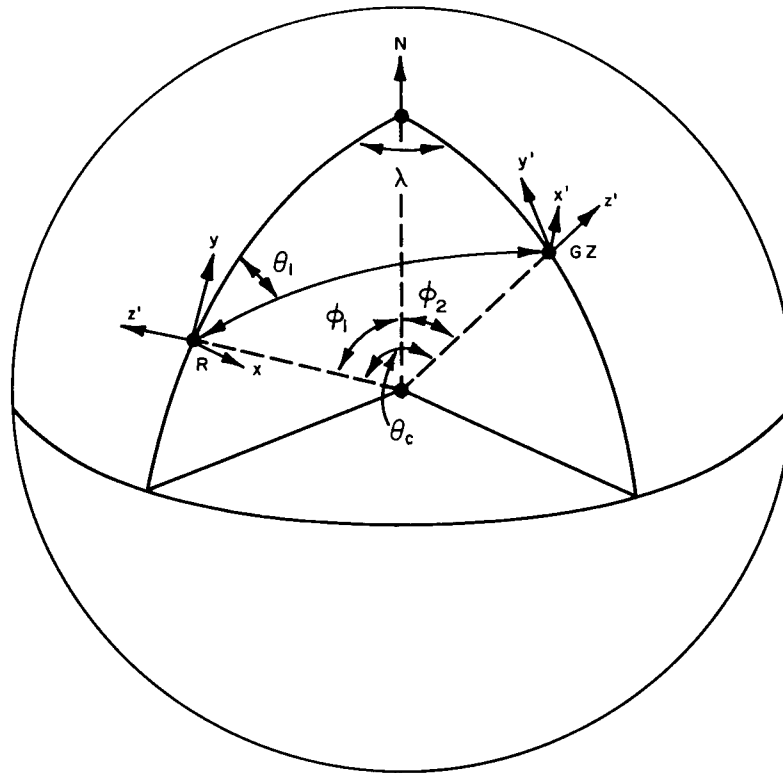


Fig. 11 - Coordinate transformation geometry

calculations. Subroutine BACOOR performs essentially the inverse of the XCOORD transformation and will not be treated in detail here. Subroutine XDRCOS transforms the components of a vector in the radar coordinate system to the corresponding components in the ground-zero coordinate system.

The relevant geometry is shown in Fig. 11. Locations for the radar and ground zero are represented by points R and GZ, respectively. In both systems the Z axis is vertical, the Y axis is directed north, and the X axis points east. Since the origins of both systems lie on the same spherical surface—namely the earth's surface—they can be algebraically related to each other via an earth-centered colatitude-longitude system. The transformation is accomplished by separate steps of translation and rotation. The known or input quantities are the range to ground zero from the radar R; the colatitude of the radar ϕ_1 ; the longitude difference λ between radar and ground zero; and the bearing or azimuthal angle θ_1 to ground zero measured clockwise from north at the radar. For these calculations terrestrial oblateness is ignored.

Figure 11 shows that the angle subtended at the center of the earth by the ground range from radar to ground zero is given by

$$\theta_c = R/RE,$$

where θ_c is given in radians and RE is the radius of the earth. The chord subtended by this angle is given by,

$$\text{Ch} = 2RE \sin (\theta_c/2),$$

and the coordinates of ground zero in the radar coordinate system (X_0B, Y_0B, Z_0B) are given by

$$\begin{aligned} X_0B &= (Ch \sin \theta_1) \cos (\theta_c / 2) \\ Y_0B &= (Ch \cos \theta_1) \cos (\theta_c / 2) \\ Z_0B &= (Ch \sin) (\theta_c / 2) . \end{aligned}$$

The coordinates of a point (X, Y, Z) in the radar coordinate system, expressed in the ground-zero coordinate system (X_T, Y_T, Z_T) , are

$$\begin{aligned} X_T &= X - X_0B \\ Y_T &= Y - Y_0B \\ Z_T &= Z + Z_0B . \end{aligned}$$

The proper rotations to orient the translated grid can be found from an examination of Fig. 11. First, a rotation is made through ϕ , the polar angle of the radar; second, a rotation through λ , the difference in longitude between radar and ground zero (GZ), is carried out; and finally, a rotation is made through ϕ_2 , the colatitude of ground zero. This colatitude ϕ_2 is determined using the law of cosines

$$\phi_2 = \cos^{-1} (\cos \phi_1 \cos \theta_c + \sin \phi_1 \sin \theta_c \cos \theta_1) .$$

The rotations can then be represented by the following three matrixes:

$$\begin{aligned} S_1 &= \begin{pmatrix} 1 & 0 & 0 \\ 0 & \cos \phi_2 & \sin \phi_2 \\ 0 & -\sin \phi_2 & \cos \phi_2 \end{pmatrix} \\ S_2 &= \begin{pmatrix} \cos \lambda & \sin \lambda & 0 \\ -\sin \lambda & \cos \lambda & 0 \\ 0 & 0 & 1 \end{pmatrix} \\ S_3 &= \begin{pmatrix} 1 & 0 & 0 \\ 0 & \cos \phi_1 & -\sin \phi_1 \\ 0 & \sin \phi_1 & \cos \phi_1 \end{pmatrix} . \end{aligned}$$

The entire transformation in matrix form is given by

$$\begin{pmatrix} X' \\ Y' \\ Z' \end{pmatrix} = (S_1) \cdot (S_2) \cdot (S_3) \cdot \begin{pmatrix} X_T \\ Y_T \\ Z_T \end{pmatrix} .$$

The algebraic expressions resulting from this matrix multiplication are

$$\begin{aligned} X' &= X_T \cos \delta + Y_T \sin \delta \cos \phi_1 - Z_T \sin \delta \sin \phi_1 \\ Y' &= -X_T \cos \phi_2 \sin \delta + Y_T (\cos \phi_2 \cos \delta \cos \phi_1 + \sin \phi_1 \sin \phi_2) \\ &\quad - Z_T (\cos \phi_2 \cos \delta \sin \phi_1 - \sin \phi_2 \cos \phi_1) \end{aligned}$$

$$Z' = X_T \sin \phi_2 \sin \delta - Y_T (\sin \phi_2 \cos \delta \cos \phi_1 - \cos \phi_2 \sin \phi_1) \\ + Z_T (\sin \phi_2 \cos \delta \sin \phi_1 + \cos \phi_2 \cos \phi_1),$$

where

$$\sin \delta = \sin \theta_c \sin \theta_1 / \sin \phi_2.$$

For Subroutine BACOOR the inverse transformation can be obtained by reversing the order of rotations;

$$X_R = X' \cos \delta - Y' \sin \delta \cos \phi_2 + Z' \sin \delta \cos \phi_2 \\ Y_R = X' \cos \phi_1 \sin \delta + Y' (\cos \phi_1 \cos \delta \cos \phi_2 + \sin \phi_1 \sin \phi_2) \\ - Z' (\cos \delta \cos \phi_1 \sin \phi_2 - \sin \phi_1 \cos \phi_2) \\ Z_R = X' \sin \phi_1 \sin \delta - Y' (\sin \phi_1 \cos \delta \cos \phi_2 - \cos \phi_1 \sin \phi_2) \\ + Z' (\cos \delta \sin \phi_1 \sin \phi_2 + \cos \phi_1 \cos \phi_2),$$

and making the translation

$$X = X_R + XB$$

$$Y = Y_R + YB$$

$$Z = Z_R - ZB.$$

Subroutine XDRCOS transforms the coordinates of a vector from the radar to the ground-zero coordinate system. It involves the same rotations as described in Subroutine XCOORD. The transformation equations are

$$\begin{pmatrix} C_1' \\ C_2' \\ C_3' \end{pmatrix} = (S_1) \cdot (S_2) \cdot (S_3) \begin{pmatrix} C_1 \\ C_2 \\ C_3 \end{pmatrix},$$

where the unprimed C's define the direction cosines of the vector in the radar coordinate system and the primed values are the corresponding quantities in the ground-zero coordinate system.

Miscellaneous Subroutines

Subroutine CONTR

Subroutine CONTR does the actual conversion of the sky-map array to a coded line-printer display. CONTR is responsible for providing all heading, coordinate, and legend data relevant to a given display.

Subroutine INIT

Subroutine INIT initializes all of the sky-map arrays by assigning a hollerith character, equivalent to a blank, to all elements of the arrays.

Subroutine INTERP

Subroutine INTERP performs a linear interpolation. It is called from Subroutine COLLF for interpolation of G-values from tabular data in the COLLF routine. It is also called from MODATM to perform a similar interpolation on the model atmosphere-ionosphere data.

Subroutine MODATM

Subroutine MODATM furnishes values for electron temperature, electron density, and neutral-species number densities (e.g., O₂, N₂, O) based on an atmospheric model which has been entered via a data statement (Appendix B). These data are subsequently used in calculations of collision frequency and refractive index when not overridden by nuclear phenomenology inputs.

Subroutine POSIT

Subroutine POSIT adjusts the position of the sky-map display so that it is centered about an azimuth AZERO (a data-input parameter) and such that the smallest elevation angle displayed corresponds to the smallest elevation angle scanned.

Subroutine SHDRAY

Subroutine SHDRAY is called for the purpose of preparing arrays used in the construction of sky maps for the various propagation and target-location parameters of interest. Inputs are the array name, the value of the parameter at the reference range, the value of the parameter limit, the azimuth and the elevation of the initial pointing direction of the ray, and the number code for the reference range. The subroutine compares the parameter value with its limit. If the parameter exceeds the limit, the array element at the given azimuth and elevation is assigned the value of the range code. Otherwise, the element value remains at its initialized value.

Subroutine SUMARY

Subroutine SUMARY presents summary data for each ray (up to 200 rays) which has been abnormally terminated. It is called by Subroutine CONTR. The data printed include the reason for termination and the range at termination, as well as the important propagation and target-location parameters.

Program Structure

A diagrammatic representation of the program structure is given in Fig. 12. This chart is intended to show subroutine interrelationships at a glance and will be helpful in understanding the operation of the program. All subroutines, as well as the main program, have been included; lines connecting the routines indicate the origins and terminations of calling instructions. The ordering of subroutines (top to bottom) has been arranged to reflect the approximate order in which they are first called from the subroutine responsible for the call instruction. It should be noted that subroutines BACOR and INTERP have more than one origin and that PRELP as called from TEST is in reality an entry point to Subroutine PRELDA.

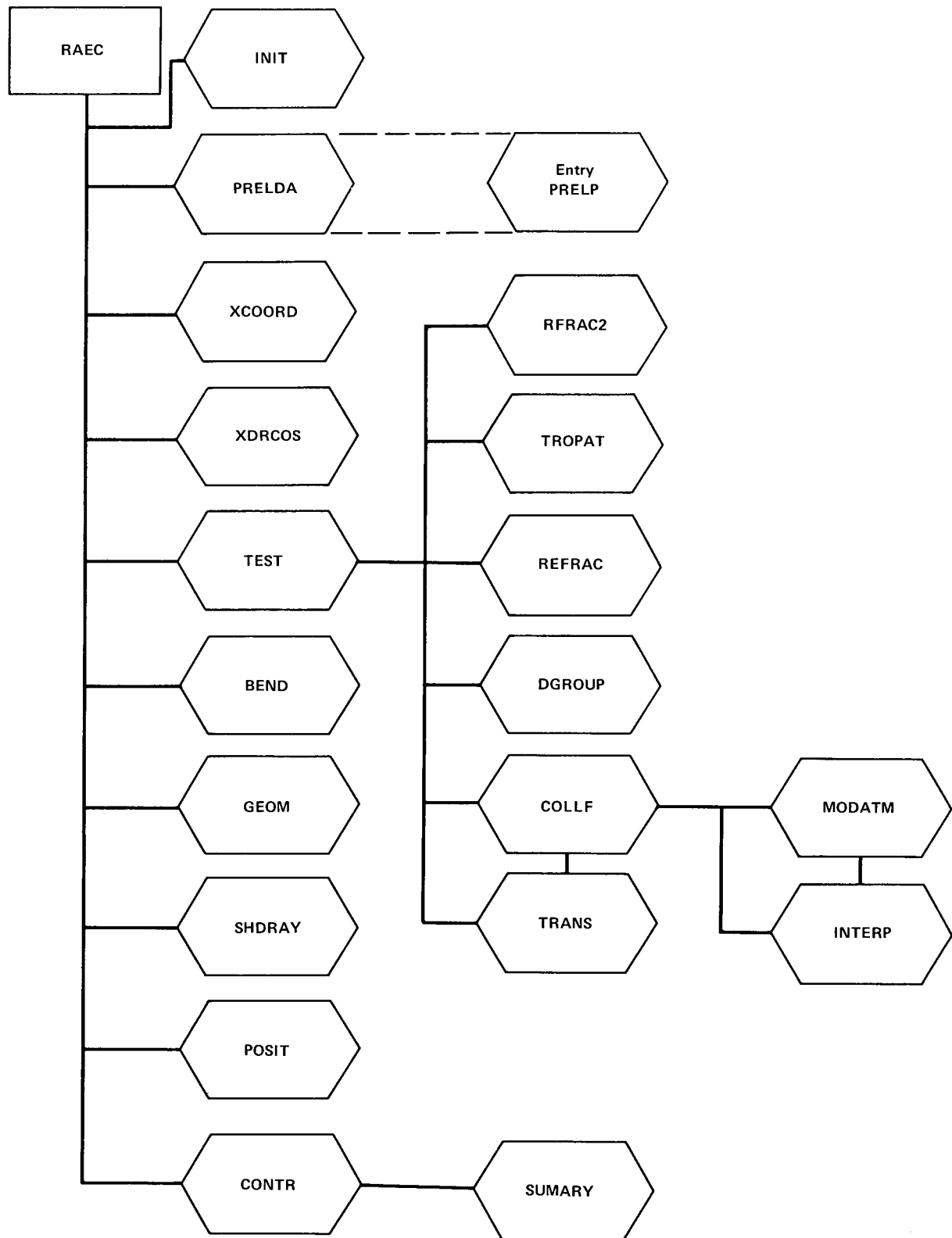


Fig. 12 - Subroutine connection diagram

TEST RUNS AND PRELIMINARY RESULTS

Description of Burst-Region Model

The RAEC program is designed to extract data on the propagation environment from phenomenology tapes which define the important physical variables at discrete points on a three-dimensional space lattice. For simplicity in testing, a fictitious analytical model of the propagation environment was employed. This avoided interface problems with the phenomenology tapes and also permitted operation on the NRL CDC-3800 computer, a convenience in terms of computer turnaround time during debugging.

The model chosen for enhanced electron density and temperature was defined by ellipsoidal surfaces of constant density and temperature, with a gaussian radial variation. The defining equations are

$$C(x, y, z) = \exp \left[- \frac{(x^2 + y^2)}{L_h^2} - \frac{(z - z_0)^2}{L_v^2} \right]$$

$$N(x, y, z) = N_0 C(x, y, z)$$

$$T(x, y, z) = T_0 C(x, y, z),$$

where N_0 and T_0 are, respectively, the electron density and electron temperature at the center of the burst, and L_h and L_v are scale factors for the major and minor axes of the family of ellipsoids. (The ratio of L_h to L_v defines the eccentricity.) T_0 was chosen to be 5000 deg. N_0 was chosen so that the ellipsoid represented by $C = \epsilon^{-1}$ represents the overdense boundary at a frequency of 400 MHz. The center of the burst region was placed at a height of 150 km (z_0), and the horizontal and vertical scale factors chosen were $L_h = 100$ and $L_v = 12.5$ km.

Ground zero of the disturbance was chosen to be 400 km due north of the radar. Figure 13 shows two contours of constant electron density (and temperature) lying in a north-south meridian plane. The contours displayed correspond to values of C equal to ϵ^{-1} and ϵ^{-2} . The inner contour corresponds to the ellipsoid within which the medium is overdense to a radar frequency of 400 MHz. The outer ellipsoid defines a boundary within which the refractive index is less than 0.80 at a frequency of 400 MHz. The space between these two curves (and their associated ellipsoids) represents the region of greatest significance to the propagation problem being studied.

This model disturbance region was used in tests of the RAEC program to evaluate the effect of varying granularity constraints and also to examine the effectiveness and intelligibility of the output displays.

Studies of the Granularity Criteria

As explained previously, the radar effects program calculates the ray path for a propagation medium which is approximated by a discrete rather than a continuous variation of electron density and temperature. In the model, the real part of the refractive index is held constant within a slab of the medium. The granularity scale for the refraction calculation is therefore determined by slab thickness. The group refractive index and the imaginary part of the phase refractive index are allowed to vary from stratum to stratum within a slab but are held constant within any given stratum. Hence the granularity scale for such quantities as absorption and radar range is the step size (stratum width) rather than the slab thickness. The parameter-limiting slab thickness is the variable LMU, where LMU represents the limit on the fractional variation of refractive index

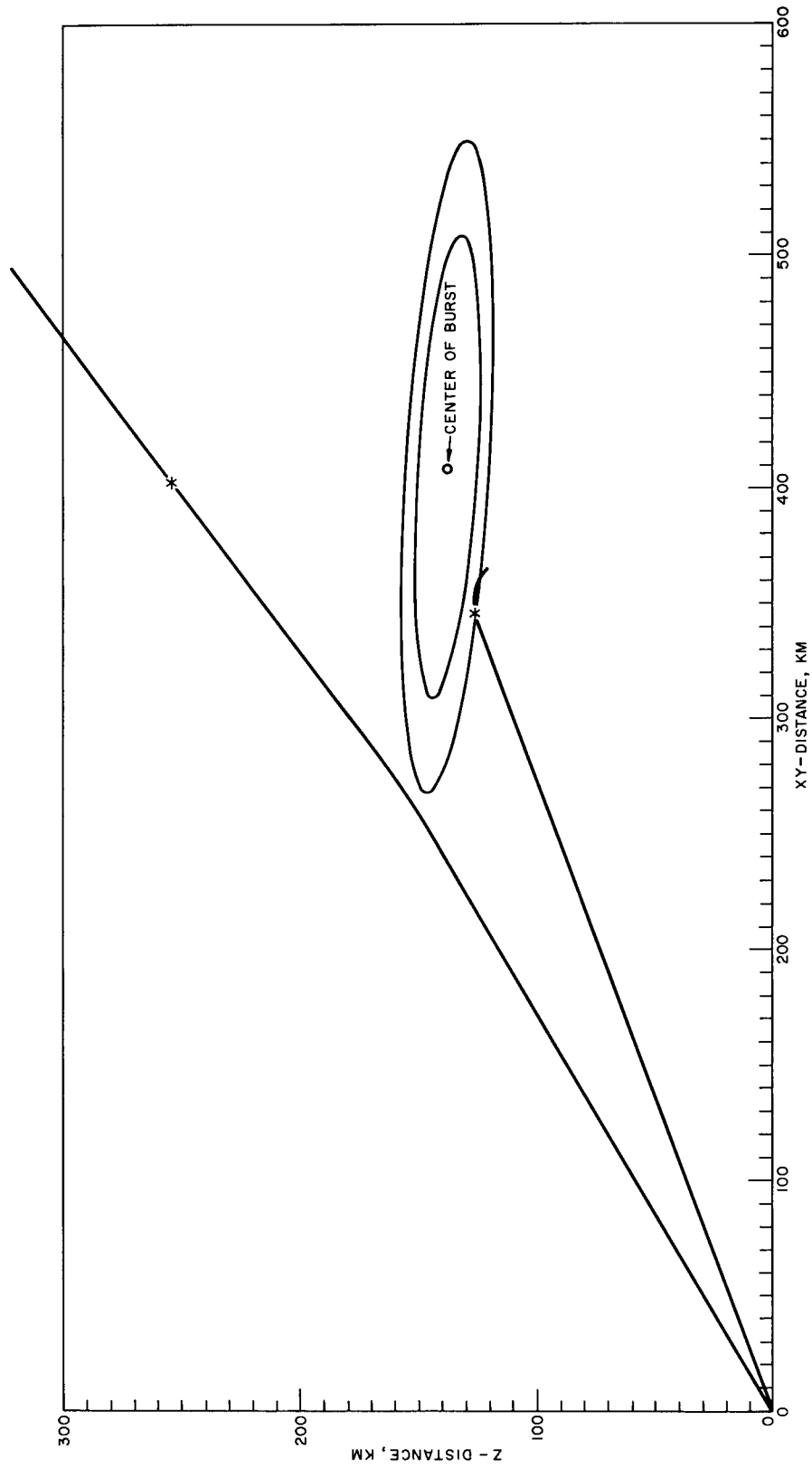


Fig. 13 - Burst region—radar geometry for granularity studies

across a slab. The parameter most important for regulating step size is the variable LABS, where LABS defines the upper limit on the allowable absorption in a given stratum of the medium. Values assigned to these variables are designated granularity constraints. In calculating physical effects, errors due to granularity can be made negligible by using sufficiently small steps but at the expense of longer calculation times. A compromise between precision and calculation time must be made. This section reports some limited studies of this problem that have been made using the NRL CDC-3800 computer.

The assumption of a constant refractive index within a slab is the primary limitation on accuracy in the ray-trace calculation. AERROR, the radar pointing error, is a useful indicator of the effect on the calculated ray path of varying LMU. Errors resulting from granularity structure of the medium on the scale of a stratum are reflected in the accuracy of the calculation of absorption. The parameter ABSDB (decibels), therefore, is a useful indicator of error due to the finiteness of the step size. Using the NRL CDC-3800 computer, studies were made of the manner in which the indicator variables AERROR and ABSDB depend on the granularity criteria LMU and LABS. Other pertinent variables considered in evaluating a given set of granularity criteria are the total number of refractive bends executed in the course of ray construction and the ray computation time.

Two rays, at initial elevation angles of 20 and 30 deg and at 0 deg azimuth propagating through the burst model that has been described, were used as representative cases. The actual ray plots, superimposed on contours of constant plasma frequency and electron temperature in the plane of the rays, are shown in Fig. 13. The asterisks appearing on the ray paths in Fig. 13 mark the points at which the granularity indicators are evaluated.

Ray 1 was used for evaluating the effect on refraction of varying the parameter LMU. A point at a distance of 475 km from the radar and well beyond the burst is chosen as a suitable evaluation point. Ray 1 represents a ray which is only mildly affected by the burst region. Differences in AERROR due to differences in the granularity criteria become evident only at substantial distances beyond the burst. A range of 475 km turned out to be a convenient test point on all test cases of ray 1. Ray 2 was used for evaluating the effect on the absorption calculation of varying the parameter LABS. The point along ray 2 at which ABSDB was evaluated is at 373 km. This distance was chosen because it is internal to the region of serious propagation disturbance and yet occurs prior to the total reflection region. The total reflection region was avoided because it forces thin slabs to be defined regardless of the refractive and absorptive granularity constraints.

To evaluate the relative merits of different granularity constraints, it is necessary to have a standard ray. The standard ray is calculated with the following very fine granularity constraints:

$$\text{LMU} = 0.001$$

$$\text{LABS} = 0.0015$$

$$\text{DEL}2 = 0.1.$$

These parameters are equivalent to a limit of 0.1 percent change in refractive index, an incremental absorption (two-way) of 0.025 dB, and a maximum step size of 0.1 km. These are rather fine granularity criteria and should produce ray traces that are virtually indistinguishable from a continuous ray trace through the medium.

Granularity constraints used for the two test rays are

Ray 1, LABS = 0.0115; LMU = 0.001, 0.002, 0.005, 0.01, 0.02, 0.05, 0.1;

Ray 2, LMU = 0.01; LABS = 0.0015, 0.003, 0.0075, 0.015, 0.03, 0.075, 0.15.

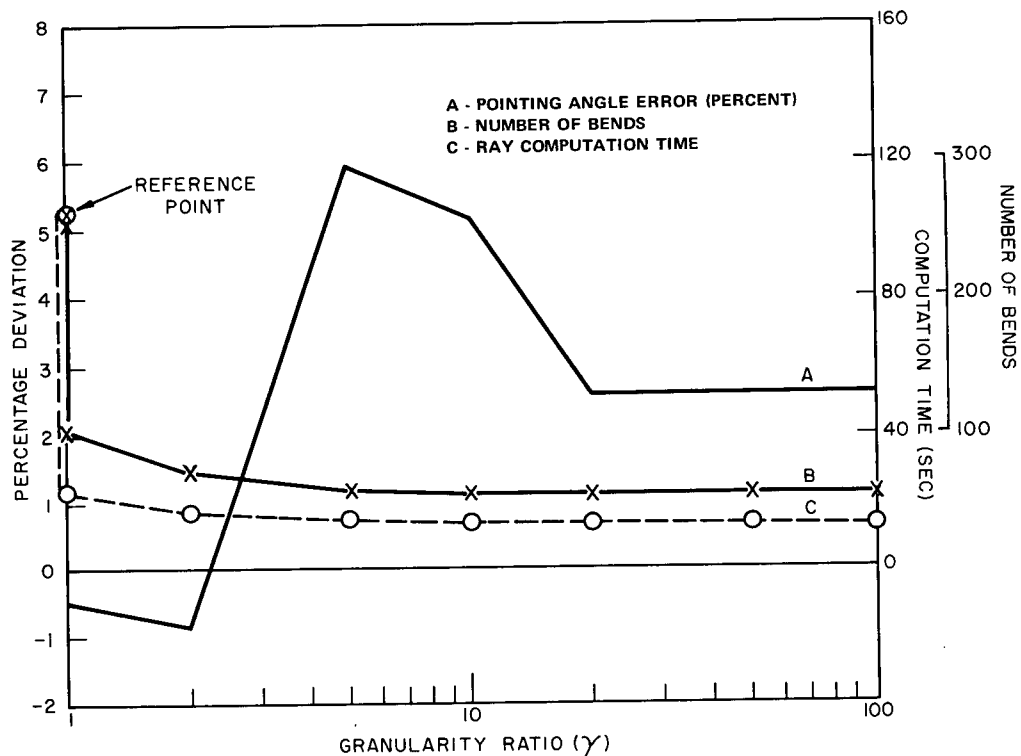


Fig. 14 - Granularity study results, ray 1

The granularity variable was chosen in multiples of 1, 2, 5, 10, 20, 50 and 100 of those of the standard ray. The maximum step size in the refracting medium was increased by a factor of 10 ($DEL2 = 1$ km) from that of the standard ray and was the same for all test cases. The results of the granularity studies are presented in Figs. 14 and 15 where the independent variable is a granularity ratio defined by $\gamma = LMU/(LMU)_{STD}$ for ray 1 and $\gamma = LABS/(LABS)_{STD}$ for ray 2.

Figure 14 is a plot of the results of the granularity study using ray 1. The results can be summarized as follows:

1. Changing maximum step size ($DEL2$) from 0.1 km to 1.0 km has a negligible effect on the accuracy of the ray trace calculation, as is evidenced by the small pointing angle error incurred by this change. It does have substantial effect on the computer running time, however.

2. Pointing angle error becomes substantial in the interval $2 < \gamma < 5$.

3. Beyond $\gamma = 5$ the pointing angle error stabilizes, which implies that for $LMU > 0.005$, slab width is controlled indirectly by $LABS$ rather than by LMU .

Figure 15 summarizes the results of varying the stratum granularity parameter $LABS$. These results can be summarized as follows:

1. Increase of $DEL2$ from 0.1 to 1.0 km results in a substantial savings in computation time without serious degradation of the absorption calculation.

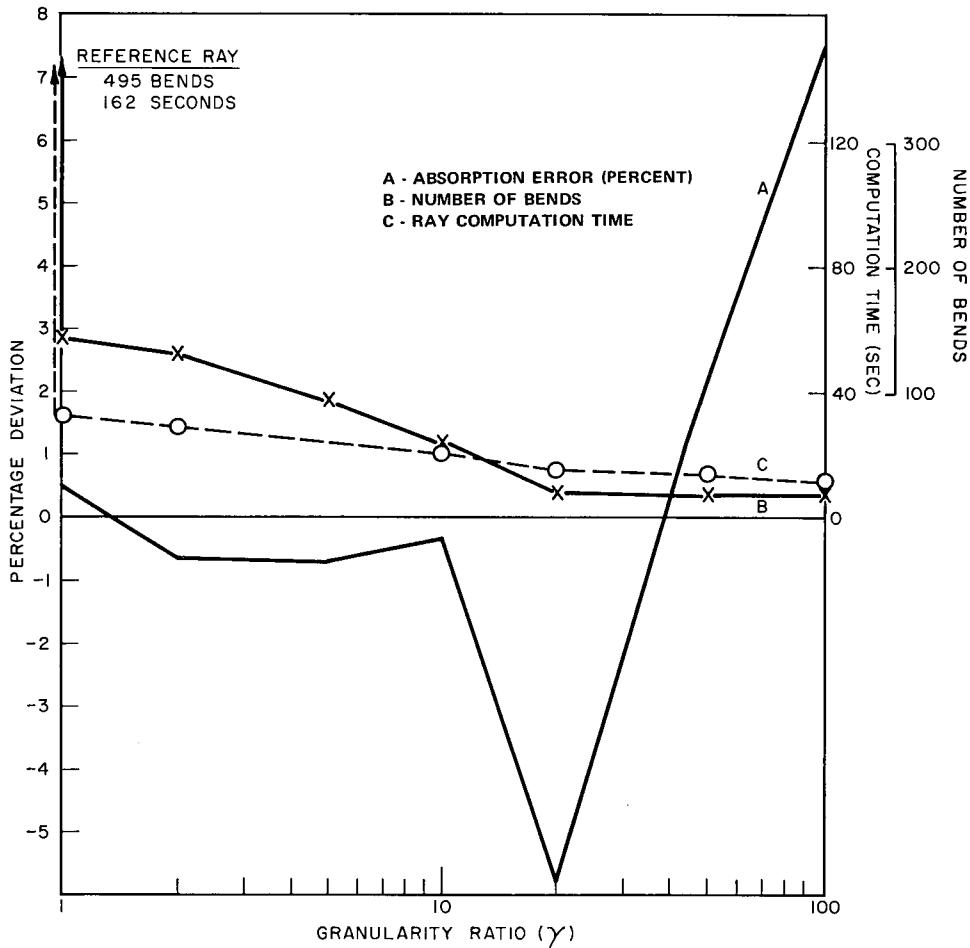


Fig. 15 - Granularity study results, ray 2

2. The absorption error starts to become large for LABS > 0.015, which corresponds to a two-way absorption limit per step of 0.25 dB.

The results of Figs. 14 and 15 suggest the following choice of granularity constraints as being optimum insofar as computer running time and calculational accuracy are concerned:

$$LMU = 0.003$$

$$LABS = 0.015$$

$$DEL 2 = 1.0 \text{ km.}$$

These conclusions are based on a very limited amount of data and on a very special set of assumptions regarding the disturbed propagation environment, however, and are therefore tentative. A firm conclusion as to an optimum set of granularity parameters must await the results of more thorough testing on better phenomenology models.

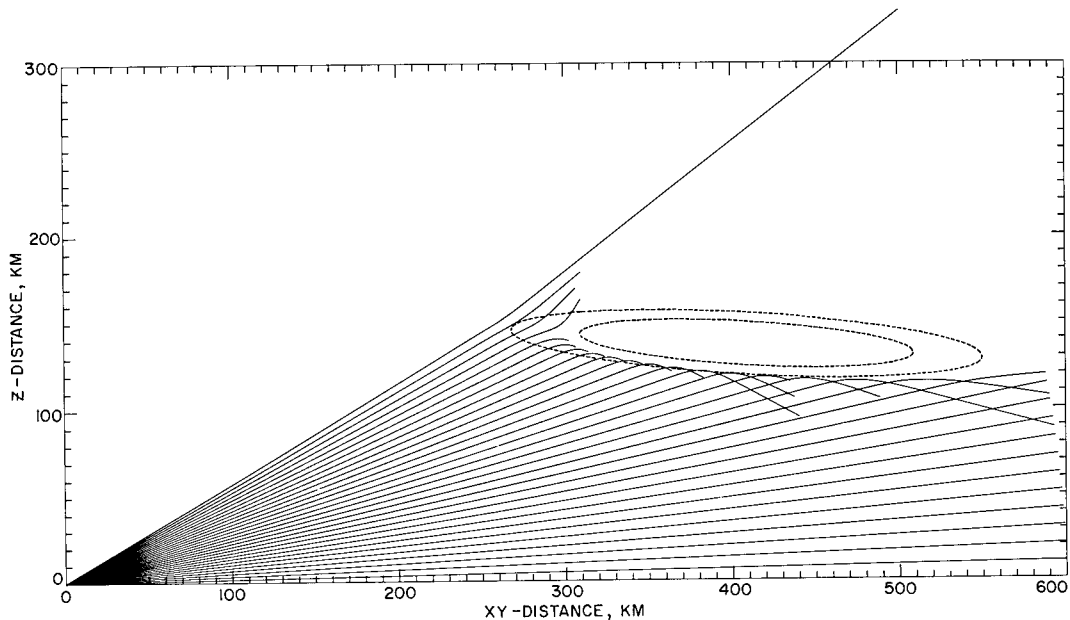


Fig. 16 - Ray paths through the central meridian of a simulated burst environment

Test Results

The model phenomenology environment as seen from the specified radar site occupies a rather large region of the sky. The burst center appears to be at 0 deg azimuth and at an elevation angle of approximately 19 deg. The region of serious propagation disturbance (within the outer contour of Fig. 13) subtends an azimuth angle of 53 deg and spans elevation angles between 15 and 29 deg as seen by an observer at the radar. The effect of the highly refracting burst region is illustrated by the ray trace contours shown in Fig. 16. These rays were launched at 0 deg azimuth and at elevation angles in the range 0 to 30 deg in steps of 1 deg. Figure 16 also contains the overdense boundary and the 0.80 refractive index contour as in Fig. 13. It is notable that all rays that are incident from beneath the disturbed region are very severely refracted and, in a sense, reflected. The absorption of these severely refracted rays was also very large and most of them were prematurely terminated either because of excessive absorption or excessive ray deviation. Rays incident on the nose of the medium are refracted away from its center as evidenced by the upper four rays. All but one of these was terminated because of excessive absorption prior to achieving maximum range. It is interesting that none of the rays ever penetrate the burst region far enough to approach the overdense boundary. In terms of grossly abnormal vs normal propagation conditions, it appears that the $n = 0.80$ boundary is more significant as a boundary of the abnormal propagation region than is the overdense medium. These conclusions pertain, however, to the condition of the model used in the present problem and cannot be extended to a more general case without extensive further tests.

In the multiple-ray calculation, advantage was taken of the azimuthal symmetry of the problem and only azimuths between 0 and 30 deg were investigated. The calculation covered elevation angles in the range of 0 to 40 deg and the angular increment between rays was 1 deg. The results of the calculations are summarized in the form of sky maps. A sky map defines a range surface within which the radar can accomplish its mission. Each propagation factor that can result in the abortion of the radar mission has associated with it a permissible upper limit, above which the mission is considered to fail. Application of this limit to the propagation calculation defines a maximum range surface which is displayed by the sky map. The important factors that are summarized in the form of sky maps

in this calculation are: absorption or path loss, radar angle error, radar range error, radar miss distance, and ray deviation. Sky maps for these quantities, for the burst region defined earlier in this section, are given in Figs. 17 through 21. The sky maps are accompanied by a data tabulation, Table 1, for those rays that were terminated prematurely (prior to RAMAX). This termination summary gives the reason for termination of each ray as well as the ray status at the time of termination.

A short discussion of two of these sky maps is given below to provide concrete examples of their interpretation.

Two-Way Absorption (Path Loss) Sky Map

The program controller has the option of obtaining a sky map for either absorption or path loss but not both. In this case (Fig. 17) the flag (IFLAG) was set so that absorption was the sky-map variable. The heading above the display defines the absorption limit (10 dB) for a successful mission, the angular resolution of the calculation, the radar frequency, and a symbol legend for interpreting the sky map. The heading beneath the display identifies the blast phenomenology and the conditions of the calculation.

Each ray-trace calculation was pursued to a maximum range (RAMAX) of 600 km, unless terminated prior to this range for reasons mentioned earlier. The numbered region on the sky-map display therefore defines the region of significant absorption. The extent of the numbered region of the display is seen to correspond roughly to the phenomenology region as defined in another part of this section.

The code symbol 5 appearing on the display signifies that the absorption limit was exceeded between the ranges of 300 and 350 km. The look angles corresponding to the symbol 5 on the display represent the directions of maximum reduction of detection range for the radar. Look angles designated by larger numerical characters indicate that the nominal detection range of the radar extends out to the range corresponding to the number code. A blank implies that the detection range extends at least to RAMAX, the maximum range of the ray trace calculation.

Refraction Sky Map (REFRAY)

The refraction sky map, Fig. 18, specifies the ranges at which the radar look-angle error exceeds the prescribed limit RFRCL, which in this case is 10 mrad. This map has the same general character as the map for absorption; the angle-error limit exceeds 10 mrad at ranges between 300 to 350 km for look angles designated by the code symbol 5. The sky map also contains a dash symbol which is an indication of the fact that in those directions the absorption limit was exceeded (and the ray terminated) at a reference range of 350 km while the angle error limit had not yet been exceeded. The surrounding 6's indicate that if the ray had not been terminated, then the angle error limit would have been exceeded at the next reference range (400 km) for many of these look angles.

The sky map again defines a maximum-range surface, with range limited by the variable of the display, in this case angle-error limit. The display indicates that usable radar angle data may be obtained at ranges less than those defined by the maximum range surface.

The final output display is one of apparent sky temperature, Fig. 22. The sky temperature includes contributions from the propagation medium, which are proportional to the temperature of the medium and its opacity to electromagnetic waves at the radar frequency. For those rays which reach the maximum range RAMAX, there is an additional contribution to apparent sky temperature due to background sky, TSKY. This contribution is reduced by the total ray attenuation. Another contributor to the apparent sky temperature

is the ground, in cases where the ray path intersects it. The calculated contribution assumes that the ground behaves like a blackbody.

The calculated apparent sky temperature is quantized into ten ranges, and a numerical code is assigned to each range. A map of coded temperature against azimuth and elevation summarizes the results of these calculations and is presented in Fig. 22.

ACKNOWLEDGMENTS

The authors are indebted to many colleagues in the development of this program. John Barry, of the Radar Division Staff, is the author of subroutines XCOORD, XDRCOS, and BACOR. He also was a major contributor to the BEND subroutine. Dr. K. Hain, of the Plasma Physics Division, is responsible for Subroutine PRELDA which interfaces plasma physics phenomenology tapes with the radar code. Mr. Kenneth Morin of the Radar Geophysics Branch was responsible for the actual programming and our success was, in large measure, the result of his efforts. Finally we express our gratitude to Lamont Blake for his guidance and criticism during all phases of the work on this program.

REFERENCES

1. Bogusch, R.L., and Hebner, C., "Examination of Starfish Data Relevant to the RANC Model (RANC III)," G.E. Tempo Report 66TMP-100 (Secret Report, Unclassified Title), Santa Barbara, Oct. 25, 1966
2. Bogusch, R.L., and Stanton, M.J., "Computer Simulation of the Effects of a Nuclear Environment on Radar (RANC II)," General Electric Tempo Report 65TMP-54 (Secret Report, Unclassified Title), Oct. 1965, reissued Oct. 1968, Santa Barbara, California
3. Blake, L.V., "A Guide to Basic Pulse-Radar Maximum-Range Calculation Part I — Equations, Definitions and Aids to Calculation," NRL Report 6930, Dec. 23, 1969
4. Ratcliffe, J.A., "The Magneto-Ionic Theory and Its Applications to the Ionosphere," Cambridge University Press, Cambridge, 1959
5. Shkarofsky, I.P., "Values of the Transport Coefficients in a Plasma for any Degree of Ionization Based on a Maxwellian Distribution," Can. J. Phys. 39:1619 (1961)
6. Shkarofsky, I.P., "Generalized Appleton-Hartree Equation for any Degree of Ionization and Application to the Ionosphere," Proc. IRE 49:1857 (Dec. 1961)
7. Hochstim, R.A., "Project Secede September 1969 Summer Study Proceedings, Vol. II — Transport Coefficients and Rates of Collisional Energy Transfer in the Upper Atmosphere," Stanford Research Institute, sponsored by ARPA, Sept. 1969
8. Kraus, J.D., "Radio Astronomy," New York, McGraw-Hill, 1966
9. Hochstim, A.R., "Collision Frequencies and Electric Conductivities of Weakly Ionized N_2 , O_2 , O , NO and Dry Air," IDA Research Paper, p. 124, Feb. 1965
10. Brillouin, L., "Wave Propagation and Group Velocity," New York, Academic Press, 1960

Table 1
Data Summary

REASON FOR TERM.	ELEVATION (DEG.)	AZIMUTH (DEG.)	RANGE (KM.)	ABSORPTION (DB)	PATH LOSS (DB)	ANGLE ERROR (RADS)	RANGE ERROR (KM.)	MISS DISTANCE (KM.)	TEMPERATURE (DEG. K)	RAY DEV (DEG.)
X ABS/PATH LOSS	37.000	0.0	353.1650	11.536	233.455	0.01178	1.1404	4.315C	487.2268	9.34
X ABS/PATH LOSS	29.000	0.0	350.3428	34.605	236.384	0.01432	2.1855	5.4797	654.6968	13.16
X ABS/PATH LOSS	28.000	0.0	350.2212	85.294	307.067	0.01635	4.3459	7.2146	722.9111	19.43
X ABS/PATH LOSS	27.000	0.0	350.2593	244.297	466.007	0.01478	11.8445	11.8734	746.3030	33.63
X ABS/PATH LOSS	26.000	0.0	351.1786	303.261	525.112	0.02241	19.8899	16.21329	765.8198	38.33
X ABS/PATH LOSS	25.000	0.0	352.6887	168.299	390.195	0.015893	41.6646	72.3992	773.9963	75.01
X ABS/PATH LOSS	24.000	0.0	350.3489	120.325	342.105	0.006921	16.7852	29.9594	774.4664	67.10
X ABS/PATH LOSS	23.000	0.0	350.0522	78.725	300.490	0.02215	1.0925	9.3647	759.1458	48.59
X ABS/PATH LOSS	22.000	0.0	350.6679	21.085	242.852	0.0	1.0925	1.8979	632.2866	14.12
X ABS/PATH LOSS	21.000	0.0	404.8357	62.879	287.170	0.013657	26.3416	63.8064	731.4419	53.57
X ABS/PATH LOSS	20.000	0.0	400.6367	53.677	277.787	0.07594	14.0889	34.0033	721.1167	49.56
X ABS/PATH LOSS	19.000	0.0	400.6707	44.781	268.893	0.03324	5.9473	14.6739	701.5330	43.08
X ABS/PATH LOSS	18.000	0.0	400.6247	15.035	239.119	0.006468	0.8384	2.0719	535.8450	16.13
X ABS/PATH LOSS	17.000	0.0	450.6853	32.688	258.843	0.05839	9.2759	28.1526	627.816	38.13
X ABS/PATH LOSS	16.000	0.0	450.6945	26.730	252.863	0.01894	2.9202	9.0332	577.6538	28.65
X ABS/PATH LOSS	15.000	0.0	500.3989	22.823	250.795	0.04907	6.8440	25.6488	515.0459	29.84
X ABS/PATH LOSS	14.000	0.0	500.3513	15.966	243.944	0.01325	1.7724	6.8877	426.3867	19.13
X ABS/PATH LOSS	13.000	0.0	590.3845	10.700	241.545	0.04156	4.2559	24.9877	347.2898	17.67
X ABS/PATH LOSS	30.000	1.000	354.5500	11.471	233.458	0.01125	1.1267	4.1437	486.2405	9.03
X ABS/PATH LOSS	29.000	1.000	350.1479	34.225	255.995	0.01422	2.1672	5.4324	653.3992	13.13
X ABS/PATH LOSS	28.000	1.000	350.0139	84.343	316.176	0.01621	4.3014	7.1388	722.4810	19.42
X ABS/PATH LOSS	27.000	1.000	350.0305	240.296	462.060	0.01367	10.3755	11.4491	746.1516	32.98
X ABS/PATH LOSS	26.000	1.000	351.3918	355.948	527.734	0.03147	95.8423	155.6655	766.7224	88.49
X ABS/PATH LOSS	25.000	1.000	352.3435	168.848	399.827	0.015544	40.8196	70.7562	773.7590	75.02
X ABS/PATH LOSS	24.000	1.000	350.1040	121.155	342.923	0.06669	16.2863	28.8570	774.1365	67.08
X ABS/PATH LOSS	23.000	1.000	350.0413	78.398	300.162	0.02182	5.1038	9.2293	759.3931	47.85
X ABS/PATH LOSS	22.000	1.000	350.0706	20.880	242.646	0.0	1.0833	1.8893	650.1119	14.24
X ABS/PATH LOSS	21.000	1.000	403.6106	63.567	287.805	0.03244	25.5708	60.7282	732.2471	53.55
X ABS/PATH LOSS	20.000	1.000	400.1316	54.007	278.093	0.07411	13.7534	33.1415	721.2407	49.55
X ABS/PATH LOSS	19.000	1.000	400.5129	44.481	268.564	0.03156	5.8567	13.9116	703.1216	42.89
X ABS/PATH LOSS	18.000	1.000	400.5283	14.960	239.044	0.06468	0.8938	2.0502	533.5549	16.00
X ABS/PATH LOSS	17.000	1.000	450.7556	32.751	258.909	0.05835	9.2703	28.1340	627.1025	38.12
X ABS/PATH LOSS	16.000	1.000	450.1370	26.847	252.781	0.01891	2.9133	9.0185	576.8735	28.63
X ABS/PATH LOSS	15.000	1.000	500.6910	22.887	250.863	0.04898	6.8308	25.6064	515.5081	29.79
X ABS/PATH LOSS	14.000	1.000	500.8721	16.255	242.244	0.01317	1.7603	6.8380	429.5271	18.79
X ABS/PATH LOSS	13.000	1.000	590.4290	10.715	241.561	0.04119	4.2612	24.7606	347.9600	17.58
X ABS/PATH LOSS	30.000	2.000	350.8574	11.019	232.824	0.01072	1.0999	3.9067	476.9858	9.12
X ABS/PATH LOSS	29.000	2.000	350.8479	33.121	254.925	0.01441	2.1221	5.4862	649.6064	13.01
X ABS/PATH LOSS	28.000	2.000	350.5454	81.746	303.536	0.01620	4.1956	7.0803	720.9529	19.32
X ABS/PATH LOSS	27.000	2.000	350.4273	229.797	451.596	0.01446	10.0171	11.2596	744.9150	32.49
X ABS/PATH LOSS	26.000	2.000	350.4199	315.094	536.878	0.031405	97.4033	157.6011	765.8779	88.93
X ABS/PATH LOSS	25.000	2.000	353.0779	170.435	392.350	0.015975	41.9971	72.9122	773.2905	75.12
X ABS/PATH LOSS	24.000	2.000	350.0420	77.480	293.244	0.06517	15.8804	28.2166	773.9426	67.36
X ABS/PATH LOSS	23.000	2.000	350.0776	20.278	242.045	0.0	1.0527	8.9581	759.6021	46.96
X ABS/PATH LOSS	22.000	2.000	403.8320	63.708	287.956	0.03237	25.5552	60.7194	732.7180	53.53
X ABS/PATH LOSS	21.000	2.000	400.1301	53.887	277.493	0.07386	13.7085	33.0273	721.2180	49.53
X ABS/PATH LOSS	19.000	2.000	400.0564	44.358	268.442	0.03127	5.6106	13.7858	701.7944	42.84
X ABS/PATH LOSS	18.000	2.000	400.0383	14.546	238.630	0.06450	0.8669	1.9849	526.0933	14.71
X ABS/PATH LOSS	17.000	2.000	450.1252	32.521	258.654	0.05687	9.0359	27.3847	625.8596	38.08
X ABS/PATH LOSS	15.000	2.000	450.2214	26.386	252.524	0.01876	2.8901	8.9507	575.1902	28.56

Table 1 (Continued)
Data Summary

X	ABSP/PATH	LOSS	15.000	2.000	500.5645	23.749	251.727	0.04789	6.6594	25.0305	520.3093	29.61
X	ABSP/PATH	LOSS	14.000	2.000	500.0527	15.573	243.534	0.01237	1.6575	6.4125	421.9883	17.62
X	ABSP/PATH	LOSS	13.000	2.000	590.5378	10.456	241.306	0.04068	4.1316	24.4533	344.4736	17.34
X	ABSP/PATH	LOSS	30.000	3.000	358.6767	16.149	232.386	0.01509	1.1389	5.5457	647.9124	9.80
X	ABSP/PATH	LOSS	28.000	3.000	350.6055	31.559	253.174	0.01668	2.1106	5.3652	453.6150	12.59
X	ABSP/PATH	LOSS	27.000	3.000	350.2229	77.733	299.506	0.01538	3.9890	6.7227	718.3653	18.75
X	ABSP/PATH	LOSS	27.000	3.000	350.8584	213.818	435.623	0.01414	9.3401	10.6027	743.8809	30.89
X	ABSP/PATH	LOSS	26.000	3.000	352.3289	330.536	552.424	0.03496	106.6577	173.5004	763.7732	89.90
X	ABSP/PATH	LOSS	25.000	3.000	350.1426	173.936	395.706	0.03288	35.4934	60.3366	771.1670	75.26
X	ABSP/PATH	LOSS	24.000	3.000	350.0361	123.404	343.168	0.06206	15.1782	26.8772	773.0386	67.15
X	ABSP/PATH	LOSS	23.000	3.000	350.0071	75.750	297.513	0.02008	4.7195	8.5011	760.2029	45.18
X	ABSP/PATH	LOSS	22.000	3.000	350.0389	19.291	241.058	0.0	1.0044	1.7410	633.0637	12.50
X	ABSP/PATH	LOSS	21.000	3.000	403.5510	63.914	288.149	0.01343	25.1931	59.7803	733.6250	53.50
X	ABSP/PATH	LOSS	20.000	3.000	400.4800	53.503	277.606	0.07381	13.6921	33.0231	721.5593	49.49
X	ABSP/PATH	LOSS	19.000	3.000	400.3501	44.845	268.943	0.03089	5.5439	13.6273	701.4802	42.75
X	ABSP/PATH	LOSS	18.000	3.000	400.0567	13.858	237.942	0.0	0.8225	1.8796	512.7236	16.60
X	ABSP/PATH	LOSS	17.000	3.000	450.0601	33.042	259.173	0.05558	8.8186	26.7501	626.6802	38.00
X	ABSP/PATH	LOSS	16.000	3.000	450.0613	26.366	252.496	0.01777	2.7463	8.4727	574.9895	28.41
X	ABSP/PATH	LOSS	15.000	3.000	500.6560	22.891	250.873	0.04781	6.6414	24.9865	514.6060	29.55
X	ABSP/PATH	LOSS	14.000	3.000	500.0771	15.428	243.389	0.01175	1.5811	6.0916	420.3181	17.46
X	ABSP/PATH	LOSS	13.000	3.000	590.5381	10.127	240.977	0.03972	4.0042	23.8712	340.3843	17.08
X	ABSP/PATH	LOSS	29.000	4.000	359.4871	23.146	251.374	0.01674	2.0149	6.3456	633.4170	12.35
X	ABSP/PATH	LOSS	28.000	4.000	350.8499	72.219	294.023	0.01532	3.7742	6.5852	713.6890	18.03
X	ABSP/PATH	LOSS	27.000	4.000	350.0381	193.324	415.088	0.01267	8.3850	9.5039	742.3967	29.17
X	ABSP/PATH	LOSS	26.000	4.000	351.3772	359.572	581.402	0.04501	110.4900	177.0159	761.7568	91.32
X	ABSP/PATH	LOSS	25.000	4.000	350.2769	179.311	401.087	0.02870	34.5641	58.5828	770.0837	75.46
X	ABSP/PATH	LOSS	24.000	4.000	350.0103	124.019	345.782	0.05900	14.5002	25.5768	772.0095	66.77
X	ABSP/PATH	LOSS	23.000	4.000	350.0366	73.446	295.210	0.01878	4.4292	7.9600	760.3259	43.09
X	ABSP/PATH	LOSS	22.000	4.000	350.0061	17.705	239.468	0.0	0.9309	1.6008	610.6865	11.29
X	ABSP/PATH	LOSS	21.000	4.000	404.1765	64.626	288.889	0.03035	25.1738	58.8148	734.2502	53.44
X	ABSP/PATH	LOSS	20.000	4.000	400.3616	54.157	278.264	0.07163	13.2856	32.0297	721.6045	49.41
X	ABSP/PATH	LOSS	19.000	4.000	400.0825	44.924	269.009	0.02890	5.1934	12.7409	701.0815	42.51
X	ABSP/PATH	LOSS	18.000	4.000	400.0742	12.928	237.013	0.0	0.7668	1.7436	492.9065	12.73
X	ABSP/PATH	LOSS	17.000	4.000	450.5876	32.818	258.969	0.05549	8.7947	26.7294	624.7786	37.88
X	ABSP/PATH	LOSS	16.000	4.000	450.0969	25.631	251.764	0.01724	2.6606	8.2179	570.6321	28.12
X	ABSP/PATH	LOSS	15.000	4.000	500.8455	23.168	251.156	0.06647	6.4253	24.2854	515.3550	29.26
X	ABSP/PATH	LOSS	14.000	4.000	500.0774	14.789	242.750	0.01113	1.4973	5.7665	412.4761	16.14
X	ABSP/PATH	LOSS	29.000	5.000	357.2686	26.504	248.524	0.01471	1.8506	5.5748	620.1245	11.74
X	ABSP/PATH	LOSS	28.000	5.000	350.6011	65.813	287.605	0.01421	3.4658	6.0783	708.4487	16.93
X	ABSP/PATH	LOSS	27.000	5.000	350.7656	171.369	393.170	0.01293	7.5398	8.8197	739.5637	27.31
X	ABSP/PATH	LOSS	26.000	5.000	351.0894	142.454	634.271	0.037607	124.8081	197.3059	759.7603	94.00
X	ABSP/PATH	LOSS	25.000	5.000	350.1157	184.891	406.659	0.02126	33.0737	55.3555	767.1250	75.80
X	ABSP/PATH	LOSS	24.000	5.000	350.1663	123.062	349.833	0.05418	13.4236	23.5307	769.4495	66.51
X	ABSP/PATH	LOSS	23.000	5.000	350.0415	73.094	291.858	0.01724	4.6737	7.3026	758.4673	41.14
X	ABSP/PATH	LOSS	22.000	5.000	350.0203	16.214	237.978	0.0	0.8586	1.4640	587.8733	10.39
X	ABSP/PATH	LOSS	21.000	5.000	401.4192	64.470	288.614	0.02052	23.3467	56.9410	736.3359	53.39
X	ABSP/PATH	LOSS	20.000	5.000	400.3706	54.204	278.303	0.07004	13.0144	31.3195	720.4407	49.38
X	ABSP/PATH	LOSS	19.000	5.000	400.0386	44.975	269.059	0.02718	4.8967	11.9823	698.3447	41.02
X	ABSP/PATH	LOSS	18.000	5.000	400.0938	12.530	236.617	0.0	0.7617	1.5940	469.2522	11.17
X	ABSP/PATH	LOSS	17.000	5.000	450.7422	33.087	259.244	0.05408	8.5547	26.0463	628.8966	37.74
X	ABSP/PATH	LOSS	16.000	5.000	450.0659	25.299	251.422	0.01597	2.4753	7.6177	568.6282	26.49
X	ABSP/PATH	LOSS	15.000	5.000	500.3323	23.054	251.025	0.04439	6.1201	23.1644	512.9689	29.14

Table 1 (Continued)
Data Summary

X ABS/PATH LOSS	14.000	500.6670	14.330	242.312	C.01072	1.4329	5.5523	405.9819	15.69
X ABS/PATH LOSS	29.000	350.8774	23.456	245.262	C.01151	1.6550	4.3637	603.1021	11.17
X ABS/PATH LOSS	28.000	350.8176	58.847	280.650	C.01316	3.1443	5.5908	709.7454	16.23
X ABS/PATH LOSS	27.000	350.5391	148.958	370.647	C.01193	6.5913	7.8232	735.1335	24.97
X ABS/PATH LOSS	24.000	350.2446	542.867	764.642	C.49086	162.2622	262.1394	742.3065	100.25
X ABS/PATH LOSS	25.000	350.1755	193.004	415.175	C.11281	31.2734	51.7297	763.2910	76.24
X ABS/PATH LOSS	24.000	350.0156	129.816	351.580	C.04764	11.9285	20.7302	767.5835	65.94
X ABS/PATH LOSS	23.000	350.2198	65.625	287.389	C.01534	3.6467	6.5071	758.8357	37.18
X ABS/PATH LOSS	22.000	350.3356	14.492	236.257	C.0	0.7786	1.3178	554.8552	9.28
X ABS/PATH LOSS	21.000	401.6945	65.743	289.895	C.11809	22.9748	53.8449	734.1667	53.31
X ABS/PATH LOSS	20.000	400.4934	55.181	279.285	C.06759	12.5564	30.2177	720.9345	48.88
X ABS/PATH LOSS	19.000	400.1423	44.556	268.645	C.02568	4.6357	11.3230	697.8184	40.78
X ABS/PATH LOSS	18.000	400.0190	10.921	235.004	C.0	0.6709	1.3852	432.1113	9.46
X ABS/PATH LOSS	17.000	450.7375	32.968	259.124	C.05227	8.2480	25.1595	621.8904	37.57
X ABS/PATH LOSS	15.000	450.3777	24.445	250.588	C.01532	2.3704	7.3073	563.4871	26.32
X ABS/PATH LOSS	15.000	500.7190	23.013	250.996	C.04287	5.8689	21.3729	511.4412	28.80
X ABS/PATH LOSS	14.000	500.6059	13.028	240.989	C.00936	1.2490	4.8353	388.6965	14.44
X ABS/PATH LOSS	26.000	355.4832	19.777	241.810	C.01212	1.5337	4.5723	582.5161	10.60
X ABS/PATH LOSS	28.000	350.5850	51.480	273.272	C.01212	2.8062	5.1009	690.5244	15.00
X ABS/PATH LOSS	27.000	350.2402	126.558	348.333	C.01099	5.6748	6.8710	728.2446	22.94
X ABS/PATH LOSS	26.000	350.0388	497.200	708.564	C.02749	18.4771	20.9472	741.0193	36.60
X ABS/PATH LOSS	25.000	350.3974	205.879	427.646	C.09933	28.2231	45.8492	761.0872	76.60
X ABS/PATH LOSS	24.000	350.0005	131.107	352.870	C.04072	10.3271	17.7667	769.3640	62.66
X ABS/PATH LOSS	23.000	350.3388	60.294	282.059	C.11351	3.7224	5.7310	755.6616	33.84
X ABS/PATH LOSS	22.000	350.0498	12.652	234.417	C.0	0.6917	1.1560	514.8181	7.71
X ABS/PATH LOSS	21.000	400.4966	66.311	290.414	C.11153	21.6550	50.6916	732.4895	53.21
X ABS/PATH LOSS	20.000	400.4500	55.249	279.351	C.06469	12.0073	28.8982	719.5339	49.12
X ABS/PATH LOSS	19.000	400.0505	43.841	267.926	C.02339	4.2346	18.3116	694.9231	39.26
X ABS/PATH LOSS	18.000	454.2573	40.312	260.604	C.09812	16.2705	48.1763	656.3467	41.41
X ABS/PATH LOSS	17.000	450.2563	33.548	259.686	C.04882	7.6960	23.4610	621.3286	37.33
X ABS/PATH LOSS	15.000	450.6819	23.892	250.046	C.01405	2.1750	6.7054	559.9204	24.70
X ABS/PATH LOSS	15.000	500.9431	23.197	251.178	C.04034	5.4934	21.0360	509.9536	28.46
X ABS/PATH LOSS	14.000	500.0352	11.877	239.837	C.00815	1.1001	4.2206	371.4885	12.87
X ABS/PATH LOSS	29.000	350.2488	16.230	238.075	C.06954	1.3406	3.6052	552.8203	9.95
X ABS/PATH LOSS	28.000	350.4709	43.979	265.765	C.01081	2.4629	4.5244	677.3271	14.05
X ABS/PATH LOSS	27.000	350.6854	106.345	328.112	C.00983	4.8340	5.9406	722.4080	20.30
X ABS/PATH LOSS	26.000	350.0867	314.360	536.127	C.01774	11.7322	13.3216	737.6951	27.37
X ABS/PATH LOSS	25.000	350.1003	224.210	446.677	C.07964	23.5063	37.1702	754.9319	77.44
X ABS/PATH LOSS	24.000	350.0371	129.243	351.908	C.03391	8.7263	14.8479	761.8293	58.25
X ABS/PATH LOSS	23.000	350.0017	53.790	275.553	C.01150	2.7666	7.8873	752.1611	30.19
X ABS/PATH LOSS	22.000	350.0625	10.834	232.600	C.0	0.6091	1.0033	464.3796	6.44
X ABS/PATH LOSS	21.000	403.7231	67.014	291.257	C.11757	22.8130	53.8324	732.1978	53.10
X ABS/PATH LOSS	20.000	400.3120	56.764	280.859	C.06036	11.2109	26.9395	718.8154	48.89
X ABS/PATH LOSS	19.000	400.0286	42.960	267.043	C.02098	3.8130	9.2460	692.2678	37.47
X ABS/PATH LOSS	18.000	455.6355	40.271	266.615	C.09776	16.1675	48.1377	655.9707	41.21
X ABS/PATH LOSS	17.000	450.0439	33.862	259.992	C.04565	7.1670	21.9110	620.0044	37.06
X ABS/PATH LOSS	16.000	450.0486	22.033	246.164	C.01175	1.8411	5.6024	548.1875	21.79
X ABS/PATH LOSS	15.000	500.5703	23.204	251.182	C.03789	5.1719	19.7503	502.3152	27.76
X ABS/PATH LOSS	14.000	500.1248	10.445	238.408	C.00707	0.9521	3.6583	346.6677	11.68
X ABS/PATH LOSS	29.000	350.4697	13.050	234.836	C.00861	1.1824	3.2320	511.7207	9.29
X ABS/PATH LOSS	28.000	350.5515	37.021	258.811	C.00996	2.1902	4.1174	654.1582	12.95
X ABS/PATH LOSS	27.000	350.3496	87.436	309.216	C.00917	4.0835	5.1975	715.2300	18.66

Table 1 (Continued)
Data Summary

X	ABS/PATH	LOSS	26.000	9.000	350.0498	448.300	0.01358	8.6047	9.8538	734.4453	23.21
X	ABS/PATH	LOSS	25.000	9.000	350.0103	467.012	0.05036	15.8921	24.0259	750.1997	72.75
X	ABS/PATH	LOSS	24.000	9.000	350.0229	121.751	0.02689	7.0212	11.8127	756.2759	50.23
X	ABS/PATH	LOSS	23.000	9.000	350.0393	47.085	0.00971	2.3469	4.1247	743.8657	25.01
X	ABS/PATH	LOSS	22.000	9.010	403.0530	85.020	0.16144	32.9290	75.1945	744.3037	57.37
X	ABS/PATH	LOSS	21.000	9.000	403.0650	68.591	0.11253	21.8264	51.2475	732.2209	52.96
X	ABS/PATH	LOSS	20.000	9.000	400.1316	57.574	0.05612	10.4600	25.0342	714.0627	48.19
X	ABS/PATH	LOSS	19.000	9.000	400.0166	41.415	0.01827	3.3391	8.0591	688.6912	34.88
X	ABS/PATH	LOSS	18.000	9.000	457.3455	40.897	0.09716	16.0151	47.9409	655.9390	40.97
X	ABS/PATH	LOSS	17.000	9.000	450.4756	35.136	0.04310	6.8057	20.7091	609.6790	36.57
X	ABS/PATH	LOSS	16.000	9.000	450.0789	20.301	0.01011	1.5969	4.8194	534.1877	19.53
X	ABS/PATH	LOSS	15.000	9.000	500.4829	22.976	0.03478	4.7024	18.1106	500.3088	26.04
X	ABS/PATH	LOSS	14.000	9.000	590.0522	15.771	0.06920	7.8472	41.8335	415.9116	21.73
X	ABS/PATH	LOSS	29.000	10.000	350.0017	10.059	0.00877	1.0447	3.2486	454.7383	9.17
X	ABS/PATH	LOSS	28.000	10.000	351.4066	29.942	0.00900	1.8796	3.6586	630.3169	11.95
X	ABS/PATH	LOSS	27.000	10.000	350.4492	71.003	0.00825	3.4238	4.4860	703.8748	16.32
X	ABS/PATH	LOSS	26.000	10.000	350.0718	163.916	0.01099	6.5774	7.6356	728.8687	19.70
X	ABS/PATH	LOSS	25.000	10.000	350.0325	213.101	0.03051	10.1080	14.8686	745.3279	48.98
X	ABS/PATH	LOSS	24.000	10.000	350.0649	109.227	0.02140	5.6619	9.4341	751.2461	41.36
X	ABS/PATH	LOSS	23.000	10.000	350.0815	40.121	0.00806	1.9666	3.4298	734.2095	20.11
X	ABS/PATH	LOSS	22.000	10.000	402.9973	87.696	0.15554	31.8406	72.4322	740.0061	57.27
X	ABS/PATH	LOSS	21.000	10.000	405.8455	71.835	0.11356	22.0362	52.1855	727.6619	52.79
X	ABS/PATH	LOSS	20.000	10.000	400.5700	57.856	0.05310	9.8892	23.6900	712.3474	47.40
X	ABS/PATH	LOSS	19.000	10.000	400.0195	33.899	0.01556	2.8564	6.8518	683.2009	32.08
X	ABS/PATH	LOSS	18.000	10.000	453.5728	41.344	0.08658	14.2654	42.3456	654.5450	40.68
X	ABS/PATH	LOSS	17.000	10.000	453.4099	34.704	0.03992	6.2942	19.1662	608.9583	35.72
X	ABS/PATH	LOSS	16.000	10.000	450.0032	17.869	0.00841	1.3386	4.0125	510.5605	16.98
X	ABS/PATH	LOSS	15.000	10.000	500.2778	23.038	0.03102	4.1594	16.1261	498.8333	25.31
X	ABS/PATH	LOSS	14.000	10.000	592.1797	14.998	0.06458	7.0779	39.1083	414.3735	20.59
X	ABS/PATH	LOSS	28.000	11.000	350.3577	23.378	0.00777	1.6018	3.1473	599.0635	10.50
X	ABS/PATH	LOSS	27.000	11.000	350.4675	56.413	0.00736	2.8357	3.8261	689.4549	14.75
X	ABS/PATH	LOSS	26.000	11.000	350.0066	126.921	0.00912	5.1038	6.0231	720.0208	16.46
X	ABS/PATH	LOSS	25.000	11.000	350.0059	163.922	0.02063	7.0715	10.1573	738.6392	27.16
X	ABS/PATH	LOSS	24.000	11.000	350.0076	92.221	0.01650	4.4170	7.2964	744.3564	32.58
X	ABS/PATH	LOSS	23.000	11.000	350.0879	33.080	0.00650	1.6145	2.7907	716.3086	15.63
X	ABS/PATH	LOSS	22.000	11.000	403.9053	91.169	0.15157	31.1631	70.7120	736.5425	57.16
X	ABS/PATH	LOSS	21.000	11.000	400.0166	72.213	0.09045	17.6958	40.9789	724.4204	52.60
X	ABS/PATH	LOSS	20.000	11.000	400.1965	59.624	0.04675	8.7480	20.8362	708.3398	47.41
X	ABS/PATH	LOSS	19.000	11.000	450.0066	35.262	0.01304	2.4009	5.7530	674.6375	27.76
X	ABS/PATH	LOSS	18.000	11.000	450.4097	42.254	0.07612	12.5139	36.9331	651.4509	40.33
X	ABS/PATH	LOSS	17.000	11.000	450.2107	35.363	0.03541	5.5649	16.9738	608.7078	34.43
X	ABS/PATH	LOSS	16.000	11.000	450.0845	15.264	0.00693	1.1116	3.3003	476.9946	14.99
X	ABS/PATH	LOSS	15.000	11.000	500.1929	22.727	0.02720	3.6169	14.1231	493.7778	24.40
X	ABS/PATH	LOSS	14.000	11.000	597.4469	13.628	0.06125	6.4165	37.3358	406.7742	19.16
X	ABS/PATH	LOSS	24.000	12.000	350.6890	17.091	0.00668	1.3442	2.6963	559.1646	9.69

Appendix A

COLLISION FREQUENCIES

The Appleton-Hartree equation for the index of refraction in a magneto-ionic medium derives from the expression for the tensor conductivity of the medium,

$$[\sigma] = \frac{Ne^2}{m} \begin{bmatrix} b + c & j(b - c) & 0 \\ -j(b - c) & b + c & 0 \\ 0 & 0 & d \end{bmatrix}, \quad (\text{A1})$$

where

$$2b = 1/[\nu + j(\omega - \omega_b)] \quad (\text{A2a})$$

$$2c = 1/[\nu + j(\omega + \omega_b)] \quad (\text{A2b})$$

$$d = 1/(\nu + j\omega). \quad (\text{A2c})$$

In this expression the ambient magnetic field is assumed to be oriented along the z-coordinate axis, ω is the angular frequency of a wave in the medium, ω_b is the angular gyro frequency of the medium $|eB/m|$, and ν is the total electron-collision frequency with all other species. Maxwell's equations applied to a plane wave propagating in a medium of conductivity (σ) lead to a dispersion relation for the wave and hence to an expression for the refractive index. Under the assumption that the collision frequency ν is the same for all electrons, one arrives at the classical Appleton-Hartree equation for the index of refraction.

The collision frequency may be related to an effective collision cross section by the expression,

$$\nu(\nu) = N_j \nu Q_j(\nu), \quad (\text{A3})$$

where N_j is the number density of the target species and Q_j the cross section for momentum transfer, generally a function of the electron velocity ν . The electron collision cross section consists of several components. Depending upon plasma concentration, electron collisions with ions (interacting via coulomb forces) can be significant. In addition, electron collisions with neutral particles (N_2 , O_2 , O) can be important depending upon the concentration of the neutral particles. The coulomb collision cross section has a ν^{-4} velocity dependence and, over the temperature range of interest, electron-neutral collisions usually have some power-law dependence on velocity (e.g., $Q_{N_2}(\nu) \propto \nu$, [A1]). The velocity dependence of the collision frequency requires that the conductivity of the medium be represented as some suitable average over the electron velocity distribution for a thermal plasma. The expression for the average conductivity has been chosen [A2] so as to closely resemble the expression obtained for the velocity-independent case and can again be represented by a tensor (Eq. (A1)) where the parameters b , c , and d are defined as [A3]

$$2b = 1/[g_- \langle \nu_g \rangle + h_- j(\omega - \omega_b)] \quad (\text{A3a})$$

$$2c = 1/[g_+ \langle \nu_g \rangle + h_+ j(\omega + \omega_g)] \quad (\text{A3b})$$

$$d = 1/(g_0 \langle \nu_g \rangle + h_0 j\omega). \quad (\text{A3c})$$

The parameter $\langle \nu_g \rangle$ is some appropriate average of $\nu(v)$ over the electron-velocity distribution. The parameters g_- , g_+ , g_0 and h_- , h_+ , h_0 are functions of $\omega/\langle \nu_g \rangle$ and other plasma variables and have a specific form which depends upon the nature of the weighting function used in the average of $\nu(v)$. Shkarofsky [A2, A3] has chosen an average

$$\langle \nu_g \rangle = -\frac{4\pi}{3N} \int_0^\infty \frac{d(f_0^0)}{dv} v^3 \nu(v) dv, \quad (\text{A4})$$

where $f_0^0(v)$ is the electron-velocity distribution function. This choice of average results in the g and h factors approaching unity in the limit as $\omega/\langle \nu_g \rangle$ becomes large. Thus, if the collision frequency is defined as in Eq. (A4), the classical Appleton-Hartree equation may be used for the refractive index in the limit of large $\omega/\langle \nu_g \rangle$. This is the so-called Shkarofsky high-frequency approximation.

For the situation where both electron-ion and electron-neutral collisions are important, the general average collision frequency is given by a sum over species:

$$\langle \nu_g \rangle = \langle \nu_{e-i} \rangle + \sum_i \langle \nu_{e-n_i} \rangle. \quad (\text{A5})$$

Assuming singly ionized ions, overall charge neutrality, a Boltzmann distribution function for the electrons, and a simple power-law velocity dependence for the electron-neutral collision frequency, i.e.,

$$f_0^0(v) = N_e \left(\frac{m_i}{2\pi\epsilon_0 k T_e} \right)^{3/2} \exp(-m_e v^2/2 k T_e)$$

$$\nu_{e-n_i} = C_n v^{r_i},$$

where r_i depends on species, the collision frequency averages become [A3]

$$\langle \nu_{e-i} \rangle = \frac{4(2\pi)^{1/2}}{3} \sum_i N_i \left(\frac{Z_i e^2}{4\pi\epsilon_0 k T_e} \right)^2 \left(\frac{k T_e}{m_e} \right)^{1/2} \ln \Lambda \quad (\text{A6})$$

where

$$\Lambda = \frac{3}{2Ze^3} \frac{(4\pi\epsilon_0 k T_e)^{3/2}}{(\pi N_e)^{1/2}}$$

and

$$\langle \nu_{e-n_i} \rangle = \frac{C_n \Gamma(S+r_i)}{\Gamma(\frac{5}{2})} \left(\frac{2k T_e}{m_e} \right)^{r_i/2}. \quad (\text{A7})$$

The neutral constituents of major importance for the altitude regions of interest are N_2 , O_2 , and O . Banks [A4] has reviewed the experimental and theoretical literature on electron-collision cross sections and has developed numerical fits for the temperature dependence:

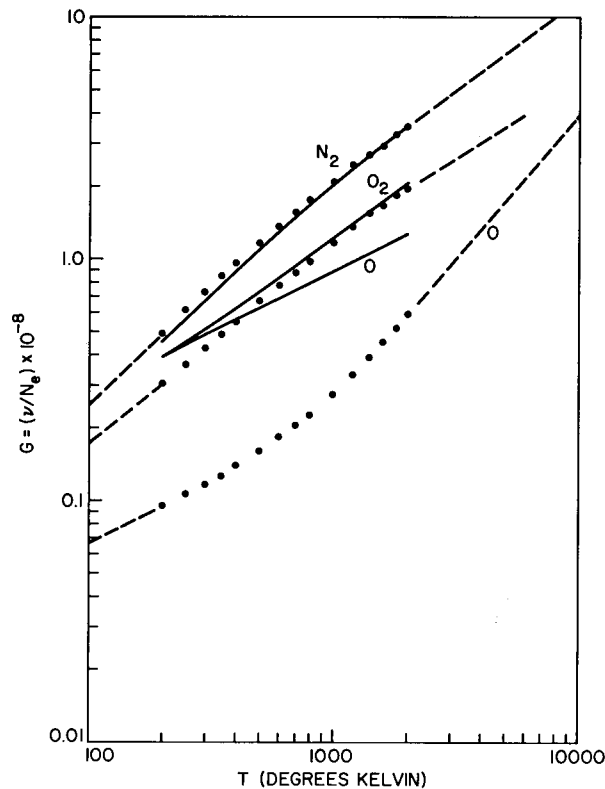


Fig. A1 - Electron neutral-collision frequencies for N_2 , O_2 , O from Banks (12) (solidlines) and Hochstim (9) (dots)

$$\nu_{e-N_2} = 2.33 \times 10^{-11} N_{N_2} (1 - 1.21 \times 10^{-4} T_e) T_e \quad (\text{A8a})$$

$$\nu_{e-O_2} = 1.82 \times 10^{-10} N_{O_2} (1 + 3.6 \times 10^{-2} T_e^{1/2}) T_e^{1/2} \quad (\text{A8b})$$

$$\nu_{e-O} = 2.8 \times 10^{-10} N_O T_e^{1/2}. \quad (\text{A8c})$$

Hochstim [A5, A6] has also calculated the temperature dependence of these cross sections by numerical integration—a technique which is believed to result in improved values. The results of Banks and Hochstim are plotted in Fig. A1. These are believed to be the most up-to-date determinations for ionospheric collision frequencies.

Agreement between the Banks and Hochstim values is quite good for the cases of O_2 and N_2 ; differences are 30% or less at 200°K and only a few percent at 1000°K. For values associated with atomic oxygen, the disagreement is by as much as a factor of 4. This is attributed by Hochstim to an incorrect energy dependence for the cross section selected by Banks.

For the COLLF Subroutine, the tabular values of collision frequency given by Hochstim [A5] have been used. These are reproduced in Table A1.

It is important to note that in the present subroutine which calculates collision frequency, neutral species concentrations are obtained from a model neutral atmosphere. The replacement of the present model atmosphere with a phenomenology-supplied neutral species roster, when available, will be straightforward.

Table A1
Collision Frequency as a Function of Temperature

Temperature (T_e °K)	Collision Frequency ($\nu \times 10^{-8}/N$)		
	N ₂	O ₂	O
200	0.490	0.302	0.094
250	0.613	0.363	0.106
300	0.733	0.423	0.117
350	0.849	0.483	0.128
400	0.962	0.543	0.139
500	1.17	0.659	0.160
600	1.37	0.772	0.182
700	1.57	0.881	0.204
800	1.75	0.986	0.227
1000	2.09	1.18	0.276
1200	2.40	1.36	0.329
1400	2.69	1.53	0.387
1600	2.97	1.68	0.448
1800	3.24	1.82	0.513
2000	3.51	1.96	0.582

Note: Table from Ref. A4.

Justification for Use of Shkarofsky High Frequency Approximation

It is instructive to examine the ratio $\omega/\langle\nu_g\rangle$ for both the ambient and disturbed ionosphere at frequencies above 100 MHz ($\omega > 6 \times 10^8$ rad/sec). Calculations of effective collision frequency $\langle\nu_g\rangle$, based upon the 1959 ARDC model atmosphere and on an average daytime electron density profile, have been made by Shkarofsky [A2] and are reproduced in Fig. A2. These values are in substantial agreement with a survey of experimental data given by Shaeffer and Inoue [A7]. A curve has been added which illustrates the ratio of $\omega/\langle\nu_g\rangle$ for the assumed atmospheric conditions and for ω corresponding to a radar frequency of 100 MHz. It is evident that for a "normal" ionosphere $\omega/\langle\nu_g\rangle$ exceeds 20 for all heights above roughly 60 km. This justifies the use of the high-frequency approximation for the normal atmosphere above 60 km.

For conditions approximating a high-altitude nuclear burst, substantial increases in temperature and electron density are to be expected. Elevated temperatures result in a reduction of the electron-ion collision frequency ($\nu_{e-i} \propto T^{-3/2}$) and an enhancement of the electron neutral collision frequency ($\nu_{e-n} \propto T^r$; r depends upon species). At low altitudes where collisions with diatomic neutrals predominate, $\nu_{e-n} \propto T$ and it is possible for the inequality on $\omega/\langle\nu_g\rangle$ to be reversed. This would require, however, a substantial temperature increase (about three orders of magnitude) at D-layer heights (60 to 80 km). This is not likely for the case of a high-altitude burst.

The conditions for Shkarofsky's high-frequency approximation could also be reversed by an electron density enhancement during a nuclear burst, since the electron-ion collision

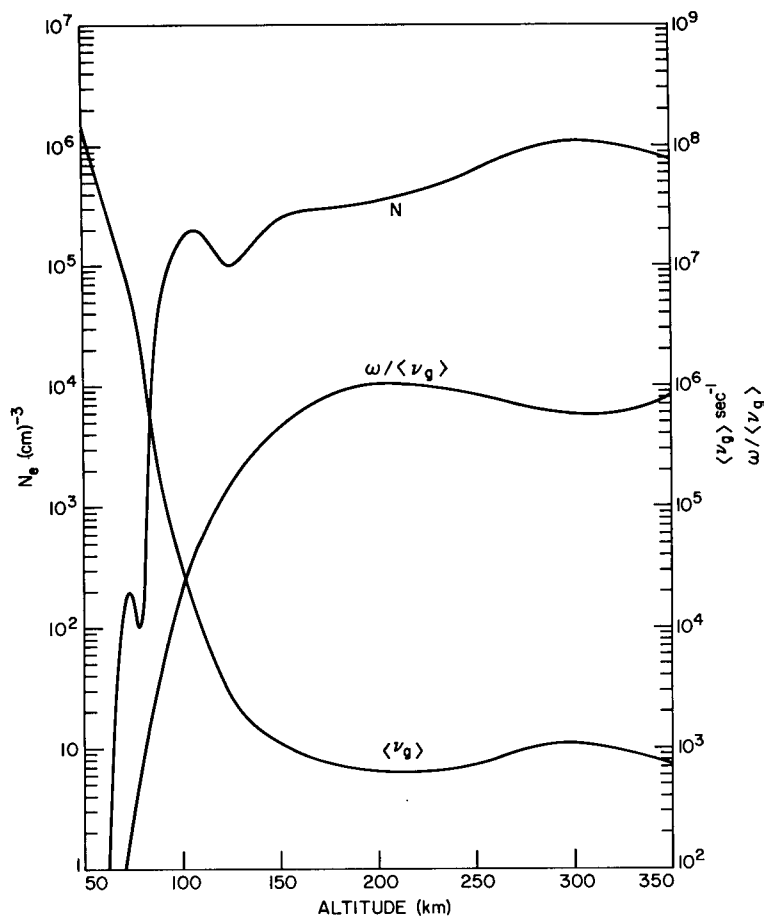


Fig. A2 - Electron density and collision frequency vs altitude, from Shkarofsky (7)

frequency (ν_{e-i}) is proportional to electron density. If we assume no further production after the initial deposition and assuming that electron density changes are controlled primarily by electron-ion recombination, at least at early times following the blast, then the time decay of electron density can be given by

$$N(t) = N_0 / (1 + N_0 \alpha t), \quad (\text{A9})$$

where N_0 = initial electron density

α = "effective" recombination coefficient.

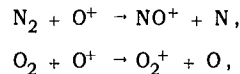
For times such that $N_0 \alpha t \ll 1$, the electron density remains relatively constant at the value N_0 . For times such that $N_0 \alpha t \gg 1$, $N(t) \doteq (\alpha t)^{-1}$. The values assigned to N_0 and α are pivotal to the discussion of changes in collision frequency.

Estimates of α

The value assigned to α depends upon whether one is dealing with monatomic or diatomic ions. For diatomic ions, dissociative recombination is the dominant reaction and $\alpha \approx 10^{-7} \text{ cm}^3/\text{sec}$ for the dominant diatomic ions in the lower ionosphere (below 200 km). For monatomic ions, the radiative recombination coefficient is $\alpha \approx 10^{-13} \text{ cm}^3/\text{sec}$

and the "effective" recombination coefficient is usually controlled by the more rapid chemical reactions of charge exchange and ion—atom interchange.

At F2-region heights, in the normal ionosphere, the primary ionic constituent is O^+ and radiative recombination is so slow that recombination occurs by the indirect route of ion—atom interchange or charge exchange,



followed by dissociative recombination. The decay time in these cases is controlled by the rate of ion—atom interchange or charge exchange and the decay times correspond to values of $\alpha \approx 10^{-9} \text{ cm}^3/\text{sec}$.

It seems to be generally accepted that complete molecular dissociation occurs within the fireball, and the effective recombination coefficient within the fireball is therefore $\alpha \approx 10^{-12} \text{ cm}^3/\text{sec}$.

External to the fireball but still in the F-layer, molecular dissociation of N_2 is probably small and the ion—atom interchange reaction previously cited becomes important in the depletion of O^+ ions. N_2^+ ions formed by the UV fireball will decay by dissociative recombination and/or ion—atom interchange, both of which are relatively rapid for the N_2^+ ion. The net result will be an "effective" recombination coefficient for this case of $\alpha \approx 10^{-8} \text{ cm}^3/\text{sec}$.

For atmospheric regions remote from the fireball region (D- and E-region heights), dissociation will again be negligible and only moderate temperature increases will be assumed. At these altitudes, diatomic molecules predominate. Dissociative recombination of the diatomic ions controls the decay of electron density, and $\alpha \approx 10^{-7} \text{ cm}^3/\text{sec}$.

Estimates of N_0

An upper limit on the initial electron density due to the blast can be established by considering the neutral air density of the undisturbed atmosphere as a limiting factor. The neutral air density at F-layer heights is of the order of $10^9/\text{cm}^3$. Taking account of dissociation, multiply-ionized atoms, and mass contributions due to the weapon, it is estimated that $N_0 \lesssim 10^{10}/\text{cm}^3$ within the fireball and $N_0 \approx 10^9/\text{cm}^3$ in the vicinity of, but external to, the fireball. At E-layer heights the neutral air density is of the order of $10^{10}/\text{cm}^3$, and this is assumed to represent an upper limit on N_0 at these heights.

Within the fireball the estimates $N_0 \approx 10^{10}/\text{cm}^3$ and $\alpha \approx 10^{-12} \text{ cm}^3/\text{sec}$ have been used, leading to the result $N(t) \approx 10^{10}/\text{cm}^3$ (see Eq. (A9)) for the first 100 sec and smaller values for later times. This represents an increase over the normal ionization density by a factor of 10^4 . Assuming nearly compensating temperature effects due to electron collisions with neutrals and with ions, the effect of raising density by a factor of 10^4 is to raise the overall collision frequency from roughly $10^3/\text{sec}$ (see Fig. A2) to $10^7/\text{sec}$ in the vicinity of the fireball. This results in $\omega/\langle\nu_g\rangle \geq 60$ for the frequency range of interest, validating the Shkarofsky high-frequency approximation within the fireball. In the vicinity of the fireball $N(t) \approx 10^9/\text{cm}^3$ for the first 10 sec and takes on smaller values thereafter, and by arguments similar to the preceding ones, the Shkarofsky approximation is validated for this region.

At E-layer heights N_0 has been estimated to be $\lesssim 10^{10}/\text{cm}^3$ and $\alpha \approx 10^{-7} \text{ cm}^3/\text{sec}$. These values imply that $N(t)$ can be as large as $10^{10}/\text{cm}^3$ for the first millisecond, dropping sharply to $5 \times 10^9/\text{cm}^3$ at 1 msec, and dropping by an order of magnitude for each

decade of time increase thereafter. The normal daytime electron density in the E-layer is $\approx 10^5/\text{cm}^3$, and the normal collision frequency is $\approx 10^4/\text{sec}$ (see Fig. A2). Initially, the increase of electron density represents an enhancement factor of 10^5 . Assuming compensating effects due to temperature changes, this would lead to a collision frequency $\approx 10^9/\text{sec}$ and a violation of the Shkarofsky high-frequency approximation. For $t \geq 100$ msec, however, the electron density at E-layer heights drops by two orders of magnitude and $\omega/\langle\nu_g\rangle \approx 60$, justifying the approximation.

The calculations of the preceding paragraphs are rough, but an attempt has been made to be conservative. They indicate that for a nuclear burst in the ionosphere, except for perhaps the first 100 msec following the blast, the Shkarofsky high-frequency approximation is well justified. For a case where $[\omega/\langle\nu_g\rangle] \geq 20$, Shkarofsky [A2] has shown that the error in using the high-frequency approximation is less than 3 percent.

REFERENCES

- A1. Phelps, A.V., and Pack, J.L., "Electron Collision Frequencies in Nitrogen and in the Lower Ionosphere," *Phys. Rev. Lett.* 3 (No. 7):340 (1959)
- A2. Shkarofsky, I.P., "Values of the Transport Coefficients in a Plasma for Any Degree of Ionization Based on a Maxwellian Distribution," *Can. J. Phys.* 39:1619 (1961)
- A3. Shkarofsky, I.P., "Generalized Appleton-Hartree Equation for Any Degree of Ionization and Application to the Ionosphere," *Proc. IRE* 49:1857 (1961)
- A4. Banks, P., "Collision Frequencies and Energy Transfer; Electrons," *Planet. Space Sci.* 14:1085 (1966)
- A5. Hochstim, R.A., "Project Secede September 1969 Summer Study Proceedings, Vol. II—Transport Coefficients and Rates of Collisional Energy Transfer in the Upper Atmosphere," Stanford Research Institute, sponsored by ARPA, Sept. 1969
- A6. Hochstim, R.A., "Collision Frequencies and Electric Conductivities of Weakly Ionized N_2 , O_2 , O , NO and Dry Air," IDA Research Paper, p. 124, Feb. 1965
- A7. Shaeffer, D.L., and Inoue, Y., "A Model Ionosphere for Mid-Day and Mid-Latitude During Sunspot Minimum," University of Pittsburgh, Space Research Coordination Center, SMUP Report 4, July 1968

Appendix B

MODEL ATMOSPHERE

Accurate ray tracing and evaluation of radar performance requires that the propagation medium be well described at all points along the radar ray path. This includes regions of the propagation medium which are affected by the nuclear blast as well as those regions that are substantially unaffected. To this end, models for the ambient troposphere and ionosphere are included as supplementary inputs in addition to the nuclear-blast phenomenology inputs.

The tropospheric model describes refraction and absorption in the lowest 30 km of the atmosphere. An analytical expression for the height dependence of the tropospheric refractive index is the basis of Subroutine RFRAC2. The refractive index in this model decreases exponentially to the free-space value with a scale height of 6.95 km, from a ground-level value of 1.000313. Tropospheric absorption is treated empirically in Subroutine TROPAT, and a detailed description of the model may be found under the description of this subroutine.

The ionospheric model atmosphere includes an ambient model for electron density and electron temperature as well as a model for neutral species number density. The electron density and temperature model is based upon a mid-day, mid-latitude model due to Shaeffer and Inoue.* The neutral atmosphere (N_2 , O_2 , O) is represented by a CIRA† Model 5 atmosphere. The data appear in Subroutine MODATM in the form of data statements, thereby reducing the size of the card deck used for input data. The model atmosphere can readily be altered to correspond to altered atmospheric conditions by making use of the EDIT feature of the O/S 360 system.

The altitude range covered is 30 to 800 km. Access to the data is obtained through a call to Subroutine MODATM which utilizes Subroutine INTERP to carry out the required interpolation between data points. The data tabulate electron density, electron temperature, and number density for molecular oxygen, molecular nitrogen, and atomic oxygen, vs altitude.

In the nuclear-blast phenomenology region, a roster of neutral species and their densities is required for the calculation of electron-neutral collision frequencies. During initial programming of the propagation expressions, there was little evidence that a species roster (of neutral number densities) would be available as one of the phenomenology-derived inputs. It was decided therefore to proceed on the assumption that the ambient composition would be essentially unaltered by the nuclear detonation in the region where collision frequencies are most dependent upon neutral composition, i.e., below 100 km.

Changes in composition for this region could result if energy transport from higher altitudes resulted in appreciable molecular dissociation or a significant change in the chemistry governing equilibrium concentrations. Discussions with phenomenology specialists in the Plasma Physics Division have led to the conclusion that ambient number densities at altitudes below 100 km will remain essentially unchanged at late times following a nuclear disturbance.

*Shaeffer, D.L., and Inoue, Y., "A Model Ionosphere for Mid-day and Mid-latitude during Sunspot Minimum," University of Pittsburgh, Space Research Coordination Center, SMUP Report 4, July 1968.

†Cospar International Reference Atmosphere.

Appendix C

FORTRAN PROGRAM LISTINGS

	DIMENSION TITLE(10)	100
	DIMENSION EL(41),ELAB(41)	200
	DIMENSION JUNKR(61,41),NUMBER(10)	300
C	PHASE 1 DECK	400
C		500
C		600
C	RAEC ... RADAR ATMOSPHERIC EFFECTS PROGRAM	800
C		800
C		900
	DIMENSION R(11)	1000
	DIMENSION ITLIM(9),LABELY(14)	1100
	DIMENSION REFLAB(3),ABSLAB(3),PTHLAB(3),GRPLAB(3),MISLAB(3),	1125
	\$ DEVLAB(3),BLNKST(3)	1150
		1200
		1300
	REAL INDEX1,INDEX2,KAPPA,INC,INC2,NUCOLL,NIT2,NOX2,NOX1,NCT	1400
	REAL NUEI,NUEM,MUU,LIMIT,MU,IN,INDEX,N1,N2,N3,NE	1500
	INTEGER GRPRAY,REFRAY,ABSRAY,RAYPRP	1600
	INTEGER TEE,GEE,ASTER,COL,BLNKS,EXL,AYE	1700
	INTEGER EL,ELAB	1800
	REAL LMU,LABS	1900
	INTEGER DEVRAY	2000
	REAL *8 TITLE,LNCRT,LRFRAY,LGPRAY,	2100
	\$ LMSRAY,LDVRAY,LITEMP,LABRAY,LPLOSS,LABEL	2200
	REAL*8 REFLAB,ABSLAB,PTHLAB,GRPLAB,MISLAB,DEVLAB,BLNKST	2250
		2300
		2400
	COMMON/AR/TEMP(61,41)	2500
	COMMON/BR/GRPRAY(61,41)	2600
	COMMON/CR/REFRAY(61,41)	2700
	COMMON/DR/ABSRAY(61,41)	2800
	COMMON/ER/NCRIT(61,41)	2900
	COMMON/GR/T	3000
	COMMON/HR/INC,NPHI,NTHETA	3100
	COMMON/IR/SPL	3200
	COMMON/JR/MISRAY(61,41)	3300
	COMMON/KR/ITEMP(61,41)	3400
	COMMON/LR/NONE,ISEMIE	3500
	COMMON/MNTP/MTP	3600
	COMMON/NR/ROERR,ROILLM,ROIULM	3700
	COMMON/OR/LMU,LABS,DEL1,DEL2,ITER1,ITER2	3800
	COMMON/PR/HGT	3900
	COMMON/QR/DEVRAY(61,41)	4000
	COMMON/SR/TRMEL(200),TRMAZ(200),TRMR(200),TRMRKK(200),TRMABS(200),	4100
	\$ TRMPL(200),TRMAER(200),TRMRER(200),TRMMSD(200),TRMTMP(200),	4200
	\$ TRMAD(200)	4300
	COMMON/FLAG/IFLAG	4400
		4500
		4600
	DATA NUMBER/' ','1','2','3','4','5','6','7','8','9'/	4700
	DATA ITLIM/200,400,600,800,1000,2000,3000,4000,5000/	4800
	DATA ICHAR/'-'/	4900
	DATA ASTER/'*'/	5000
	DATA BLNKS/' '/	5100
	DATA EXL/'&'/	5200
	DATA COL/'\$'/	5300
	DATA TEE/'\$'/	5400
	DATA GEE/'=''/	5500
	DATA AYE/'-'/	5600
	DATA LABELY/	5700
	\$ 'E',	5800

\$	'L',	5900
\$	'E',	6000
\$	'V',	6100
\$	'A',	6200
\$	'T',	6300
\$	'I',	6400
\$	'U',	6500
\$	'N',	6600
\$	'A',	6700
\$	'N',	6800
\$	'G',	6900
\$	'L',	7000
\$	'E'/'	7100
	DATA LNCRT/' NCRIT '/',LRFRAY/' REFRAY '/', LGPRAY/' GRPRAY '/'	7200
	DATA LMSRAY/' MISRAY '/',LDVRAY/' DEVRAY '/',LITEMP/' ITEMP '/'	7300
	DATA LABRAY/' ABSRAY '/',LPLUS/' PATHLOSS'/'	7400
	DATA REFLAB/'ANGLE ERR. DISPLAY LIMIT'/'	7405
	DATA ABSLAB/'ABSORPTION DISPLAY LIMIT'/'	7410
	DATA PTHLAB/'PATH LOSS DISPLAY LIMIT '/'	7420
	DATA GRPLAB/'RANGE ERR. DISPLAY LIMIT'/'	7430
	DATA MISLAB/'MISS DIST. DISPLAY LIMIT'/'	7440
	DATA DEVLAB/'RAY DEV. DISPLAY LIMIT '/'	7450
	DATA BLNKST/' '/'	7460
	DATA DEGREE/'DEG'/'	7470
	DATA DBS/'DB.'/'	7480
	DATA KMS/'KM.'/'	7490
		7500
		7600
		7700
1	FORMAT(10F8)	7700
2	FORMAT(6F8,I8,F8)	7800
3	FORMAT(E10.4)	7900
4	FORMAT(4I5)	8000
5	FORMAT(8F10)	8100
6	FORMAT(' READ R')	8200
7	FORMAT(4X,4HABSL,	8300
\$	5X,5HRFRCL,	8400
\$	5X,4HGRPL,	8500
\$	6X,4HMISL,	8600
\$	5X,6HRTRGET,	8700
\$	6X,5HPATHL,	8800
\$	6X,5HIFLAG,	8900
\$	4X,4HDEVL)	9000
8	FORMAT(1X,'ELEV =',F11.4,5X,	9100
\$	'AZIMUTH =',F11.4,5X,	9200
\$	'DIST1 =',F11.4,5X,	9300
\$	'RKK =',F7.1,5X,	9400
\$	'ABSDB =',F13.4,/,	9500
\$	1X,'PTHLDB =',F13.4,5X,	9600
\$	'AERROR =',F15.4,5X,	9700
\$	'KERROR =',F13.4,5X,	9800
\$	'DISMIS =',F15.4,5X,	9900
\$	'TEMP =',F15.4,/,	10000
\$	1X,'ADEV =',F15.4)	10100
9	FORMAT(' FR =',E11.4)	10200
10	FORMAT(' NREC '	10300
11	FORMAT(2X,6HTHETMN,4X,6HTHETMX,4X,6HTHETAU,5X,5HELMIN,5X,	10400
\$	5HELMAX,5X,4HELU,7X,3HINC,9X,5HAZERU)	10500
12	FORMAT(' READ TSKY')	10600
13	FORMAT(2H *,' SIGNIFIES OUTPUT AT REFERENCE RANGE',/,	10700
\$	5X,'X, Y, Z ARE IN RADAR COORD SYSTEM RATHER THAN GRND ZERO '	10800
\$	'COORD SYST',/,	10900

```

$ 5X,'ABSDB IS PRINTED INSTEAD OF ABS',/, 11000
$ 5X,'TEMP IS PRINTED INSTEAD OF T') 11100
14 FORMAT(6F10.4,I10,F10.4) 11200
15 FORMAT(2F10,2I10) 11300
16 FORMAT(' DEL1 =',F8.2,5X,'DEL2 =',F8.2,5X,'ITER1 =',I5,5X, 11400
$ 'ITER2 =',I5) 11500
17 FORMAT(///,' THETA R =',F10.4,' DEG.',/, 11600
$ ' PHI =',F10.4,' DEG.',/, 11700
$ ' ELEVATION ANGLE =',F8.2,' DEG.',/,2X, 11800
$ ' K ', ' I ', 11900
$ ' X ', ' Y ', ' Z ', 12000
$ ' DL ', ' PL ', ' DIST1 ', 12100
$ 'ABS/ABSDB ', 'T/TEMP ', 12200
$ ' INDEX2 ', ' DRGRP ', 12300
$ ' WPE ', ' NUCOLL ', 'L3 ', 12400
$ ' RGRP ', ' AERRUR ', 'RERROR ', 'DISMIS') 12500
18 FORMAT(1X,A1, 12600
$ 2I3,3F6,F7.2,F8.2,F7.1,F10.5,F7.1,F8.4,F7.3,F8.1,1X,E10.3, 12700
$ I3,F7.1,F10.6,2F7.2) 12800
19 FORMAT(I3) 12900
20 FORMAT(' TOO MANY LAYERS') 13000
21 FORMAT(10A8) 13100
22 FORMAT(//) 13200
23 FORMAT(' RAMAX =',F7.2,5X,'RANGE =',F7.2,5X,' THETA =',F7.2,5X, 13300
$ 'COLATI =',F7.2) 13400
24 FORMAT(' TITLE: ',10A8) 13500
25 FORMAT(4F5) 13600
26 FORMAT(' LMU =',F10.6,5X,'LABS =',F10.6,5X, 13700
$ 'ISEMI E =',I5) 13800
27 FORMAT(5A3) 13900
31 FORMAT(10E13.3) 14000
44 FORMAT(3E13.3,3I13) 14100
51 FORMAT(' ABSDB IS ',F14.2) 14200
114 FORMAT(8F10.4) 14300
176 FORMAT ( ' FIRST ENCOUNTER OF CRITICAL ANGLE ... IN TEST ' ) 14400
1247 FORMAT ( ' PTHLDB .GT. PATHL ' ) 14500
1248 FORMAT( ' ABSDB .GT. ABSL ' ) 14600
1400 FORMAT( ' ANTENNA TEMPERATURE = ',F12.1,/, ' ABSORPTION = ',F12.1, 14700
C' DB ' ) 14800
1541 FORMAT(' RAY PATH INTERSECTS THE GROUND, RAY TERMINATED, THETAR=' 14900
$ ',F10.5,' PHI =',F10.5,' DIST1 =',E13.4) 15000
1551 FORMAT(' IMPOSSIBLE SET OF DIRECTION COSINES. THETAR =',F10.5, 15100
$ ' PHI =',F10.5,' DIST1 =',E13.4) 15200
1601 FORMAT(' OVERDENSE MEDIUM ENCOUNTERED. THETAR =',F10.5,' PHI =', 15300
$ F10.5,' DIST1 =',E13.3) 15400
1651 FORMAT(' RAY DEVIATION EXCESSIVE . THETAR =',F10.5,' PHI =',F10.5, 15500
$ ' DIST1 =',E13.3) 15600
19191 FORMAT(' PATH LOSS =',E14.5) 15700
6000 FORMAT(' DIST1.GT.RAMAX') 15800
99997 FORMAT ( ' KKK IS UNDEFINED IN TEST... RESET KKR=0, KKK=0' ) 15900
16000
16100
C''''R = RANGE ARRAY. 16200
C''''ABS L = ABSORPTION LIMIT. 16300
C''''RFRCL = ANGLE ERROR LIMIT. 16400
C''''GRPL IS RADAR RANGE-ERROR LIMIT 16500
C''''MISSL IS RADAR MISS DISTANCE LIMIT 16600
C''''ROERR IS A ROUND OFF ERROR PARAMETER 16700
C''''DEL1 DETERMINES MAXIMUM RAY PATH STEP SIZE IN A NON-REFRACTING 16800
C ENVIRONMENT 16900
C''''ROERR IS A ROUND OFF ERROR PARAMETER 17000

```

C''''DEL2 DETERMINES MAXIMUM STEP SIZE IN A REFRACTING ENVIRONMENT	17100
C''''ITER1 DETERMINES MINIMUM RAY PATH STEP SIZE IN A NON-REFRACTING ENVIRONMENT	17200
C''''ITER2 DETERMINES MINIMUM STEP SIZE IN A REFRACTING ENVIRONMENT	17300
C''''LMU IS THE GRANULARITY LIMIT ON REFRACTIVE INDEX	17400
C''''LABS IS THE GRANULARITY LIMIT ON INCREMENTAL ABSORPTION	17500
C''''DEVL IS THE RAY DEVIATION LIMIT IN DEGREES	17600
C''''NONE AND ISEMIE ARE PARAMETERS WHICH CONTROL THE EXTENT OF THE ON-LINE PRINTOUT	17700
C''''COLATI = COLAT1 IS THE COLATITUDE OF THE RADAR IN DEGREES.	17800
C''''THETAR IS POINTING AZIMUTH OF RADAR IN RADIANS	17900
C''''THETA IS AZMUTH OF GROUND ZERO, MEASURED FROM THE RADAR, IN RADIAN	18000
C''''RAMAX IS THE MAXIMUM DISTANCE TO WHICH THE RAY IS TRACED	18100
C''''NREC IS THE NUMBER OF THE TIME STEP	18200
C''''DIST1 IS LENGTH OF CHORD SUBTENDEED BY RAY PATH	18300
C''''WR IS THE RADAR ANGULAR FREQUENCY IN MEGA-RADIANS PER SECOND	18400
C''''ATF IS ATTENUATION FACTOR.	18500
C''''NRAY IS NUMBER OF RAY	18600
C''''NPLA IS NUMBER OF POLAR ANGLES AROUND BURST.	18700
C''''THETMN IS THE SMALLEST ANGLE IN THE AZIMUTH LOOP. READ IN IN DEGREES.	18800
C''''THETMX IS THE LARGEST ANGLE IN THE AZIMUTH LOOP. READ IN IN DEGREE	18900
C''''THETAO IS THE AZIMUTHAL ANGLE FOR THE ENGAGEMENT COMPUTATION. READ IN IN DEGREES.	19000
C''''PHIMN IS THE SMALLEST ANGLE IN THE ZENITH ANGLE LOOP. READ IN IN DEGREES.	19100
C''''PHIMX IS THE LARGEST ANGLE IN THE ZENITH ANGLE LOOP. READ IN IN DEGREES.	19200
C''''PHIU IS THE ZENITH ANGLE FOR AN ENGAGEMENT COMPUTATION. READ IN IN DEGREES.	19300
C''''INC IS THE ANGULAR RESOLUTION OF THE CALCULATION. READ IN IN DEGREE	19400
C''''RADAR ZENITH ANGLE IS DEFINED AS THE COMPLEMENT OF RADAR BORESIGHT	19500
C''''TSKY IS AVERAGE SKY TEMPERATURE.	19600
LL=1	20100
NI=61	20200
MI=41	20300
DO 1355 ILJ = 1,MI	20400
ELAB(ILJ) = BLNKS	20500
1355 EL(ILJ) = BLNKS	20600
ROERR= 1. E-5.	20700
RO1LLM=1.-ROERR	20800
RO1ULM=1.+ROERR	20900
READ 27, ELAB(41), ELAB(31), ELAB(21), ELAB(11), ELAB(1)	21000
READ 21,TITLE	21100
READ 15,DEL1,DEL2,ITER1,ITER2	21200
READ 15,LMU,LABS,ISEMIE	21300
READ 25,RAMAX,RANGE,THETA,COLATI	21400
READ 1,(R(I),I=1,10)	21500
READ 2,ABSL,RFRCL,GRPL,MISL,RTRGET,PATHL,IFLAG,DEVL	21600
READ 3,FR	21700
READ 4,NREC	21800
READ 5,THETMN,THETMX,THETAO,ELMIN,ELMAX,EL EU,INC,AZERU	21900
READ 1,TSKY	22000
PRINT 24,TITLE	22100
PRINT 16,DEL1,DEL2,ITER1,ITER2	22200
	22300
	22400
	22500
	22600
	22700
	22800
	22900
	23000
	23100

```

PRINT 26,LMU,LABS,      ISEMIE                23200
PRINT 23,RAMAX,RANGE,THETA,COLATI            23300
PRINT 6                                                    23400
PRINT 1,R                                                    23500
PRINT 7                                                    23600
PRINT 14,ABSL,RFRCL,GRPL,MISL,RTRGET,PATHL,IFLAG,DEVL    23700
PRINT 9,FR                                                    23800
PRINT 10                                                    23900
PRINT 4,NREC                                                24000
PRINT 11                                                    24100
PRINT 114,THETMN,THETMX,THETAU,ELMIN,ELMAX,ELEU,INC,AZERU 24200
PRINT 12                                                    24300
PRINT 1,TSKY                                                24400
                                                    24500
                                                    24600
EDGE L=AZERO-INC*NI/2                                     24700
EDGE R=AZERO+INC*NI/2                                     24800
IF(THETMN.GE.EDGE L.AND.THETMX.LE.EDGER) GO TO 70        24900
IF(THETMN.GE.EDGE L) GO TO 60                            25000
THETMN=EDGE L                                            25100
60 IF(THETMX.LE.EDGER) GO TO 70                            25200
THETMX=EDGER                                             25300
70 CONTINUE                                              25400
EDGE L=THETMN                                            25500
EDGER=THETMX                                             25600
99998 CONTINUE                                           25700
                                                    25800
                                                    25900
C''''''INITIALIZE SHADEPLUT ARRAYS                       26000
I=0                                                       26100
CALL INIT(NCRIT,NI,MI)                                   26200
CALL INIT(ITEMP,NI,MI)                                   26300
CALL INIT(GRPRAY,NI,MI)                                   26400
CALL INIT(REFRAY,NI,MI)                                   26500
CALL INIT(ABSRAY,NI,MI)                                   26600
CALL INIT(MISRAY,NI,MI)                                   26700
CALL INIT(DEVRAY,NI,MI)                                   26800
DO 50 I = 1,NI                                           26900
DO 50 J = 1,MI                                           27000
TEMP(I,J)=0.0                                           27100
50 CONTINUE                                              27200
                                                    27300
                                                    27400
C''''''DEFINE ELEVENTH REFERENCE RANGE SO THAT IT IS GREATER THAN RAMAX 27500
DO 99999 I=2,11                                          27600
99999 IF(R(I).LT.R(I-1))R(I)=RAMAX+11.                  27700
                                                    27800
                                                    27900
C''''''CONVERT ALL ANGLES FROM DEGREES INTO RADIAN      28000
RADS=1.7453292512E-2                                     28100
PI=3.141592654                                           28200
PHIMN=90.0-ELMAX                                          28300
PHIMX=90.0-ELMIN                                          28400
PHIU=90.0-ELEU                                           28500
ELEV=ELMAX                                                28600
COLATI =COLATI*RADS                                       28700
THETA=THETA*RADS                                          28800
DEVL=DEVL*RADS                                           28900
THETMN=THETMN*RADS                                       29000
THETMX=THETMX*RADS                                       29100
THETAU=THETAU*RADS                                       29200

```

PHIMN=PHIMN*RADS	29300
PHIMX=PHIMX*RADS	29400
PHIU=PHIU*RADS	29500
INC=INC*RADS	29600
INC2 = INC/2.0	29700
WR=2.*PI*FR	29800
	29900
	30000
C''''''READ IN PHENOMENOLGY DATA AT TIME STEP PRESCRIBED BY NREC	30100
C NA IS THE NUMBER OF THE LAST RECORD READ	30200
C RANGE IS DISTANCE BETWEEN RADAR AND GROUND ZERO.	30300
C RMAX IS THE MAX RADIUS OF THE PHENOM REGION	30400
C HGT IS THE HEIGHT OF THE CENTER OF THE PHENOM REGION	30500
NA=0	30600
	30700
100 CALL PRELDA(NREC,NA,WR,RMAX,HGT)	30800
	30900
	31000
C''''''INITIAL CONDITIONS AT START OF TIME STEP	31100
NTHETA=1	31200
NPHI=1	31300
IPLC=0	31400
110 CONTINUE	31500
NHTA=1	31600
NPH=1	31700
	31800
	31900
	32000
C'''''' START RAY PATH SIMULATION	32100
	32200
150 CONTINUE	32300
149 CONTINUE	32400
	32500
	32600
C''''''ADVANCE ELEVATION AND AZIMUTH TO STARTING POINT OF SECTOR SCAN	32700
PHI = (NPH - 1) * INC	32800
JPR=PHI*1000.	32900
JPM=PHIMN*1000.	33000
IF(JPR.LT.JPM)GO TO 151	33100
GO TO 152	33200
151 NPH =NPH +1	33300
GO TO 149	33400
152 CONTINUE	33500
155 CONTINUE	33600
THETAR = (NTH TA-1) * INC - PI/2.0	33700
JTR=THETAR*1000.	33800
JTM = THETMN * 1000.	33900
IF(JTR.LT.JTM)GO TO 156	34000
GO TO 157	34100
156 NTH TA=NTH TA+1	34200
GO TO 155	34300
	34400
	34500
157 CONTINUE	34600
	34700
	34800
C'''''' INITIAL CONDITIONS AT START OF RAY	34900
KA=0	35000
K=0	35100
SPL=0.0	35200
RKK=0.0	35300

KKR=0	35400
KKK=0	35500
ABS=0.	35600
RGRP=0	35700
DEL=DEL1	35800
ITER=ITER1	35900
ITROP=0	36000
	36100
C KA IS 0 IF RAY IS NOT YET BENT--SET TO 2 AFTER THE FIRST BEND.	36200
C K IS NUMBER OF THE BEND IN PROCESS	36300
C SPL = ARC LENGTH ALONG CURVED RAY PATH	36400
	36500
	36600
C*****FREE SPACE CONDITIONS	36700
INDEX1=1.0	36800
KAPPA=0	36900
DRGRP=1.	37000
I=1	37100
	37200
	37300
C INITIAL POSITION OF THE RAY IN THE RADAR COORDINATE SYSTEM	37400
XPL=0.0	37500
YPL=0.0	37600
ZPL=0.0	37700
	37800
	37900
	38000
C*****C1,C2,C3, ARE DIRECTION COSINES OF RAY IN RADAR COORDINATE SYSTEM	38100
C*****THETAR IS THE POINTING AZIMUTH OF THE RADAR IN RADIANS	38200
C PHI IS RADAR ZENITH ANGLE IN RADIANS	38300
APHI=PHI*(180.0/PI)	38400
C1=SIN(PHI)*SIN(THETAR)	38500
C2=SIN(PHI)*COS(THETAR)	38600
C3=COS(PHI)	38700
C10 = C1	38800
C20 = C2	38900
C30= C3	39000
	39100
	39200
C*****R1,R2,R3 ARE THE DIRECTION COSINES OF THE REFRACTED RAY	39300
R1=C1	39400
R2=C2	39500
R3=C3	39600
	39700
	39800
C*****RADAR POSITION IS	39900
X=0.0	40000
Y=0.0	40100
Z=0.0	40200
	40300
	40400
C*****CONVERT RADAR POSITION COORDINATES TO GROUND ZERO COORDINATE SYSTEM	40500
CALL XCOORD(X,Y,Z,XB,YB,ZB,RANGE,COLATI,THETA)	40600
	40700
C*****XPLU,YPLO,ZPLO ARE THE RADAR POSITION COORDS IN GROUND ZERO	40800
C COORDINATE SYSTEM	40900
XPLU=XB	41000
YPLU=YB	41100
ZPLU=ZB	41200
	41300
	41400
C*****CONVERT RADAR POINTING VECTOR TO VECTOR IN GROUND ZERO COORD	

C	SYSTEM	41500
	CALL XDRCUS(C1,C2,C3,XB,YB,ZB,RANGE,CULATI,THETA)	41600
	C1=XB	41700
	C2=YB	41800
	C3=ZB	41900
	THETAD=THETAR/RADS	42000
	PHID=PHI/RADS	42100
	PRINT 13	42200
	PRINT 17,THETAD,PHID,ELEV	42300
		42400
		42500
		42600
	C'''''' START OF STRAIGHT LINE RAY PATH SEGMENT	42700
C	PL IS THE LENGTH OF A STRAIGHT LINE SEGMENT	42800
C	KU IS NUMBER OF BENDS PRIOR TO CURRENT STEP	42900
		43000
200	L3=1	43100
	DABS=0.0	43200
	PL=0.0	43300
	KU=K	43400
	K=K+1	43500
	IRMAX=11.*DEL	43600
	XPL1=XPL	43700
	YPL1=YPL	43800
	ZPL1=ZPL	43900
		44000
	C'''''' START OF RAY PATH ITERATION LOUP (CONSTRUCTION OF BEND SEGMENT)	44100
		44200
	DO 400 J=1,IRMAX	44300
	DL=DEL/(10** (L3-1))	44400
		44500
		44600
	C'''''' STEPPING ROUTINE TO BE FOLLOWED IN THE VICINITY OF A CRITICAL	44700
C	KKR IS INITIALIZED TO ZERO	44800
C	KKK IS INITIALIZED TO ZERO	44900
C	KKR IS SET TO FIVE AT THE FIRST 1 KM. STEP THAT EXCEEDS THE	45000
C	CRITICAL ANGLE.	45100
C	IT CAUSES THE RAY TO STEP BACK A DISTANCE DL AND ALSO TO REDUCE	45200
C	THE MAXIMUM STEP SIZE BY A FACTOR OF 10.	45300
C	KKK IS SET TO 1 WHEN THE CRITICAL ANGLE IS EXCEEDED AND THEREAFTER	45400
C	CUUNT STEPS UNTIL THE ANGLE IS EXCEEDED AGAIN	45500
C	KKR=5 AND KKK GREATER THAN 1 FORCES THE RAY TO BEND AFTER EACH 100	45600
C	METER STEP.	45700
C	THE SECOND ENCOUNTER OF THE CRITICAL ANGLE SETS KKR=6, FORCES THE	45800
C	RAY TO STEP BACK DL, AND FORCES A REDUCTION OF STEP SIZE BY AN	45900
C	ADDITIONAL FACTOR OF 10 WITH A BEND AFTER EACH STEP.	46000
C	THE THIRD ENCOUNTER OF THE CRITICAL ANGLE RESETS KKR=7 THE RAY	46100
C	DOES NOT STEP BACK AND A CRITICAL REFLECTION IS EXECUTED IN BEND	46200
C	KKR AND KKK ARE RESET TO ZERO IN BEND AFTER CRITICAL REFLECTION IS	46300
C	THE OBJECT OF TAKING SMALL STEPS AT THE CRITICAL REFLECTION	46400
C	POINT IS TO MAKE THE CRITICAL ANGLE AS CLOSE TO PI/2. AS IS	46500
C	PRACTICAL, THUS MINIMIZING THE DISTINCTION	46600
C	BETWEEN A CONTINUOUS MEDIUM AND THE SLAB APPROXIMATION TO THE	46700
C	CONTINUOUS MEDIUM.	46800
		46900
		47000
	C'''''' CHECK ON STATUS OF CRITICAL REFLECTION FLAG	47100
	IF (KKR .EQ. 0) GO TO 180	47200
	IF (KKR .EQ. 5) GO TO 171	47300
	IF (KKR .EQ. 6) GO TO 172	47400
	PRINT 99997	47500

KKR=0	47600
KKK=0	47700
GU TU 180	47800
	47900
	48000
C''''SET STEP SIZE IN CRITICAL REFLECTION REGION	48100
171 DL=DEL/(10**L3)	48200
KKK=KKK+1	48300
GU TU 180	48400
172 DL=DEL/(10**(L3+1))	48500
KKK=KKK+1	48600
GU TU 180	48700
175 DL=0.0	48800
KKK=1	48900
IF(ISEMIE.EQ.0)GO TO 180	49000
PRINT 176	49100
	49200
	49300
	49400
180 CONTINUE	49500
IF(ITER-L3.LT.0.AND.KKR.EQ.6) GO TO 455	49600
PL=PL+DL	49700
IF(KU.EQ.0)GO TO 300	49800
250 X=XPL1 +PL*C1	49900
Y=YPL1 +PL*C2	50000
Z=ZPL1 +PL*C3	50100
GO TU 350	50200
300 X=XPLU+PL*C1	50300
Y=YPLU+PL*C2	50400
Z=ZPLU+PL*C3	50500
350 XPL =X	50600
YPL = Y	50700
ZPL = Z	50800
DIST=(XPL -XPLU)**2+(YPL -YPLU)**2+(ZPL -ZPLU)**2	50900
IF (DIST .LE. ROERR) DIST=0.	51000
DIST1=SQRT(DIST)	51100
	51200
	51300
C''''CHECK FOR TARGET ENGAGEMENT RANGE	51400
C IF YES AND L3EQUALS ITER , GO TO BEND	51500
C IF YES AND L3 IS LESS THAN ITER THEN STEP BACKAND REDUCE SIZE OF	51600
C SUBSEQUENT STEPS	51700
IF(RTRGET.GE.DIST1-DL.AND.RTRGET.LT.DIST1.AND.ITER.EQ.L3) GO TO455	51800
IF(RTRGET.GE.DIST1-DL .AND.RTRGET.LT.DIST1) GO TO 399	51900
	52000
C ''' CHECK TO SEE IF RAMAX IS EXCEEDED, IF YES STEP BACK AND TAKE	52100
C SMALLER STEPS.	52200
IF(DIST.GT.RAMAX**2.AND.L3.LT.ITER)GO TO 399	52300
IF(DIST.GE.RAMAX**2.AND.L3.GE.ITER)GO TU 550	52400
	52500
	52600
C''''GO TO TEST FOR CHECK ON GRANULARITY CRITERIA AND CRITICAL REFLECTI	52700
C CONDITIONS	52800
	52900
CALL TEST(X,Y,Z,PL,L3,INDEX1,RKK,DEL,DL,DABS,INDEX2,XPLU,YPLU,	53000
\$ ZPLU,RAMAX,T,I,NUCOLL,WR,WPE,KAPPA,RGRP,DRGRP,	53100
\$ TEMP(NTHETA,NPHI),ABSDB,ITER,ABS,N1,N2,N3,DWP,C1,C2,C3,KKR,	53200
\$ KKK,IRMAX,DIST,ARGIN,ITROP)	53300
	53400
IF (DIST .LE. ROERR) DIST=0.	53500
DIST1=SQRT(DIST)	53600

	53700
	53800
C''''''CHECK ON TERMINATION CONDITIONS	53900
C OVERDENSE MEDIUM	54000
C IMPOSSIBLE SET OF DIRECTIONS	54100
C RAY INTERSECTION WITH GROUND	54200
IF(RKK.NE.5.AND.RKK.NE.25.AND.RKK.NE.100)GO TO 88	54300
	54400
	54500
C''''''RAY TERMINATED...CALCULATE ERROR QUANTITIES	54600
CALL GEUM(X,Y,Z,C10,C20,C30,RGRP,DIST1,RError,AError,DISMIS,RANGE,	54700
\$ COLATI,THETA,XB,YB,ZB)	54800
IAST=ASTER	54900
PRINT 18,IAST,	55000
\$ K,I,XB,YB,ZB,DL,PL,DIST1,ABSDB,TEMP(NTHETA,NPHI),INDEX2,	55100
\$ DRGRP,WPE,NUCOLL,L3,	55200
\$ RGRP,AError,RError,DISMIS	55300
IF(RKK.EQ.5)GO TO 1540	55400
IF(RKK.EQ.25)GO TO 1600	55500
IF(RKK.EQ.100)GO TO 1550	55600
360 CONTINUE	55700
88 CONTINUE	55800
	55900
	56000
C''''''CHECK ON STATUS OF REFLECTION FLAG	56100
IF(KKR.EQ.5.AND.KKK.EQ.0)GO TO 175	56200
IF(KKR.EQ.5.AND.KKK.GE.1)GO TO 450	56300
IF (KKR .EQ. 6 .AND. KKK .LT. 0) GO TO 175	56400
IF (KKR .EQ. 6 .AND. KKK .GE. 1) GO TO 450	56500
IF (KKR .EQ. 7) GO TO 450	56600
	56700
	56800
C EXIT POINT FOR BEND	56900
IF(L3.GT.ITER) GO TO 450	57000
	57100
	57200
C TEST FOR DISPLAY RANGE IF YES, INCREMENT I	57300
IF(DIST1.LT.R(I)) GO TO 400	57400
TEMP(NTHETA,NPHI)=TEMP(NTHETA,NPHI)+	57500
\$EXP(-2.*ABS)* (1.-EXP(-2.*DABS)) * T	57600
SPL=SPL+PL	57700
ABS=ABS+DABS	57800
DBPNP=8.685896	57900
ABSDB=2.*DBPNP*ABS	58000
GO TO 1200	58100
C''''''STATEMENT 1200 IS THE POINT AT WHICH ERROR QUANTITIES ARE CALCULAT	58200
C PRIOR TO SETTING UP THE SHADEPLOT ARRAYS FOR THE OUTPUT SKYMAPS	58300
	58400
	58500
399 PL=PL-DL	58600
L3=L3+1	58700
ITER=ITER1	58800
IRMAX=IRMAX+1	58900
400 CONTINUE	59000
C''''''END OF STRAIGHT LINE RAY PATH SEGMENT TERMINAL STATEMENT OF	59100
C RAY STEPPING LOUP	59200
	59300
	59400
GO TO 455	59500
450 CONTINUE	59600
KA=2	59700

	59800
	59900
	60000
C''''''PREPARATIONS FOR BEND SUBROUTINE	60100
	60200
	60300
DABS=DABS+KAPPA*DL	60400
RGRP=RGRP+DRGRP*DL	60500
PL=PL+DL	60600
DIST=(X-XPLU)**2+(Y-YPLU)**2+(Z-ZPLU)**2	60700
IF (DIST .LE. ROERR) DIST=0.	60800
DIST1=SQRT(DIST)	60900
455 CONTINUE	61000
SPL=SPL+PL	61100
TEMP(NTHETA,NPHI)=TEMP(NTHETA,NPHI)+	61200
\$EXP(-2.*ABS)* (1.-EXP(-2.*DABS)) * T	61300
ABS=ABS+DABS	61400
DBPNP=8.685896	61500
ABSDB=2.*DBPNP*ABS	61600
IF(DIST1.LT.R(I))GO TO 460	61700
GO TO 1200	61800
460 CONTINUE	61900
	62000
C''''''DU A REFRACTIVE BEND	62100
CALL BEND(X,Y,Z,C1,C2,C3,INDEX1,R1,R2,R3,INDEX2,RKK,WR,WPE	62200
C,NUCOLL,N1,N2,N3,DWP,KKR,KKK,ARGIN,RANGE,COLATI,THETA)	62300
	62400
C1=R1	62500
C2=R2	62600
C3=R3	62700
NUM=1	62800
IF(ISEMIE.EQ.0)GO TO 462	62900
IAST=BLNKS	63000
PRINT 18,IAST,	63100
\$ K,I,X,Y,Z,DL,PL,DIST1,ABS,T,INDEX2,DRGRP,WPE,NUCOLL,L3	63200
462 CONTINUE	63300
465 CONTINUE	63400
	63500
	63600
	63700
INDEX1 = INDEX2	63800
	63900
	64000
C''''''TEST FOR REFERENCE RANGE ,YES ...GO TO SHDRAY PROCESSING	64100
C NO.....PROCEED TO NEXT BEND	64200
IF(RTRGET.GE.DIST1-DL.AND.RTRGET.LT.DIST1) GO TO 650	64300
	64400
	64500
C''''''CHECK RAY DISPLACEMENT AGAINST RAMAX IN EXCESS, BACKTRACK,	64600
C USE SMALLER STEPS	64700
IF(DIST.GE.RAMA X**2) GO TO 550	64800
	64900
	65000
C''''''CHECK NO. OF BENDS AGAINST 999 LIMIT, YES ... PRINTOUT	65100
IF(998-K.LT.0)GO TO 500	65200
	65300
	65400
C''''''IN THE BEND REGION USE DEL=DEL2, ITER=ITER2	65500
DEL=DEL2	65600
ITER=ITER2	65700
	65800
C''''''GO TO START OF NEXT STRAIGHT LINE SEGMENT	

GO TO 200	65900
	66000
	66100
C''''RAY TERMINATED BECAUSE OF TOO MANY BENDS...CALCULATE ERROR QUANTIT	66200
500 CONTINUE	66300
PRINT 20	66400
RKK=200	66500
CALL GEUM(X,Y,Z,C10,C20,C30,RGRP,DIST1,RERROR,AERROR,DISMIS,RANGE,	66600
\$ COLATI,THETA,XB,YB,ZB)	66700
IAST=ASTER	66800
PRINT 18,IAST,	66900
\$ K,I,XB,YB,ZB,DL,PL,DIST1,ABSDB,TEMP(NTHETA,NPHI),INDEX2,	67000
\$ DRGRP,WPE,NUCOLL,L3,	67100
\$ RGRP,AERROR,RERROR,DISMIS	67200
IP=TEE	67300
GO TO 1700	67400
	67500
	67600
C''''DISTANCE TO RAY TIP EXCEEDS MAX RANGE...ADD CONTRIBUTION OF TSKY	67700
C TO APPARENT SKY TEMPERATURE AND THEN PROCEED TO NEXT RAY	67800
550 CONTINUE	67900
PRINT 6000	68000
875 CONTINUE	68100
CALL GEUM(X,Y,Z,C10,C20,C30,RGRP,DIST1,RERROR,AERROR,DISMIS,RANGE,	68200
\$ COLATI,THETA,XB,YB,ZB)	68300
890 CONTINUE	68400
TEMP(NTHETA,NPHI)=TEMP(NTHETA,NPHI)+EXP(-2.0*ABS)*TSKY	68500
GO TO 1250	68600
	68700
	68800
C''''TEST FOR TARGET ENGAGEMENT DIRECTION	68900
650 CONTINUE	69000
IF(THETA.GE.THETAU-INC2.AND.THETA.LE.THETAU+INC2.AND.	69100
\$ PHI.GE.PHI0-INC2.AND.PHI.LE.PHI0+INC2) GO TO 700	69200
GO TO 851	69300
	69400
C''''CALCULATE ERROR QUANTITIES	69500
700 CONTINUE	69600
750 CALL GEUM(X,Y,Z,C10,C20,C30,RGRP,DIST1,RERROR,AERROR,DISMIS,RANGE,	69700
\$ COLATI,THETA,XB,YB,ZB)	69800
IAST=ASTER	69900
PRINT 18,IAST,	70000
\$ K,I,XB,YB,ZB,DL,PL,DIST1,ABSDB,TEMP(NTHETA,NPHI),INDEX2,	70100
\$ DRGRP,WPE,NUCOLL,L3,	70200
\$ RGRP,AERROR,RERROR,DISMIS	70300
IF(IFLAG.EQ.0) GO TO 812	70400
PTHLDB=ABSDB+120.0+40.0*ALOG10(DIST1)	70500
PRINT 19191,PTHLDB	70600
812 CONTINUE	70700
850 CONTINUE	70800
851 CONTINUE	70900
DEL=DEL2	71000
ITER=ITER2	71100
	71200
C''''GO TO START OF NEXT STRAIGHT LINE SEGMENT	71300
GO TO 200	71400
	71500
	71600
C''''RANGE EQUALS A REFERENCE RANGE...CALCULATE ERROR QUANTITIES	71700
	71800
1200 CONTINUE	71900

```

CALL GEOM(X,Y,Z,C10,C20,C30,RGRP,DIST1,RERROR,AERROR,DISMIS,RANGE, 72000
$ COLATI,THETA,XB,YB,ZB) 72100
IAST=ASTER 72200
PRINT 18,IAST, 72300
$ K,I,XB,YB,ZB,DL,PL,DIST1,ABSDB,TEMP(NTHETA,NPHI),INDEX2, 72400
$ DRGRP,WPE,NUCOLL,L3, 72500
$ RGRP,AERRUR,RERROR,DISMIS 72600
72700
72800
C''''''SETUP SHADEPLOT ARRAYS FOR OUTPUT 72900
1240 CONTINUE 73000
CALL SHDRAY(AERROR,RFRCL,REFRAY,I,NTHETA,NPHI) 73100
SCLPRD=C10*R1+C20*R2+C30*R3 73200
IF(SCLPRD.GE.R01LLM.AND.SCLPRD.LE.R01ULM) SCLPRD=1.0 73300
ADEV=ARCOS(SCLPRD) 73400
ADEV0=ADEV/RADS 73500
CALL SHDRAY(ADEV,DEVL,DEVRAY,I,NTHETA,NPHI) 73600
CALL SHDRAY(RERROR,GRPL,GRPRAY,I,NTHETA,NPHI) 73700
CALL SHDRAY(DISMIS,MISL,MISRAY,I,NTHETA,NPHI) 73800
73900
C''''''IF IFLAG EQUALS 0, MONITOR ABSORPTION...OTHERWISE MONITOR PATHLOSS 74000
IF(IFLAG.EQ.0) GO TO 1241 74100
PTHLDB=ABSDB+120.0+40.0*ALOG10(DIST1) 74200
CALL SHDRAY(PTHLDB,PATHL,ABSRAY,I,NTHETA,NPHI) 74300
C CHECK ON PATH-LOSS ... IF .GT. PATHL, TERMINATE THE RAY 74400
IF ( PTHLDB .GE. PATHL ) GO TO 1249 74500
GO TO 1245 74600
1241 CONTINUE 74700
CALL SHDRAY(ABSDB,ABSL,ABSRAY,I,NTHETA,NPHI) 74800
C CHECK ON ABSORPTION...IF .GT. ABSL, TERMINATE THE RAY 74900
IF(ABSDB .GE. ABSL)GO TO 1249 75000
1245 CONTINUE 75100
I=I+1 75200
75300
75400
C''''''CHECK ON RAY DEVIATION...IF GREATER THAN LIMIT, TERMINATE THE RAY 75500
XDEV=COS(DEVL) 75600
IF(SCLPRD.LE.XDEV.AND.RKK.NE.100.0)GO TO 1650 75700
75800
GO TO 460 75900
C''''''STATEMENT 460 PRECEDES THE BEND SUBROUTINE ... A SLAB OF THE 76000
C MEDIUM IS ALWAYS TERMINATED AT A REFERENCE RANGE. 76100
76200
76300
C''''''MARK SHADEPLOT ARRAYS ACCORDING TO REASON FOR TERMINATIUN 76400
1249 IF(REFRAY(NTHETA,NPHI).EQ.BLNKS )REFRAY(NTHETA,NPHI)=ICHR 76500
IF(ABSRAY(NTHETA,NPHI).EQ.BLNKS )ABSRAY(NTHETA,NPHI)=ICHR 76600
IF(GRPRAY(NTHETA,NPHI).EQ.BLNKS )GRPRAY(NTHETA,NPHI)=ICHR 76700
IF(MISRAY(NTHETA,NPHI).EQ.BLNKS )MISRAY(NTHETA,NPHI)=ICHR 76800
IF(DEVRAY(NTHETA,NPHI).EQ.BLNKS )DEVRAY(NTHETA,NPHI)=ICHR 76900
IP=AYE 77000
RKK=1 77100
IF ( IFLAG .EQ. 0) GO TO 1242 77200
PRINT 1247 77300
GO TO 1250 77400
1242 CONTINUE 77500
PRINT 1248 77600
77700
77800
77900
C''''''PREPARE TO GO TO NEXT RAY 78000

```

		78100
1250	CONTINUE	78200
	PRINT 1400,TEMP(NTHETA,NPHI),ABSDB	78300
	PTHLDB=ABSDB+120.0+40.0*ALOG10(DIST1)	78400
	PRINT 19191,PTHLDB	78500
1260	CONTINUE	78600
	IF(RKK.EQ.0.OR.LL.GT.200)GO TO 1265	78700
	IF(RKK.NE.100.AND.RKK.NE.200)GO TO 1263	78800
	ABSDB=0	78900
	PTHLDB=0	79000
	AERRUR=0	79100
	RERRUR=0	79200
	DISMIS=0	79300
	TEMP(NTHETA,NPHI)=0	79400
		79500
		79600
		79700
C''''	SET UP TERMINATION SUMMARY DATA	79800
1263	TRMEL(LL)=ELEV	79900
	TRMAZ(LL)=THETAR/RADS	80000
	TRMK(LL)=DIST1	80100
	TRMKKK(LL)=RKK	80200
	TRMABS(LL)=ABSDB	80300
	TRMPL(LL)=PTHLDB	80400
	TRMAER(LL)=AERRUR	80500
	TRMRER(LL)=RERRUR	80600
	TRMMSD(LL)=DISMIS	80700
	TRMTMP(LL)=TEMP(NTHETA,NPHI)	80800
	TRMAD(LL)=ADEVD	80900
	LL=LL+1	81000
1265	CONTINUE	81100
	TD=THETAR/RADS	81200
	PRINT 8,ELEV,TD,DIST1,RKK,ABSDB,PTHLDB,AERRUR,RERRUR,DISMIS,	81300
	\$ TEMP(NTHETA,NPHI),ADEVD	81400
		81500
C''''	CONVERT TEMPERATURE TO QUANTIZED VALUES AS DEFINED IN ITLIM ARRAY	81600
	DO 5000 IK=1,9	81700
	IF(ITEMP(NTHETA,NPHI).EQ.COL.OR.ITEMP(NTHETA,NPHI).EQ.EXL)	81800
	\$ GO TO 5050	81900
	IF(TEMP(NTHETA,NPHI).LT.ITLIM(IK))GO TO 4050	82000
	GO TO 5000	82100
4050	ITEMP(NTHETA,NPHI)=NUMBER(IK)	82200
	GO TO 5050	82300
5000	CONTINUE	82400
	ITEMP(NTHETA,NPHI)=NUMBER(10)	82500
		82600
		82700
		82800
5050	CONTINUE	82900
5060	IP=BLNKS	83000
		83100
C'''	STEP ZENITH ANGLE AND CHECK TO SEE IF THE AZIMUTH ANGLE MUST BE	83200
C	STEPPED.	83300
	NPH=NPH+1	83400
	NPHI=NPHI+1	83500
	PHI = (NPH -1) * INC	83600
	ELEV=ELEV-INC/RADS	83700
	JPR=PHI*1000.	83800
	JPM=PHI*M*1000.	83900
	IF(NPHI.GT.MI)GO TO 1300	84000
	IF(JPR.GT.JPM)GO TO 1300	84100

GU TU 150	84200
	84300
	84400
C INCREMENT AZIMUTH ANGLE	84500
1300 NTHETA=NTHETA+1	84600
IF(NTHETA.EQ.2)NPHIMX=NPHI-1	84700
NPH=1	84800
NHTA=NHTA+1	84900
NPHI=1	85000
ELEV=ELMAX	85100
THETAR = (NTH TA-1) *INC - PI/2.0	85200
JTR=THETAR*1000.	85300
JTM = THETMX * 1000.	85400
IF(NTHETA.GT.NI) GU TU 1350	85500
IF(JTR.GT.JTM)GU TU 1350	85600
GU TU 150	85700
	85800
C''''''NURMAL POINT OF RAY TERMINATION	85900
C GU TU NEXT RAY....STATEMENT 150 OR	86000
C GU TU END OF PROGRAM FOR OUTPUT OF DATA...STATEMENT 1350	86100
	86200
	86300
1540 CONTINUE	86400
PRINT 1541,THETAR,PHI,DIST1	86500
IP=GEE	86600
TEMP(NTHETA,NPHI)=TEMP(NTHETA,NPHI) +EXP(-2.*ABS)*290.	86700
GU TU 1750	86800
	86900
	87000
1550 CONTINUE	87100
IP=COL	87200
PRINT 1551,THETAR,PHI,DIST1	87300
GU TU 1700	87400
	87500
	87600
1600 CONTINUE	87700
IP=ASTER	87800
PRINT 1601,THETAR,PHI,DIST1	87900
GU TU 1750	88000
	88100
	88200
1650 CONTINUE	88300
RKK=10	88400
IP=EXL	88500
PRINT 1651,THETAR,PHI,DIST1	88600
	88700
	88800
1700 ITEMP(NTHETA,NPHI)=IP	88900
	89000
	89100
C'''''' MARK SHADEPLOT ARRAYS ACCORDING TO REASON FOR TERMINATION	89200
1750 CONTINUE	89300
IF (REFRAY(NTHETA,NPHI).NE.BLNKS .AND.IP.NE.COL)GU TU 1800	89400
REFRAY(NTHETA,NPHI)=IP	89500
1800 IF (ABSRAY(NTHETA,NPHI).NE.BLNKS .AND.IP.NE.COL)GU TU 1850	89600
ABSRAY(NTHETA,NPHI)=IP	89700
1850 IF (GRPRAY(NTHETA,NPHI).NE.BLNKS .AND.IP.NE.COL)GU TU 1900	89800
GRPRAY(NTHETA,NPHI)=IP	89900
1900 IF (MISRAY(NTHETA,NPHI).NE.BLNKS .AND.IP.NE.COL)GU TU 1950	90000
MISRAY(NTHETA,NPHI)=IP	90100
1950 IF (NCRIT(NTHETA,NPHI).NE.BLNKS .AND.IP.NE.COL)GU TU 2000	90200

NCRIT(NTHETA,NPHI)=IP	90300
2000 IF(DEVRAY(NTHETA,NPHI).NE.BLNKS .AND.IP.NE.COL)GO TU 1250	90400
DEVRAY(NTHETA,NPHI)=IP	90500
	90600
	90700
C''''STATEMENT 1250 IS PREPARATORY TO STARTING A NEW RAY	90800
GO TO 1250	90900
	91000
	91100
C''''PRINT OUTPUT SKYMAPS ON LINE PRINTER	91200
	91300
1350 CONTINUE	91400
N=NI	91500
M=MI	91600
IF(IFLAG.EQ.1)ABSL=PATHL	91700
AL=ELMIN	91800
AS=INC/RADS	91900
RF=WR/(PI*2.0)	92000
BA=HGT	92100
AGZ=THETA/RADS	92200
RGZ=RANGE	92300
TS=NREC	92400
RC=COLATI/RADS	92500
EL(8)=LABELY(1)	92600
EL(10)=LABELY(2)	92700
EL(12)=LABELY(3)	92800
EL(14)=LABELY(4)	92900
EL(16)=LABELY(5)	93000
EL(18)=LABELY(6)	93100
EL(20)=LABELY(7)	93200
EL(22)=LABELY(8)	93300
EL(24)=LABELY(9)	93400
EL(30)=LABELY(10)	93500
EL(32)=LABELY(11)	93600
EL(34)=LABELY(12)	93700
EL(36)=LABELY(13)	93800
EL(38)=LABELY(14)	93900
CALL POSIT(REFRAY,JUNKR,BLNKS,AZERO,EDGEL,AS,NPHIMX,NI,MI)	94300
CALL CONTR(JUNKR,LRFRAY ,RFRCL,AS,RF,R,TITLE,BA,RC,AGZ,RGZ,INC,	94400
\$TS,THETA,PHI,N,M,LL,EL,ELAB,REFLAB,DEGREE)	94500
IF(IFLAG.EQ.0) GO TO 1351	94600
GO TO 1352	94700
1351 LABEL=LABRAY	94800
GO TU 1353	94900
1352 LABEL=LGLOSS	95000
ABSLAB(1)=PTHLAB(1)	95025
ABSLAB(2)=PTHLAB(2)	95050
ABSLAB(3)=PTHLAB(3)	95075
1353 CONTINUE	95100
CALL POSIT(ABSRAY,JUNKR,BLNKS,AZERO,EDGEL,AS,NPHIMX,NI,MI)	95200
CALL CONTR(JUNKR, LABEL, ABSL,AS,RF,R,TITLE,BA,RC,AGZ,RGZ,INC,	95300
\$TS,THETA,PHI,N,M,LL,EL,ELAB,ABSLAB,DBS)	95400
CALL POSIT(GRPRAY,JUNKR,BLNKS,AZERO,EDGEL,AS,NPHIMX,NI,MI)	95500
CALL CONTR(JUNKR,LGPRAY ,GRPL,AS,RF,R,TITLE,BA,RC,AGZ,RGZ,INC,	95600
\$TS,THETA,PHI,N,M,LL,EL,ELAB,GRPLAB,KMS)	95700
CALL POSIT(MISRAY,JUNKR,BLNKS,AZERO,EDGEL,AS,NPHIMX,NI,MI)	95800
CALL CONTR(JUNKR,LMSRAY ,MISL,AS,RF,R,TITLE,BA,RC,AGZ,RGZ,INC,	95900
\$TS,THETA,PHI,N,M,LL,EL,ELAB,MISLAB,KMS)	96000
CALL POSIT(DEVRAY,JUNKR,BLNKS,AZERO,EDGEL,AS,NPHIMX,NI,MI)	96100
CALL CONTR(JUNKR,LDVRAY ,DEVL,AS,RF,R,TITLE,BA,RC,AGZ,RGZ,INC,	96200
\$TS,THETA,PHI,N,M,LL,EL,ELAB,DEVLAB,DEGREE)	96300

NRL REPORT 7284

75

CALL POSIT(ITEMP, JUNKR, BLNKS, AZERO, EDGEL, AS, NPHIMX, NI, MI)	96400
CALL CONTR(JUNKR, LITEMP, U.O, AS, RF, ITLIM,	96500
\$ TITLE, BA, RC, AGZ, RGZ, INC,	96600
\$ TS, THETA, PHI, N, M, -5, EL, ELAB, BLNKST, BLNKS)	96700
1360 CONTINUE	96800
STOP	96900
	97000
	97100
END	97200
	97300

SUBROUTINE BACOUR(X,Y,Z,XB,YB,ZB,RANGE,COLAT1,THETA)	97400
	97500
	97600
REAL INDEX1,INDEX2,KAPPA,INC,INC2,NUCOLL,NIT2,NUX2,NOX1,NCT	97700
REAL NUEI,NUEM,MUU,LIMIT,MU,IN,INDEX,N1,N2,N3,NE	97800
	97900
RE=6371.2	98000
THETAC=RANGE/RE	98100
STC2=SIN(THETAC/2.0)	98200
CTC2=COS(THETAC/2.0)	98300
SINT=SIN(THETA)	98400
COST=COS(THETA)	98500
COSC1=COS(COLAT1)	98600
SINC1=SIN(COLAT1)	98700
COSTC=COS(THETAC)	98800
SINTC=SIN(THETAC)	98900
CHORD=2.0*RE*STC2	99000
PROJ=CHORD*CTC2	99100
XU=PROJ*SINT	99200
YU=PROJ*COST	99300
ZU=CHORD*STC2	99400
COLAT2=ARCOS(COSC1*COSTC+SINC1*SINTC*COST)	99500
SINC2=SIN(COLAT2)	99600
COSC2=COS(COLAT2)	99700
DELTA=ARCSIN(SINTC*SINT/SINC2)	99800
COSD=COS(DELTA)	99900
SIND=SIN(DELTA)	100000
XB=COSD*X-SIND*COSC2*Y+SIND*SINC2*Z	100100
YB=COSC1*SIND*X+(COSC1*COSD*COSC2+SINC1*SINC2)*Y-	100200
\$ (COSD*COSC1*SINC2-SINC1*COSC2)*Z	100300
ZB=-SINC1*SIND*X-(SINC1*COSD*COSC2-COSC1*SINC2)*Y+	100400
\$ (COSD*SINC1*SINC2+COSC1*COSC2)*Z	100500
XB=XB+XU	100600
YB=YB+YU	100700
ZB=ZB-ZU	100800
RETURN	100900
END	101000
	101100

```

SUBROUTINE BEND(X,Y,Z,C1,C2,C3,INDEX1,R1,R2,R3,INDEX2,RKK,WR,WPE      101200
C,NUCOLL,N1,N2,N3,DWP,KKR,KKK,ARGIN,RANGE,CULAT1,THETA)              101300
                                                                    101400
                                                                    101500
COMMUN/LR/NONE,ISEMIE                                              101600
                                                                    101700
                                                                    101800
REAL INDEX1,INDEX2,KAPPA,INC,INC2,NUCOLL,NIT2,NOX2,NOX1,NCT        101900
REAL NU EI,NU EM,MUU,LIMIT,MU,IN,INDEX,N1,N2,N3,NE                 102000
                                                                    102100
                                                                    102200
C''''CHECK FOR OVERDENSE MEDIUM                                     102300
IF(WPE.EQ.-1.) GO TO 300                                           102400
                                                                    102500
                                                                    102600
C''''KKR IS INITIALIZED TO ZERO                                     102700
C   KKK IS INITIALIZED TO ZERO                                     102800
C   KKR IS SET TO FIVE AT THE FIRST 1 KM. STEP THAT EXCEEDS THE   102900
C   CRITICAL ANGLE.                                              103000
C   IT CAUSES THE RAY TO STEP BACK A DISTANCE DL AND ALSO TO REDUCE 103100
C   THE MAXIMUM STEP SIZE BY A FACTOR OF 10.                      103200
C   KKK IS SET TO 1 WHEN THE CRITICAL ANGLE IS EXCEEDED AND THEREAFTER 103300
C   COUNT STEPS UNTIL THE ANGLE IS EXCEEDED AGAIN                 103400
C   KKR=5 AND KKK GREATER THAN 1 FORCES THE RAY TO BEND AFTER EACH 100 103500
C   METER STEP.                                                  103600
C   THE SECOND ENCOUNTER OF THE CRITICAL ANGLE SETS KKR=6, FORCES THE 103700
C   RAY TO STEP BACK DL, AND FORCES A REDUCTION OF STEP SIZE BY AN 103800
C   ADDITIONAL FACTOR OF 10 WITH A BEND AFTER EACH STEP.         103900
C   THE THIRD ENCOUNTER OF THE CRITICAL ANGLE RESETS KKR=7 THE RAY 104000
C   DOES NOT STEP BACK AND A CRITICAL REFLECTION IS EXECUTED IN BEND 104100
C   KKR AND KKK ARE RESET TO ZERO IN BEND AFTER CRITICAL REFLECTION IS 104200
C   THE OBJECT OF TAKING SMALL STEPS AT THE CRITICAL REFLECTION   104300
C   THE OBJECT OF TAKING SMALL STEPS AT THE CRITICAL REFLECTION   104400
C   POINT IS TO MAKE THE CRITICAL ANGLE AS CLOSE TO PI/2. AS IS   104500
C   PRACTICAL, THUS MINIMIZING THE DISTINCTION                   104600
C   BETWEEN A CONTINUOUS MEDIUM AND THE SLAB APPROXIMATION TO THE 104700
C   CONTINUOUS MEDIUM.                                           104800
C   RKK=10 ... RAY DEVIATION EXCESSIVE                            104900
                                                                    105000
                                                                    105100
PI = 3.141592654                                                  105200
                                                                    105300
                                                                    105400
IF (ABS(ARGIN) .EQ. 1. ) GO TO 310                                  105500
IN=ARCOS(ARGIN)                                                    105600
DIV = INDEX1/INDEX2                                                105700
RARG = DIV * SIN(IN)                                               105800
                                                                    105900
                                                                    106000
C''''CHECK CRITICAL REFLECTION CRITERION                           106100
IF(KKR.EQ.7) GO TO 301                                            106200
                                                                    106300
                                                                    106400
C''''IMPLEMENT STANDARD REFRACTION CALCULATION...SNELL,S LAW      106500
R = ARSIN(RARG)                                                    106600
IF (ABS(IN) .GE. PI/2. ) R= PI-R                                  106700
ARGIN2 = COS(R)                                                    106800
FACT = ARGIN2 - DIV * ARGIN                                        106900
R1 = DIV * C1 + FACT * N1                                          107000
R2 = DIV * C2 + FACT * N2                                          107100
R3 = DIV * C3 + FACT * N3                                          107200

```

GO TO 500	107300
	107400
	107500
C''''RAY PARALLEL TO DENSITY GRADIENT...NO REFRACTION	107600
310 R1 = C1	107700
R2 = C2	107800
R3 = C3	107900
RFLTC = ((INDEX2/INDEX1 -1.0)/(INDEX2/INDEX1 + 1.0))**2	108000
GO TO 500	108100
	108200
	108300
C''''MEDIUM OVERDENSE...SET FLAG AND PRINT OUT.	108400
300 CONTINUE	108500
PRINT 217	108600
217 FORMAT(' WPE = -1. MEDIUM IS OVERDENSE IN BEND')	108700
RKK = 25.	108800
GO TO 500	108900
	109000
	109100
C''''EXECUTE CRITICAL REFLECTION	109200
301 CONTINUE	109300
R1=C1-2.0*ARGIN*N1	109400
R2=C2-2.0*ARGIN*N2	109500
R3=C3-2.0*ARGIN*N3	109600
KKK=0	109700
KKR=0	109800
PRINT 218	109900
218 FORMAT(1X,'R GREATER THAN PI/2. WAVE CRITICALLY REFLECTED.')	110000
150 CONTINUE	110100
ANG=(PI/2.0)-IN	110200
ANG=((PI/2.0)-IN)/1.7453292512E-2	110300
CALL BACOUR(X,Y,Z,XBB,YBB,ZBB,RANGE,CULAT1,THETA)	110400
PRINT 1001 , ANG,XBB,YBB,ZBB	110500
1001 FORMAT(' GRAZING ANGLE = ',F10.5,' DEG.',	110600
\$ ' XB =',F10.5,' YB =',F10.5,	110700
\$ ' ZB =',F10.5)	110800
RETURN	110900
	111000
	111100
500 CONTINUE	111200
	111300
	111400
C''''CHECK NU. OF BENDS IN CRITICAL REGION AGAINST ARBITRARY LIMIT	111500
IF (KKK .LT. 20) GO TO 399	111600
KKR=0	111700
KKK=0	111800
399 RETURN	111900
END	112000
	112100

```

SUBROUTINE COLLF(
$      X,Y,Z,TEP,WPE,NUCOLL,NUEI,NUEM,NIT2,NOX2,NOX1,T,NE,
$N1,N2,N3      )
112200
112300
112400
112500
112600
112700
C'''''' CALCULATION OF NUCOLL, THE GENERAL AVERAGE COLLISION FREQUENCY AS
C      DEFINED BY SHKAKOVSKY. IT IS THE ALGEBRAIC SUM OF ELECTRON-
C      NEUTRAL AND ELECTRON-ION COLLISION FREQUENCIES.
112800
112900
113000
113100
C'''''' REVISED COLLISION FREQUENCIES.
113200
113300
113400
C'''''' COLLISION FREQUENCIES ARE INTERPOLATED FROM TABULAR VALUES OF
C      HOCHSTIM IN THE TEMPERATURE RANGE FROM 200 TO 2000 DEGREES K.
C      OUTSIDE THIS RANGE THEY ARE CALCULATED FROM A POWER LAW FIT
C      TO THE EXTRAPOLATED TABULAR VALUES.
113500
113600
113700
113800
113900
C'''''' POWER LAW FIT PARAMETERS--G = A * PWRF(T,R) ABOVE 2000 DEG.
C      G = B * POWRF(T,S) BELOW 200 DEG.
114000
114100
114200
114300
C'''''' WPE IS PLASMA FREQUENCY IN MEGA-RADIANS PER SECOND.
114400
C'''''' COLLISION FREQUENCIES ARE IN MEGA-COLLISIONS PER SECOND.
114500
C'''''' TE IS ELECTRON TEMPERATURE IN ELECTRON VOLTS.
114600
C'''''' TEP IS PHENOMENOLOGY ELECTRON TEMPERATURE IN ELECTRON VOLTS.
114700
C'''''' T IS ELECTRON TEMPERATURE IN DEGREES KELVIN.
114800
C'''''' NE IS ELECTRON DENSITY IN CM-3 DERIVED FROM WPE.
114900
C'''''' NIT2,NOX2,NOX1 ARE NEUTRAL NUMBER DENSITIES IN CM-3 FOR
C      MOLECULAR NITROGEN, MOLECULAR OXYGEN, AND ATOMIC OXYGEN
C      RESPECTIVELY.
115000
115100
C'''''' GNIT2,GNOX2,GNOX1, ARE THE G-FACTORS FOR THE ABOVE SPECIES AS
C      DEFINED BY HOCHSTIM-- ELECTRON NEUTRAL COLL. FREQ. = G * NO.
C      DENSITY(CM-3) * 1.E-14
115200
115300
115400
115500
115600
115700
115800
115900
DIMENSION TABT(15),TABG02(15),TABGN2(15),TABG01(15)
116000
116100
116200
116300
116400
116500
116600
116700
116800
116900
117000
117100
117200
117300
117400
117500
117600
117700
117800
117900
118000
118100
118200
POWER LAW FIT PARAMETERS--G=A*PWRF(T,R) ABOVE 2000 DEG.

```

```

C          G=B*POWRF(T,S) BELOW 200 DEG.                                118300
                                                                    118400
                                                                    118500
DATA RNIT2/0.741/                                                    118600
DATA RNUX2/0.697/                                                    118700
DATA RNOX1/1.179/                                                    118800
DATA ANIT2/1.259E-2/                                                  118900
DATA ANUX2/9.803E-3/                                                  119000
DATA ANOX1/7.463E-5/                                                  119100
DATA SNIT2/0.974/                                                    119200
DATA SNOX1/0.517/                                                    119300
DATA SNUX2/0.834/                                                    119400
DATA BNIT2/2.811E-3/                                                  119500
DATA BNUX2/3.639E-3/                                                  119600
DATA BNOX1/6.076E-3/                                                  119700
DATA A/550562.0/                                                      119800
DATA B/6.06318E+17/                                                  119900
DATA IN1/0/                                                            120000
                                                                    120100
                                                                    120200
C'''''' SELECT LARGER OF TEMPERATURES AND ELECTRON DENSITIES FROM
C          PHENOMENOLOGY AND MODEL ATMOSPHERE.                        120300
                                                                    120400
                                                                    120500
C'''''' STORE DIRECTION COSINES DERIVED FROM PRELP AS CALLED FROM TEST. 120600
          NA1 = N1                                                    120700
          NA2 = N2                                                    120800
          NA3 = N3                                                    120900
          CALL TRANS(X,Y,Z,RA,N1,N2,N3 )                             121000
          IF(RA.LT.0)RETURN                                           121100
                                                                    121200
C'''''' DIRECTION COSINES NOW REFER TO MODEL ATMOSPHERE--SIGN HAS NOT YET
C          BEEN ESTABLISHED FOR ELECTRON DENSITY GRADIENT.          121300
                                                                    121400
          RB = RA + .01                                              121500
          RS = 30.                                                    121600
          RT = 800.                                                    121700
          IF(RB.LE.30.) GO TO 3                                       121800
          IF(RB.GE.800.) GO TO 4                                       121900
          CALL MODATM(NIT2,NUX2,NOX1,NE,T,RB)                          122000
          GO TO 5                                                       122100
          3 CALL MODATM(NIT2,NUX2,NOX1,NE,T,RS)                        122200
          GO TO 5                                                       122300
          4 CALL MODATM(NIT2,NUX2,NOX1,NE,T,RT)                        122400
          5 CONTINUE                                                    122500
          NE2 = NE                                                      122600
          IF(RA.LE.30.) GO TO 7                                       122700
          IF(RA.GE.800.) GO TO 8                                       122800
          CALL MODATM(NIT2,NUX2,NOX1,NE,T,RA)                          122900
          GO TO 9                                                       123000
          7 CALL MODATM(NIT2,NUX2,NOX1,NE,T,RS)                        123100
          GO TO 9                                                       123200
          8 CALL MODATM(NIT2,NUX2,NOX1,NE,T,RT)                        123300
          9 CONTINUE                                                    123400
                                                                    123500
C'''''' ESTABLISH SIGNS FOR DIRECTION COSINES.                       123600
          IF(NE.LE.NE2)GO TO 50                                         123700
          N1=-N1                                                       123800
          N2=-N2                                                       123900
          N3=-N3                                                       124000
          50 CONTINUE                                                  124100
          TP = 11605.0 * TEP                                           124200
C'''''' CONVERSION OF PLASMA FREQUENCY TO ELECTRON DENSITY.        124300

```

	124400
NEP = 314.2196 * WPE * WPE	124500
IF (NE .LE. NEP) GO TO 10	124600
GO TO 20	124700
10 NE = NEP	124800
N1 = NA1	124900
N2 = NA2	125000
N3 = NA3	125100
20 CONTINUE	125200
C'''' PLASMA FREQ. RECALCULATED FROM SELECTED VALUE OF ELEC. DENSITY.	125300
WPE = SQRT(NE/314.2196)	125400
IF(T.LT.TP) T = TP	125500
VTHERM = A * SQRT(T)	125600
IF(NE.LE.O.OR.T.LE.O)GO TO 100	125700
200 CONTINUE	125800
ARG1 = 7.423795E-14 * (VTHERM**3) / SQRT(NE)	125900
TLOG =ALOG (ARG1)	126000
	126100
C'''' CALCULATE ELECTRON-ION COLLISION FREQUENCY.	126200
NUEI = NE * B * TLOG / (VTHERM**3)	126300
NUEI = NUEI * 1E-6	126400
GO TO 300	126500
100 NUEI=0	126600
	126700
C'''' CALCULATE ELECTRON-NEUTRAL COLLISION FREQUENCY.	126800
300 CONTINUE	126900
IF(T.GE.2000.) GO TO 800	127000
600 IF(T.LE.200.) GO TO 900	127100
700 CONTINUE	127200
	127300
C'''' CALCULATE G-VALUES FROM TABLE.	127400
CALL INTERP(TABT,T,TABGN2, GNIT2, 14)	127500
CALL INTERP(TABT,T,TABG02,GNOX2, 14)	127600
CALL INTERP(TABT,T,TABG01,GNOX1, 14)	127700
GO TO 1000	127800
	127900
C'''' POWER LAW FIT ABOVE 2000 DEGREES K.	128000
800 GNIT2 = ANIT2 * POWRF(T,RNIT2)	128100
GNOX2 = ANOX2 * POWRF(T,RNOX2)	128200
GNOX1 = ANOX1 * POWRF(T,RNOX1)	128300
GO TO 1000	128400
	128500
C'''' POWER LAW FIT BELOW 200 DEGREES K.	128600
900 GNIT2 = BNIT2 * POWRF(T,SNIT2)	128700
GNOX2 = BNOX2 * POWRF(T,SNOX2)	128800
GNOX1 = BNOX1 * POWRF(T,SNOX1)	128900
1000 NUEM = 1.E-14 * (GNIT2*NIT2 + GNOX2 * NOX2 + GNOX1 * NOX1)	129000
NUCULL = NUEM + NUEI	129100
RETURN	129200
END	129300
	129400

	SUBROUTINE CONTR(A,ALAB,LIMIT,AS,RF,R,TITLE,BA,RC,AGZ,RGZ,INC,TS,	129500
\$	THETA,PHI,N,M,LL,EL,ELAB,LABELS,UNITS)	129600
		129700
		129800
	DIMENSION A(N,M),R(11),TITLE(10),AZLAB(7),EL(41),ELAB(41),L(10)	129900
	DIMENSION LABELS(3)	129950
		130000
		130100
	REAL INC	130200
	REAL*8 TITLE,ALAB,LABELS	130300
	INTEGER AZLAB	130400
		130500
		130600
	COMMON/FLAG/IFLAG	130700
		130800
		130900
	ANC=INC/1.7453292512E-2	131000
	THETAU=THETA/1.7453292512E-2	131100
	AZINC=ANC*10.0	131200
	AZLAB(1)=-AZINC*3.0	131300
	AZLAB(2)=-AZINC*2.0	131400
	AZLAB(3)=-AZINC	131500
	AZLAB(4)=0	131600
	AZLAB(5)=AZINC	131700
	AZLAB(6)=AZINC*2.0	131800
	AZLAB(7)=AZINC*3.0	131900
	IF(LL.EQ.-5) GO TO 20	132000
	CALL SUMMARY(LL-1)	132100
	GO TO 21	132200
20	CONTINUE	132300
	PRINT 12	132400
	PRINT 12	132500
	PRINT 12	132600
	PRINT 12	132700
21	CONTINUE	132800
		132900
C		133000
C		133100
C	ARRAYS EL AND ELAB ARE TO BE LOADED WITH BLANKS OR ELEVATION LABEL	133200
		133300
		133400
	1 FORMAT(28X,A8)	133500
	2 FORMAT(5X,3A8,'/',F6.1,A3,	133600
	\$' ANGULAR RES/',F5.1,' DEG.',	133700
	\$' RADAR FREQ/',F7.1,' MHZ')	133800
	3 FORMAT(5X,'REFERENCE RANGES',10I10)	133900
	4 FORMAT(5X,'RANGE CODES',5X,10(I9,1X))	134000
5	FORMAT(5X,'TERMINATION CODES/ -=ABSORPTION(PATHLOSS) EXCEEDS ',	134100
	\$'LIMIT. &=RAY DEVIATION EXCESSIVE. ',1H*,'=OVERDENSE '	134200
	\$ 'MEDIUM ENCOUNTERED.',/,	134300
	\$5X,'TERMINATION CODES/ ==GROUND REFLECTION ',	134400
	\$5X,'\$=IMPOSSIBLE DIRECTION COSINES ',	134500
	\$5X,'\$=TOO MANY BENDS')	134600
	6 FORMAT(46X,'A Z I M U T H',F8,5X,'A Z I M U T H')	134700
	7 FORMAT(4X,3(I4,16X),I3,17X,I4,2(16X,I4))	134800
	8 FORMAT(6X,6I(2H+))	134900
	9 FORMAT(1X,A1,A3,1H+,6I(A1,1X),1H+,A3)	135000
10	FORMAT(5X,10A8)	135100
11	FORMAT(5X,'BLAST ALTITUDE IS ',F5,' KM.',	135200
	\$ 5X,'AZIMUTH OF GROUND ZERO IS ',F5,' DEG.',	135300
	\$ 5X,'TIME STEP IS ',F5,' SEC.',/,	135400
	\$ 5X,'RANGE TO GROUND ZERO IS ',F5,' KM.',	

\$	5X,'RADAR COLATITUDE IS ',F5.1,' DEG.')	135500
12	FORMAT(1H)	135600
13	FORMAT(5X,'TEMP QUANT. LIMITS/ ', 'UPPER',9I10)	135700
14	FORMAT(25X,'LOWER',10X,9I10)	135800
15	FORMAT(5X,'TEMPERATURE CODES/',17X, 9(19,1X))	135900
16	FORMAT(5X,'PATH LOSS DISPLAY LIMIT/',F6.1,' DB',	136000
\$	' ANGULAR RES/',F5.1,' DEG.',	136100
\$	' RADAR FREQ/',F7.1,' MHZ')	136200
		136300
		136400
	PRINT 1,ALAB	136500
	PRINT 12	136600
	PRINT 2,LABELS,LIMIT,UNITS,AS,RF	136700
	IF(LL.NE.-5) GO TO 25	137200
	PRINT 13,(R(I),I=1,9)	137300
	PRINT 14,(R(I),I=1,9)	137400
	PRINT 12	137500
	II=0	137600
	PRINT 15,(I,I= 1,9)	137700
	GO TO 35	137800
25	CONTINUE	137900
	DO 150 I = 1,10	138000
150	L(I) = R(I)	138100
	PRINT 3,(L(I),I=1,10)	138200
	II=0	138300
	PRINT 4,(I,I=II,9)	138400
	PRINT 12	138500
	PRINT 5	138600
35	CONTINUE	138700
	PRINT 12	138800
	PRINT 7,AZLAB	138900
	PRINT 8	139000
	DO 100 J=1,M	139100
100	PRINT 9,EL(J),ELAB(J),(A(I,J),I=1,N),ELAB(J)	139200
	PRINT 8	139300
	PRINT 7,AZLAB	139400
	PRINT 6,THETAU	139500
	PRINT 12	139600
	PRINT 10,TITLE	139700
	PRINT 11,BA,AGZ,TS,RGZ,RC	139800
	RETURN	139900
	END	140000
		140100


```

SUBROUTINE GEUM(X,Y,Z,C10,C20,C30,RGRP,DIST1,RERROR,AERROR,DISMIS, 143400
$   RANGE,CULATI,THETA,XB,YB,ZB) 143500
                                   143600
                                   143700
COMMON/IR/SPL 143800
COMMON/LR/NONE,ISEMIE 143900
COMMON/NR/ROERR,ROILLM,ROIULM 144000
                                   144100
                                   144200
C ERR COMPUTES REFRACTION ANGLE ERROR USING LAW OF COSINES. 144300
C   AERROR IS THE ERROR IN RADAR POINTING ANGLE. 144400
C   RERROR IS THE ERROR IN RADAR RANGE TO TARGET. 144500
C   DISMIS IS THE RADAR MISS DISTANCE (SPATIAL SEPARATION IN KM. 144600
C     BETWEEN APPARENT RADAR TARGET POSITION AND ACTUAL TARGET 144700
C     POSITION). 144800
                                   144900
                                   145000
PRX=RGRP*C10 145100
PRY=RGRP*C20 145200
PRZ=RGRP*C30 145300
CALL BACOR(X,Y,Z,XB,YB,ZB,RANGE,CULATI,THETA) 145400
RERROR=RGRP-DIST1 145500
DISMIS=SQRT((PRX-XB)**2+(PRY-YB)**2+(PRZ-ZB)**2) 145600
AERROR=(DIST1**2+RGRP**2-DISMIS**2)/(2.0*DIST1*RGRP) 145700
IF(AERROR.GE.ROILLM.AND.AERROR.LE.ROIULM)AERROR=1.0 145800
AERROR=ARCUS(AERROR) 145900
RETURN 146000
END 146100
                                   146200

```

SUBROUTINE INIT(SHGRAY,N,M)	146300
	146400
INTEGER SHGRAY,BLNKS	146500
	146600
	146700
DATA BLNKS/' '/	146800
DIMENSION SHGRAY(N,M)	146900
	147000
	147100
DO 100 I=1,N	147200
DO 100 J=1,M	147300
100 SHGRAY(I,J)=BLNKS	147400
RETURN	147500
END	147600
	147700
	147800

```
SUBROUTINE INTERP(TABZ,Z,TAB,VAL, LPC)
147900
148000
148100
DIMENSION TABZ(134),TAB(134)
148200
148300
148400
N=0
148500
DO 800 I=1,LPC
148600
IF(Z.EQ.TABZ(I))GO TO 500
148700
GO TO 600
148800
500 VAL=TAB(I)
148900
RETURN
149000
600 IF(Z.LT.TABZ(I+1).AND.Z.GT.TABZ(I))GO TO 700
149100
GO TO 800
149200
700 DELTA=(TAB(I)-TAB(I+1))/(TABZ(I)-TABZ(I+1))
149300
VAL=TAB(I)+DELTA*(Z-TABZ(I))
149400
RETURN
149500
800 CONTINUE
149600
RETURN
149700
END
149800
149900
```

```

SUBROUTINE MUDATM(NIT2,NOX2,NOX1,NE,T,Z)
C..... READS IN DATA CARDS FOR MODEL IONOSPHERE-ATMOSPHERE AND
C          CARRIES OUT INTERPOLATION IN ALTITUDE.
REAL INDEX1,INDEX2,KAPPA,INC,INC2,NUCULL,NIT2,NOX2,NOX1,NCT
REAL NUENI,NUEM,MOU,LIMIT,MU,IN,INDEX,N1,N2,N3,NE
DIMENSION TABZ(134),TARN1(134),TABN2(134),TABN3(134),
$          TABNE(134),TABT(134)
DATA TABZ/
$ 30.0, 31.0, 32.0, 33.0, 34.0, 35.0, 36.0, 37.0,
$ 38.0, 39.0, 40.0, 41.0, 42.0, 43.0, 44.0, 45.0,
$ 46.0, 47.0, 48.0, 49.0, 50.0, 51.0, 52.0, 53.0,
$ 54.0, 55.0, 56.0, 57.0, 58.0, 59.0, 60.0, 61.0,
$ 62.0, 63.0, 64.0, 65.0, 66.0, 67.0, 68.0, 69.0,
$ 70.0, 71.0, 72.0, 73.0, 74.0, 75.0, 76.0, 77.0,
$ 78.0, 79.0, 80.0, 81.0, 82.0, 83.0, 84.0, 85.0,
$ 86.0, 87.0, 88.0, 89.0, 90.0, 91.0, 92.0, 93.0,
$ 94.0, 95.0, 96.0, 97.0, 98.0, 99.0, 100.0, 101.0,
$ 102.0, 103.0, 104.0, 105.0, 106.0, 107.0, 108.0, 109.0,
$ 110.0, 111.0, 112.0, 113.0, 114.0, 115.0, 116.0, 117.0,
$ 118.0, 119.0, 120.0, 130.0, 140.0, 150.0, 160.0, 170.0,
$ 180.0, 190.0, 200.0, 210.0, 220.0, 230.0, 240.0, 250.0,
$ 260.0, 270.0, 280.0, 290.0, 300.0, 320.0, 340.0, 360.0,
$ 380.0, 400.0, 420.0, 440.0, 460.0, 480.0, 500.0, 520.0,
$ 540.0, 560.0, 580.0, 600.0, 620.0, 640.0, 660.0, 680.0,
$ 700.0, 720.0, 740.0, 760.0, 780.0, 800.0/
DATA TABN1/
$ 3.004+017, 2.573+017, 2.205+017, 1.894+017, 1.629+017, 1.402+017,
$ 1.209+017, 1.044+017, 9.023+016, 7.808+016, 6.769+016, 5.871+016,
$ 5.098+016, 4.433+016, 3.860+016, 3.365+016, 2.937+016, 2.565+016,
$ 2.242+016, 1.963+016, 1.720+016, 1.535+016, 1.344+016, 1.204+016,
$ 1.063+016, 9.500+015, 8.367+015, 7.460+015, 6.553+015, 5.829+015,
$ 5.105+015, 4.529+015, 3.952+015, 3.497+015, 3.041+015, 2.684+015,
$ 2.328+015, 2.050+015, 1.771+015, 1.554+015, 1.337+015, 1.172+015,
$ 1.007+015, 8.800+014, 7.517+014, 6.543+014, 5.568+014, 4.826+014,
$ 4.083+014, 3.523+014, 2.963+014, 2.478+014, 2.072+014, 1.733+014,
$ 1.449+014, 1.212+014, 1.014+014, 8.480+013, 7.095+013, 5.934+013,
$ 4.965+013, 4.103+013, 3.544+013, 2.831+013, 2.349+013, 1.947+013,
$ 1.626+013, 1.362+013, 1.146+013, 9.673+012, 8.178+012, 6.817+012,
$ 5.704+012, 4.804+012, 4.060+012, 3.453+012, 2.950+012, 2.529+012,
$ 2.174+012, 1.875+012, 1.620+012, 1.365+012, 1.164+012, 9.983+011,
$ 8.606+011, 7.460+011, 6.513+011, 5.723+011, 5.057+011, 4.478+011,
$ 4.000+011, 1.383+011, 6.302+010, 3.308+010, 1.891+010, 1.147+010,
$ 7.284+009, 4.794+009, 3.249+009, 2.254+009, 1.594+009, 1.146+009,
$ 8.340+008, 6.138+008, 4.558+008, 3.411+008, 2.569+008, 1.945+008,
$ 1.480+008, 8.666+007, 5.137+007, 3.075+007, 1.854+007, 1.125+007,
$ 6.837+006, 4.189+006, 2.577+006, 1.591+006, 9.858+005, 6.128+005,
$ 3.821+005, 2.390+005, 1.499+005, 9.428+004, 5.947+004, 3.762+004,
$ 2.386+004, 1.517+004, 9.673+003, 6.184+003, 3.963+003, 2.546+003,
$ 1.640+003, 1.059+003/
DATA TABN2 /
$ 7.745+016, 6.636+016, 5.687+016, 4.885+016, 4.200+016, 3.616+016,
$ 3.118+016, 2.692+016, 2.327+016, 2.013+016, 1.745+016, 1.514+016,
$ 1.315+016, 1.143+016, 9.953+015, 8.678+015, 7.573+015, 6.615+015,

```

\$ 5.781+015,	5.061+015,	4.436+015,	3.959+015,	3.605+015,	3.229+015,	151705
\$ 2.853+015,	2.549+015,	2.245+015,	2.002+015,	1.758+015,	1.564+015,	151706
\$ 1.370+015,	1.215+015,	1.060+015,	9.380+014,	8.160+014,	7.200+014,	151707
\$ 6.246+014,	5.499+014,	4.752+014,	4.170+014,	3.588+014,	3.145+014,	151708
\$ 2.702+014,	2.360+014,	2.017+014,	1.756+014,	1.494+014,	1.295+014,	151709
\$ 1.096+014,	9.455+013,	7.950+013,	6.649+013,	5.559+013,	4.648+013,	151710
\$ 3.888+013,	3.251+013,	2.721+013,	2.275+013,	1.906+013,	1.598+013,	151711
\$ 1.332+013,	1.101+013,	9.188+012,	7.361+012,	6.146+012,	5.190+012,	151712
\$ 4.296+012,	3.553+012,	2.936+012,	2.423+012,	1.994+012,	1.644+012,	151713
\$ 1.359+012,	1.131+012,	9.443+011,	7.932+011,	6.693+011,	5.665+011,	151714
\$ 4.809+011,	4.093+011,	3.492+011,	2.903+011,	2.443+011,	2.066+011,	151715
\$ 1.757+011,	1.501+011,	1.292+011,	1.119+011,	9.744+010,	8.501+010,	151716
\$ 7.500+010,	2.325+010,	9.729+009,	4.746+009,	2.542+009,	1.454+009,	151717
\$ 8.737+008,	5.463+008,	3.527+008,	2.336+008,	1.581+008,	1.088+008,	151718
\$ 7.596+007,	5.367+007,	3.829+007,	2.755+007,	1.996+007,	1.455+007,	151719
\$ 1.066+007,	5.797+006,	3.195+006,	1.779+006,	9.991+005,	5.650+005,	151720
\$ 3.200+005,	1.829+005,	1.050+005,	6.058+004,	3.507+004,	2.038+004,	151721
\$ 1.188+004,	6.954+003,	4.081+003,	2.404+003,	1.420+003,	8.417+002,	151722
\$ 5.004+002,	2.984+002,	1.785+002,	1.071+002,	6.442+001,	3.887+001,	151723
\$ 2.352+001,	1.427+001/					151724

DATA TABT /

\$ 230.1,	232.1,	234.2,	236.2,	238.3,	240.3,	242.3,	244.4,	151802
\$ 246.4,	248.5,	250.5,	252.6,	254.6,	256.7,	258.7,	260.8,	151803
\$ 262.8,	264.9,	266.9,	269.0,	271.0,	268.2,	265.5,	262.7,	151804
\$ 259.9,	257.2,	254.4,	251.6,	248.8,	246.1,	243.3,	240.6,	151805
\$ 238.0,	235.3,	232.6,	230.0,	227.3,	224.6,	221.9,	219.3,	151806
\$ 216.6,	213.5,	210.5,	207.4,	204.4,	201.3,	198.2,	195.2,	151807
\$ 192.1,	189.1,	186.0,	186.0,	186.4,	186.0,	186.0,	185.9,	151808
\$ 185.9,	185.9,	185.9,	185.8,	185.8,	188.4,	190.9,	193.5,	151809
\$ 195.9,	198.2,	200.4,	202.4,	204.4,	206.3,	208.1,	212.2,	151810
\$ 215.7,	220.0,	224.6,	229.0,	233.4,	237.9,	242.3,	246.8,	151811
\$ 251.1,	261.6,	271.9,	282.3,	292.7,	302.9,	313.1,	323.6,	151812
\$ 334.0,	344.4,	355.0,	445.0,	540.0,	630.0,	720.0,	810.0,	151813
\$ 900.0,	1100.0,	1310.0,	1400.0,	1520.0,	1630.0,	1730.0,	1839.0,	151814
\$ 1907.0,	1975.0,	2043.0,	2111.0,	2178.0,	2151.0,	2224.0,	2395.0,	151815
\$ 2468.0,	2541.0,	2566.0,	2591.0,	2615.0,	2040.0,	2665.0,	2673.0,	151816
\$ 2681.0,	2687.0,	2695.0,	2703.0,	2703.0,	2703.0,	2704.0,	2704.0,	151817
\$ 2704.0,	2699.0,	2694.0,	2690.0,	2685.0,	2680.0/			151818

DATA TABN3 /

\$ 0.000+000,	0.000+000,	0.000+000,	0.000+000,	0.000+000,	0.000+000,	0.000+000,	151902
\$ 0.000+000,	0.000+000,	0.000+000,	0.000+000,	0.000+000,	0.000+000,	0.000+000,	151903
\$ 0.000+000,	0.000+000,	0.000+000,	0.000+000,	0.000+000,	0.000+000,	0.000+000,	151904
\$ 0.000+000,	0.000+000,	0.000+000,	0.000+000,	0.000+000,	0.000+000,	0.000+000,	151905
\$ 0.000+000,	0.000+000,	0.000+000,	0.000+000,	0.000+000,	0.000+000,	0.000+000,	151906
\$ 0.000+000,	0.000+000,	0.000+000,	0.000+000,	0.000+000,	0.000+000,	0.000+000,	151907
\$ 0.000+000,	0.000+000,	0.000+000,	0.000+000,	0.000+000,	0.000+000,	0.000+000,	151908
\$ 0.000+000,	0.000+000,	0.000+000,	0.000+000,	0.000+000,	0.000+000,	0.000+000,	151909
\$ 0.000+000,	0.000+000,	8.500+010,	8.700+010,	8.930+010,	9.210+010,		151910
\$ 9.500+010,	9.800+010,	1.015+011,	1.055+011,	1.105+011,	1.165+011,		151911
\$ 1.250+011,	1.420+011,	1.680+011,	2.060+011,	2.660+011,	3.410+011,		151912
\$ 4.100+011,	4.515+011,	4.800+011,	4.935+011,	5.000+011,	4.945+011,		151913
\$ 4.760+011,	4.425+011,	4.050+011,	3.610+011,	3.210+011,	2.835+011,		151914
\$ 2.510+011,	2.230+011,	2.000+011,	1.812+011,	1.642+011,	1.487+011,		151915
\$ 1.347+011,	1.235+011,	1.125+011,	1.020+011,	9.250+010,	8.400+010,		151916
\$ 7.600+010,	3.650+010,	2.154+010,	1.411+010,	9.817+009,	7.122+009,		151917
\$ 5.335+009,	4.099+009,	3.216+009,	2.565+009,	2.075+009,	1.698+009,		151918
\$ 1.403+009,	1.168+009,	9.783+008,	8.242+008,	6.975+008,	5.927+008,		151919
\$ 5.053+008,	3.702+008,	2.035+008,	1.522+008,	1.142+008,	8.588+007,		151920
\$ 6.487+007,	4.913+007,	3.729+007,	2.836+007,	2.161+007,	2.161+007,		151921
\$ 1.650+007,	1.262+007,	9.667+006,	7.418+006,	5.701+006,	4.389+006,		151922
\$ 3.384+006,	2.613+006,	2.021+006,	1.565+006,	1.214+006,	9.429+005,		151923

```

$ 7.334+005, 5.713+005/ 151924
DATA TABNE / 152001
$ 0.000+000, 0.000+000, 0.000+000, 0.000+000, 0.000+000, 0.000+000, 152002
$ 0.000+000, 0.000+000, 0.000+000, 0.000+000, 0.000+000, 0.000+000, 152003
$ 0.000+000, 0.000+000, 0.000+000, 0.000+000, 0.000+000, 0.000+000, 152004
$ 0.000+000, 0.000+000, 0.000+000, 0.000+000, 0.000+000, 0.000+000, 152005
$ 5.000+001, 6.000+001, 7.000+001, 1.100+002, 1.500+002, 1.375+002, 152006
$ 1.250+002, 9.750+001, 7.000+001, 5.500+001, 4.000+001, 4.950+001, 152007
$ 5.900+001, 1.295+002, 2.000+002, 3.250+002, 4.500+002, 6.000+002, 152008
$ 7.500+002, 8.000+002, 8.500+002, 9.000+002, 9.500+002, 9.750+002, 152009
$ 1.000+003, 1.125+003, 1.250+003, 1.525+003, 1.800+003, 1.870+003, 152010
$ 1.940+003, 2.470+003, 3.000+003, 3.800+003, 4.600+003, 5.040+003, 152011
$ 5.480+003, 8.140+003, 1.080+004, 1.500+004, 1.920+004, 1.270+004, 152012
$ 2.630+004, 2.880+004, 3.140+004, 3.540+004, 3.930+004, 4.320+004, 152013
$ 4.700+004, 5.180+004, 5.650+004, 6.080+004, 6.500+004, 7.050+004, 152014
$ 7.600+004, 7.900+004, 8.200+004, 8.650+004, 9.100+004, 9.550+004, 152015
$ 1.000+005, 9.850+004, 9.700+004, 9.550+004, 9.400+004, 9.350+004, 152016
$ 9.300+004, 1.000+005, 1.200+005, 1.400+005, 1.600+005, 1.800+005, 152017
$ 2.300+005, 3.000+005, 3.400+005, 4.000+005, 4.500+005, 4.700+005, 152018
$ 4.800+005, 4.600+005, 4.320+005, 4.040+005, 3.760+005, 3.480+005, 152019
$ 3.200+005, 2.840+005, 2.480+005, 2.120+005, 1.760+005, 1.400+005, 152020
$ 1.270+005, 1.140+005, 1.010+005, 8.800+004, 7.500+004, 6.900+004, 152021
$ 6.300+004, 5.700+004, 5.100+004, 4.500+004, 4.250+004, 4.000+004, 152022
$ 3.800+004, 3.600+004, 3.400+004, 3.200+004, 3.000+004, 2.800+004, 152023
$ 2.600+004, 2.400+004/ 152024
CALL INTERP(TABZ,Z,TABNE,NE, 133) 152200
CALL INTERP(TABZ,Z,TABT,T, 133) 152300
100 CALL INTERP(TABZ,Z,TABN1,NIT2, 133) 152400
CALL INTERP(TABZ,Z,TABN2,NOX2, 133) 152500
CALL INTERP(TABZ,Z,TABN3,NOX1, 133) 152600
RETURN 152700
END 152800
152900

```

SUBROUTINE POSIT(A, JUNKR, BLNKS, AZERU, THMN, INC, NPMX, N, M)	153000
	153100
	153200
DIMENSION A(N,M), JUNKR(N,M)	153300
	153400
	153500
INTEGER A, BLNKS	153600
REAL INC	153700
	153800
	153900
1 FORMAT(54H THE FOLLOWING DISPLAY IS BLANK DUE TO AN ERROR IN THE,	154000
\$ 51H PROGRAM, THETA MIN. IS COMPLETELY OFF THE DISPLAY.,/,	154100
'59H CHECK THE STATEMENTS STARTING JUST BEFORE STATEMENT NO. 60)	154200
	154300
	154400
DO 200 I=1,N	154500
DO 100 J=1,M	154600
JUNKR(I,J)=BLNKS	154700
100 CONTINUE	154800
200 CONTINUE	154900
IC=1	155000
N2=N/2	155100
SINC=AZERU-(INC*N2)	155200
300 IF(SINC.LE.THMN.AND.SINC+INC.GT.THMN) GO TO 500	155300
SINC=SINC+INC	155400
IC=IC+1	155500
IF(IC.GT.N) GO TO 400	155600
GO TO 300	155700
400 PRINT 1	155800
RETURN	155900
500 CONTINUE	156000
NPM=NPMX	156100
MB=M	156200
I=1	156300
600 JUNKR(IC,MB)=A(I,NPM)	156400
MB=MB-1	156500
NPM=NPM-1	156600
IF(MB.LE.O.OR.NPM.LE.O) GO TO 700	156700
GO TO 600	156800
700 CONTINUE	156900
MB=M	157000
NPM=NPMX	157100
IC=IC+1	157200
I=I+1	157300
IF(IC.GT.N.OR.I.GT.N) GO TO 800	157400
GO TO 600	157500
800 CONTINUE	157600
RETURN	157700
END	157800
	157900

```

          SUBROUTINE PRELDA(NEXT, LAST, WR1, RMAX, HGT1)
C          INPUT IS TAPE FROM LATE CHEMISTRY
C
          COMMON/SCRACH/SKIP(26,51,2)
C          DIMENSIONS ARE GIVEN IN TAPE READ SEGMENTS
          DIMENSION CONST(26),COORD(3), COORDA(26,7), COORDB(26,8),
1             ZCONST(7), ZC(51),ZH(51),
2             PLASMA(26,51,2), PLASMB(26,51,2), PLASMC(26,51),
3             BFIELD(26,51,2), BFIELDA(26,51),
4             CHECOA(26,51,2), CHECOB(26,51,2), CHECOC(26,51,2),
5             CHECOD(26,51), TE(26,51), RHO(26,51), CHECUE(26,51),
6             WPN(11), AMBNT(90,5), SPEC(100,3)
C
          TE IN EV AND DENE IN NUMBER DENSITY IN CHECOM
C          IS USED FOR TE AND RHO.
C          DIMENSION FOR DATA TO BE EQUIVALENCED TO BE USED BY NAME
          DIMENSION R(26), PDR(26)
C          EQUIVALENCE FOR DATA TO BE USED BY NAME
          EQUIVALENCE (CONST(5),NTIME), (CONST(14),RB),
1             (COORD(2),NR1), (COORDA(1,1),R(1)), (COORDA(1,7),PDR(1)),
2             (ZCONST(3),PDZ), (ZCONST(6),NZ1), (WPN(4),HGT)
C          EQUIVALENCE FOR DATA TO BE SKIPPED
C
          EQUIVALENCE (SKIP(1,1,1), COORDB(1,1),ZH(1),
1             PLASMA(1,1,1), PLASMB(1,1,1), PLASMC(1,1),
2             BFIELD(1,1,1), BFIELDA(1,1), CHECOA(1,1,1),
3             CHECOB(1,1,1), CHECOC(1,1,1), CHECOD(1,1),
4             CHECUE(1,1), AMBNT(1,1), SPEC(1,1))
          DATA NREAD/0/, NCON/1/
          IF(NCON.EQ.0) GOTO 1
C          CONVERSION FACTOR FOR RHO= 4*PI*E**2/ME
          CONV=12.56637*4.8024E-10**2/9.1066E-28
          CONV = SQRT(CONV)
C          CONVERT PLASMA FREQUENCY FROM RADS/SEC TO MEGA-RADS/SEC.
          CONV = CONV * 1.E-6
          NCON=0
1          IF(NREAD.NE.-1000) GOTO 2
          PRINT 100
100          FORMAT(' EOF NOTICE IGNORED')
          STOP
C
2          NREAD=NEXT-LAST-1
          IF(NREAD.LE.0) GOTO 4
C          SKIP NREAD RECORDS
          DO 3 K=1,NREAD
          READ(9,END=10)
3          CONTINUE
C
4          READ(9,END=10) CONST, COORD, COORDA, COORDB,NDX,
1             ZCONST, ZC, ZH, PLASMA, PLASMB, PLASMC,
2             BA, BFIELD, BFIELDA,
3             CHECOA, CHECOB, CHECOC, CHECOD, TE, RHO, CHECUE,
4             WPN
C
          RMAX=RB
          HGT1=HGT
          WR =WR1
          DO 5 K=1,NZ1
          DO 5 J=1,NR1
5          RHO(J,K)= CONV*SQRT(RHO(J,K))
          RETURN

```

```

CR2 = .5          *RTWO*RPLUS*ROME          170200
CR3 = .5          *RTWO*RPLUS*DXR          170300
CR4 = -.1666667 *DXR*ROME *RPLUS          170400
C INTERPOLATE IN R                          170500
WPE = CR1 *ZWPE(1) +CR2*ZWPE(2) +CR3*ZWPE(3) +CR4*ZWPE(4) 170600
TEP = CR1 *ZTEP(1) +CR2*ZTEP(2) +CR3*ZTEP(3) +CR4*ZTEP(4) 170700
C CHECK FOR OVER DENSITY                    170800
IF(WPE.LE.WR) GO TO 30                      170900
PRINT 200, WPE                              171000
PRINT 201, TEP                              171100
200 FORMAT(' WPE = ',E12.3)                 171200
201 FORMAT(' TEP = ',E12.3 )                171300
WPE = -1.                                    171400
RETURN                                       171500
C                                           171600
C CHECK FOR ROUNDING ERRORS                 171700
30 IF(WPE.LT.1.E-5) RETURN                  171800
C                                           171900
C COMPUTE DERIVATE IN Z                     172000
DCZ1 = -.1666667*PDZ*(ZONE*ZTWO- DXZ *(ZTWO +ZONE)) 172100
DCZ2 = -.5          *PDZ*(ZTWO*ZPLUS+ZONE*(ZPLUS- ZTWO)) 172200
DCZ3 = -.5          *PDZ*(ZPLUS*DXZ- ZTWO*(DXZ +ZPLUS)) 172300
DCZ4 = -.1666667*PDZ*(ZONE* DXZ+ZPLUS*(ZONE - DXZ )) 172400
DU 35 I=1,4                                  172500
JB = JA+I-2                                  172600
IF(JB.EQ.0) JB=2                              172700
DZWPE(I) = DCZ1*RHO(JB,KA-1) +DCZ2*RHO(JB,KA) 172800
          +DCZ3*RHO(JB,KA+1) +DCZ4*RHO(JB,KA+2) 172900
35 CONTINUE                                  173000
C                                           173100
DWPPEZ = CR1*DZWPE(1) +CR2*DZWPE(2) +CR3*DZWPE(3)+CR4*DZWPE(4) 173200
C                                           173300
C COMPUTE DERIVATE IN R                     173400
DCR1 = -.1666667*PDR(1)*(ROME *RTWO -DXR *(RTWO +ROME )) 173500
DCR2 = -.5          *PDR(1)*(RTWO *RPLUS +ROME*(RPLUS-RTWO )) 173600
DCR3 = -.5          *PDR(1)*(RPLUS*DXR - RTWO*(DXR +RPLUS)) 173700
DCR4 = -.1666667*PDR(1)*(ROME *DXR +RPLUS*(ROME -DXR )) 173800
DWPPEX = DCR1*ZWPE(1) +DCR2*ZWPE(2) +DCR3*ZWPE(3)+DCR4*ZWPE(4) 173900
C                                           174000
C                                           174100
IF(RXY.EQ.0) GOTO 40                          174200
DWPPEX = DWPPEX*X/RXY                         174300
DWPPEY = DWPPEX*Y/RXY                         174400
GO TO 45                                       174500
40 DWPPEX = 0.                                174600
DWPPEY = 0.                                    174700
45 DWPE = SQRT (DWPPEX**2 +DWPPEY**2 +DWPEZ**2) 174800
IF(DWPE.EQ.0) GOTO 50                          174900
COSX = DWPPEX/DWPE                             175000
COSY = DWPPEY/DWPE                             175100
COSZ = DWPEZ/DWPE                             175200
RETURN                                          175300
C                                           175400
50 COSX = 0.                                    175500
COSY = 0.                                    175600
COSZ = 1.                                    175700
RETURN                                          175800
END                                            175900

```

C		164100
10	NREAD=-1000	164200
	NEXT= -1	164300
	PRINT 101	164400
101	FORMAT(' END OF FILE REACHED')	164500
	RETURN	164600
C		164700
C*****		164800
	ENTRY PRELP(X,Y,Z, COSX, COSY, COSZ, WPE, DWPE, TEP)	164900
C	THIS PRELP IS WRITTEN FOR EQUAL SPACING IN R AND Z	165000
C		165100
	DIMENSION ZWPE(4), ZTEP(4), DZWPE(4)	165200
	TEP= 0.	165300
	WPE=0.	165400
	DWPE=0.	165500
C	CHECK IF IN RANGE	165600
	Z1 = Z-HGT	165700
	IF(Z1.LT.ZC(1).OR.Z1.GT.ZC(NZ1)) RETURN	165800
	RXY=SQRT(X**2+Y**2)	165900
	IF(RXY.GT.R(NR1)) RETURN	166000
C		166100
	Z1=Z1-ZC(1)	166200
	ZA=Z1*PDZ	166300
C	GET INDEX AND KEEP IN RANGE N-1,N,N+1,N+2	166400
	KA=ZA	166500
	KA=KA+1	166600
	KA=MAX(2,KA)	166700
	KA=MIN(NZ1-2,KA)	166800
C		166900
	RA=RXY*PDR(1)	167000
	JA=RA	167100
	JA=JA+1	167200
	JA=MIN(NR1-2,JA)	167300
C		167400
C	COMPUTE COEFFICIENT FOR Z	167500
	DXZ=ZA- (KA-1)	167600
	ZONE=1.-DXZ	167700
	ZTWO=2.-DXZ	167800
	ZPLUS=1.+DXZ	167900
	CZ1 = -.1666667*DXZ*ZONE*ZTWO	168000
	CZ2 = .5 *ZTWO*ZPLUS*ZONE	168100
	CZ3 = .5 *ZTWO*ZPLUS*DXZ	168200
	CZ4 = -.1666667*DXZ*ZONE*ZPLUS	168300
C	INTERPOLATE IN Z	168400
	DO 20 I=1,4	168500
	JB= JA+I-2	168600
C	TEST FOR R - ORIGIN	168700
	IF(JB.EQ.0) JB=2	168800
	ZWPE(I)=CZ1*RHO(JB,KA-1)+CZ2*RHO(JB,KA)+CZ3*RHO(JB,KA+1)	168900
	+CZ4*RHO(JB,KA+2)	169000
	ZTEP(I)=CZ1*TE(JB,KA-1)+CZ2*TE(JB,KA)+CZ3*TE(JB,KA+1)	169100
	+CZ4*TE(JB,KA+2)	169200
20	CONTINUE	169300
C		169400
C	COEFFICIENTS FOR R	169500
	DXR=RA- (JA-1)	169600
	RONE= 1.-DXR	169700
	RTWO= 2.-DXR	169800
	RPLUS=1.+DXR	169900
		170000
	CR1 =-.1666667 *DXR *RONE *RTWO	170100

```

SUBROUTINE REFRAC(WPE,NUCOLL,WR,KAPPA,INDEX2,RKK)
176100
176200
176300
C   CALCULATES REAL AND IMAGINARY PARTS OF REFRACTIVE INDEX BASED UPON
C   COLLISION FREQUENCY, SHKAROFSKY FORM OF AVERAGE, AND UPON ZERO
C   MAGNETIC FIELD.
176400
176500
176600
C   SHKAROFSKY G AND H FACTORS OMITTED, HIGH FREQUENCY APPROX.
176700
C   WPE IS ELECTRON PLASMA FREQUENCY IN MEGA-RADIANS PER SECOND.
176800
C   INDEX2 IS REAL PART OF REFRACTIVE INDEX.
176900
C   KAPPA IS IMAGINARY PART OF INDEX OF REFRACTION.
177000
C   NUCOLL IS COLLISION FREQUENCY IN MEGA-RADIANS PER SECOND.
177100
C   WR IS RADAR FREQUENCY IN MEGA-RADIANS PER SECOND.
177200
177300
177400
COMMON/LR/NONE,ISEMIE
177500
COMMON/NR/ROERR,RO1LLM,RO1ULM
177600
177700
177800
REAL NU EI,NU EM,MUU,LIMIT,MU,IN,INDEX,N1,N2,N3,NE
REAL INDEX1,INDEX2,KAPPA,INC,INC2,NUCOLL,NIT2,NUX2,NOX1,NC T
177900
178000
178100
178200
178300
RATIO = WPE / WR
178400
X=RATIO**2
178500
IF(X.LT.ROERR)X=0
178600
178700
C   IF WPE RETURNED BY PRELP IS -1, MEDIUM IS OVERDENSE.
178800
IF(WPE - 0.)20,10,10
178900
179000
179100
C   IF PLASMA FREQ. IS GREATER THAN RADAR FREQ., MEDIUM IS OVERDENSE.
179200
10 IF(RATIO - 1.) 30,20,20
179300
20 CONTINUE
179400
PRINT 21
179500
21 FORMAT( ' OVERDENSE MEDIUM ENCOUNTERED ' )
179600
RETURN
179700
30 IF(NUCOLL - 0.) 40,70,50
179800
40 CONTINUE
179900
PRINT 41
180000
41 FORMAT( ' COLLISION FREQUENCY IS NEGATIVE-CHECK SUBROUTINES COLL
180100
CF AND MODATM ' )
180200
RETURN
180300
50 CONTINUE
180400
IF(X.EQ.0) GO TO 80
180500
60 C = 299793.0
180600
Z=NUCOLL/WR
180700
ALPHA=1.0+Z**2
180800
RESULT=(ALPHA-X)**2+(X*Z)**2
180900
STEP1=SQRT(RESULT)
181000
RESULT=(STEP1+ALPHA-X)/(2.*ALPHA)
181100
IF(RESULT)61,62,63
181200
61 PRINT 65,RESULT
181300
62 FORMAT( ' ----- RESULT IN REFRAC =',E13.3,' CHECK FOR A MALFUNCTI
181400
$ON -----' )
181500
RESULT = 0
181600
62 RKK=25
181700
INDEX2=0
181800
KAPPA=0.
181900
RETURN
182000
63 INDEX2=SQRT(RESULT)
182100

```

63	INDEX2=DSORT(RESET)	182200
	CHI=X*Z/(2.*ALPHA*INDEX2)	182300
	KAPPA=10**6*WR*CHI/C	182400
	RETURN	182500
70	KAPPA = 0.0	182600
	INDEX2 = SQRT(1.0 - X)	182700
	RETURN	182800
80	KAPPA = 0.0	182900
	INDEX2 = 1.0	183000
	RETURN	183100
	END	183200
		183300

```

SUBROUTINE RFRAC2(INDEX2)
C''''CALCULATES REFRACTIVE INDEX IN TROPOSPHERE FOR ALTITUDES BELOW
C      30RM. AN EXPONENTIAL HEIGHT DEPENDENCE IS USED - SCALE FACTOR
C      IS GAMMA IN UNITS OF 1/KM.
COMMON RA
REAL NS ,INDEX2
DATA GAMMA/0.143859/
IF(RA.GE.30.) GO TO 5
GO TO 3
5 CONTINUE
INDEX2 = 1.0
RETURN
3 CONTINUE
NS = 313.
INDEX2 = 1. + (NS*1.E-6)*EXP(-GAMMA*RA)
IF(INDEX2.LT.0) GO TO 10
GO TO 20
10 PRINT 15,INDEX2
15 FORMAT( ' INDEX2 IS ', E15.3, ' CHECK FOR MALFUNCTION ',/)
20 RETURN
END
183400
183500
183600
183700
183800
183900
184000
184100
184200
184300
184400
184500
184600
184700
184800
184900
185000
185100
185200
185300
185400
185500
185600
185700
185800
185900
186000
186100
186200
186300
186400
186500

```

SUBROUTINE SHDRAY(VAR,LIMIT,ARRAY,I,NT,NP)	186600
	186700
INTEGER ARRAY,BLNKS	186800
REAL LIMIT	186900
	187000
	187100
DIMENSION ARRAY(61,41),NUM(10)	187200
	187300
	187400
DATA NUM/'0','1','2','3','4','5','6','7','8','9'/	187500
DATA BLNKS/' '/	187600
	187700
	187800
	187900
C SHDRAY CONSTRUCTS A 2-D ARRAY WHOSE ELEMENTS ARE INTEGERS,I,	188000
C ARRAY(M,N)=I-1 IF VAR(M,N) EXCEEDS LIMIT AT RANGE R(I)	188100
	188200
	188300
IF(I.GT.10) GO TO 150	188400
IF(ABS(VAR).GT.LIMIT.AND.ARRAY(NT,NP).EQ.BLNKS)GO TO 100	188500
GO TO 200	188600
100 ARRAY(NT,NP)=NUM(I)	188700
GO TO 200	188800
150 ARRAY(NT,NP)=BLNKS	188900
200 RETURN	189000
END	189100
	189200

SUBROUTINE SUMARY(LL)	189300
	189400
	189500
DIMENSION IRKK(16)	189600
DIMENSION LUSSP(16), IGRND(16), IRAYD(16), MEDOD(16), IMPDC(16),	189700
\$ MANYB(16), ILLRK(16)	189800
	189900
	190000
COMMON/SR/EL(200), AZ(200), R(200), RKK(200), ABS(200), PL(200),	190100
\$ AER(200), RER(200), MSD(200), TMP(200), ADEV(200)	190200
	190300
	190400
	190500
DATA LUSSP/	190600
\$ 'X',	190700
\$ ' ',	190800
\$ 'A',	190900
\$ 'B',	191000
\$ 'S',	191100
\$ ' /',	191200
\$ 'P', 'A', 'T',	191300
\$ 'H', ' ', 'L',	191400
\$ 'O', 'S', 'S', ' ' /	191500
DATA IGRND/	191600
\$ 'G', 'R', 'N',	191700
\$ 'D', ' ', 'R',	191800
\$ 'E', 'F', 'L',	191900
\$ 'E', 'C', 'T',	192000
\$ 'I', 'O', 'N', ' ' /	192100
DATA IRAYD/	192200
\$ 'E', 'X', 'C',	192300
\$ 'E', 'S', 'S',	192400
\$ ' ', ' ', 'R',	192500
\$ 'A', 'Y', ' ',	192600
\$ 'D', 'E', 'V', ' ', ' /	192700
DATA MEDOD/	192800
\$ 'O', 'V', 'E',	192900
\$ 'R', ' ', 'D',	193000
\$ 'E', 'N', 'S',	193100
\$ 'E', ' ', 'M',	193200
\$ 'E', 'D', ' ', ' ' /	193300
DATA IMPDC/	193400
\$ 'I', 'M', 'P',	193500
\$ ' ', ' ', 'D',	193600
\$ 'I', 'R', ' ',	193700
\$ ' ', 'C', 'U',	193800
\$ 'S', ' ', ' ', ' ' /	193900
DATA MANYB/	194000
\$ 'T', 'O', 'U',	194100
\$ ' ', 'M', 'A',	194200
\$ 'N', 'Y', ' ',	194300
\$ 'B', 'E', 'N',	194400
\$ 'D', 'S', ' ', ' ' /	194500
DATA ILLRK/	194600
\$ 'I', 'L', 'L',	194700
\$ 'E', 'G', 'A',	194800
\$ 'L', ' ', 'R',	194900
\$ 'K', 'K', ' ',	195000
\$ ' ', ' ', ' ', ' ', ' ' /	195100
	195200
1 FORMAT(30X, 'S U M M A R Y', /)	195300

2	FORMAT(1X,' REASON FOR TERM. ',	195400
	\$ 'ELEVATION',	195500
	\$ 2X,'AZIMUTH',	195600
	\$ 6X,'RANGE',	195700
	\$ 2X,'ABSORPTION',	195800
	\$ 2X,'PATH LOSS',	195900
	\$ 2X,'ANGLE ERROR',	196000
	\$ 1X,'RANGE ERROR',	196100
	\$ 2X,'MISS DISTANCE',	196200
	\$ 2X,'TEMPERATURE',	196300
	\$ 1X,8H RAY DEV)	196400
3	FORMAT(2X,16A1,	196500
	\$ F10.3,	196600
	\$ F9.3,	196700
	\$ F11.4,	196800
	\$ F12.3,	196900
	\$ F11.3,	197000
	\$ F13.5,	197100
	\$ F12.4,	197200
	\$ F15.4,	197300
	\$ F13.4,	197400
	\$ F9.2)	197500
4	FORMAT(1H1)	197600
5	FORMAT(21X,' (DEG.)',	197700
	\$ 3X,' (DEG.)',	197800
	\$ 6X,'(KM.)',	197900
	\$ 5X,'(DB)',	198000
	\$ 8X,'(DB)',	198100
	\$ 6X,'(RADS)',	198200
	\$ 7X,'(KM.)',	198300
	\$ 9X,'(KM.)',	198400
	\$ 8X,'(DEG. K)',	198500
	\$ 2X'(DEG.)')	198600
		198700
		198800
	PRINT 4	198900
	PRINT1	199000
	PRINT2	199100
	PRINT 5	199200
	DU 80 I=1,LL	199300
	IF(RKK(I).NE.1.0)GU TO 10	199400
	DU 51 J=1,16	199500
51	IRKK(J)=LOSSP(J)	199600
	GU TO 70	199700
10	IF(RKK(I).NE.5.0)GU TO 20	199800
	DU 15 J=1,16	199900
15	IRKK(J)=IGRND(J)	200000
	GU TO 70	200100
20	IF(RKK(I).NE.10.0) GU TO 30	200200
	DU 25 J=1,16	200300
25	IRKK(J)=IRAYD(J)	200400
	GU TO 70	200500
30	IF(RKK(I).NE.25.0) GU TO 40	200600
	DU 35 J=1,16	200700
35	IRKK(J)=MEDUD(J)	200800
	GU TO 70	200900
40	IF(RKK(I).NE.100.0) GU TO 50	201000
	DU 45 J=1,16	201100
45	IRKK(J)=IMPDC(J)	201200
	GU TO 70	201300
50	IF(RKK(I).NE.200.0)GU TO 60	201400

DU 55 J=1,16	201500
55 IRKK(J)=MANYB(J)	201600
GO TO 70	201700
60 DU 65 J=1,16	201800
65 IRKK(J)=ILLRK(J)	201900
70 CONTINUE	202000
PRINT 3,IRKK,EL(I),AZ(I),R(I),ABS(I),PL(I),AER(I),RER(I),MSD(I),	202100
\$ TMP(I),ADEV(I)	202200
80 CONTINUE	202300
PRINT 4	202400
RETURN	202500
END	202600
	202700


```

CALL TROPAT(WR,PHI,ATTR0)                208900
TTRUP=280.                                209000
GO TO 221                                  209100

90 IF (ITRUP .NE. 1) GO TO 91              209200
TEMP=TEMP+ (1.- EXP(-ATTR0))*TTRUP        209300
ITRUP=0.                                   209400

C''''SUBROUTINE PRELP INTERPOLATES WITHIN THE PHENOMENOLOGY GRID TO GIV 209500
C ELECTRON DENSITY, AND ITS VECTOR GRADIENT AND TEMPERATURE AT THE      209600
C RAY TIP POSITION (X,Y,Z)                                                 209700
C TEP IS PHENOMENOLOGY REGION TEMPERATURE IN ELECTRON VOLTS           209800
C WPE IS PLASMA FREQUENCY IN MEGA-RADIANS PER SECOND.                   209900
C COLLISION FREQUENCIES ARE IN MEGAHERTZ.                               210000
91 CALL PRELP(X,Y,Z,N1,N2,N3,WPE,DWP,TEP )                                210100
                                                                              210200
                                                                              210300
                                                                              210400
                                                                              210500
                                                                              210600
                                                                              210700
C''''CHECK FOR OVERDENSE MEDIUM                                          210800
IF(WPE.EQ.-1.0) GO TO 100                                                  210900
GO TO 200                                                                    211000
100 IF(L3.LT.ITER) GO TO 150                                               211100
                                                                              211200
                                                                              211300
C''''PREPARE FOR RAY TERMINATION                                         211400
NCRIT(NTHETA,NPHI)=NUM(I)                                                  211500
CALL COLLF(X,Y,Z,TEP,WPE,NUCOLL,NUEI,NUEM,NIT2,NOX2,NOX1,T,NE,          211600
$N1,N2,N3 )                                                                211700
TEMP=TEMP+EXP(-2.0*ABSD)*T                                                211800
INDEX2=0.                                                                    211900
101 FORMAT(' OVERDENSE MEDIUM HIT IN TEST')                               212000
PRINT 101                                                                    212100
110 CONTINUE                                                                212200
RGRP=RGRP+DL*DRGRP                                                         212300
WPE = -1.                                                                    212400
RKK=25                                                                      212500
RETURN                                                                      212600
                                                                              212700
                                                                              212800
C''''STEP BACK...REDUCE STEP SIZE...ADVANCE IN SMALLER STEPS          212900
150 PL=PL-DL                                                                213000
WPE=0.0                                                                      213100
L3=L3+1                                                                      213200
IR=IR+1                                                                      213300
GO TO 7000                                                                    213400
                                                                              213500
                                                                              213600
C''''NOT IN TROPO REGION...PHENOMENOLOGY REGION NOT OVERDENSE...GO TO 213700
C COLLF FOR CALCULATION OF COLLISION FREQUENCY                          213800
200 CALL COLLF(X,Y,Z,TEP,WPE,NUCOLL,NUEI,NUEM,NIT2,NOX2,NOX1,T,NE,      213900
$N1,N2,N3 )                                                                214000
                                                                              214100
                                                                              214200
IF(WR-NUCOLL) 700,720,720                                                  214300
700 CONTINUE                                                                214400
PRINT 710                                                                    214500
710 FORMAT(' SHKAROFSKY HIGH FREQUENCY APPROXIMATION IS INVALID FOR     214600
CTHIS CALCULATION ' )                                                       214700
PRINT 715,RA,T,NE,WPE,WR,NUCOLL,NUEI,NUEM                                214800
715 FORMAT(' ALTITUDE = ',E13.3,'T = ',E13.3,'NE = ',E13.3,'WPE = ',    214900
$E13.3, / , ' WR = ',E13.3,'NUCOLL = ',E13.3,'NUEI = ',E13.3,

```


C''''RAY INTERSECTS GROUND...TERMINATE RAY OR STEP BACK AND TAKE SMALLER	221100
C STEPS	221200
625 IF(ITER-L3.GT.0)GO TO 500	221300
RKK=5	221400
RETURN	221500
	221600
	221700
	221800
C''''BEND CRITERIA HAVE BEEN EXCEEDED,... STEP BACK AND PROCEED FORWARD	221900
C AGAIN, BUT IN SMALLER STEPS	222000
500 PL=PL-DL	222100
RGRP=RGRP-DRGRP*DL	222200
DABS=DABS-KAPPA*DL	222300
L3=L3+1	222400
IR=IR+1	222500
GO TO 7000	222600
	222700
	222800
600 RETURN	222900
650 PL=PL-DL	223000
7000 DIST = ((X-DL*C1)-XPLU)**2+((Y-DL*C2)-YPLU)**2+((Z-DL*C3)-ZPLU)**2	223100
RETURN	223200
END	223300
	223400

```
SUBROUTINE TRANS(X,Y,Z,RA, N1, N2, N3          ) 223500
                                                    223600
                                                    223700
REAL N1,N2,N3 223800
                                                    223900
                                                    224000
C PERFORMS COORDINATE TRANSFORM TO CALCULATE HEIGHT ABOVE 224100
C EARTH SURFACE FOR CORRECT MODEL ATMOSPHERE PARAMETERS, 224200
C AND ALSO CALCULATES MAGNITUDE OF DIRECTION COSINES 224300
C OF ELECTRON DENSITY GRADIENT DERIVED FROM MODEL ATMOSPHERE. 224400
C RE IS EARTH MEAN RADIUS IN KM. 224500
                                                    224600
                                                    224700
                                                    224800
RE = 6371.2 224900
QA = Z + RE 225000
QB = X**2 + Y**2 + QA**2 225100
QC = SQRT(QB) 225200
RA = QC - RE 225300
N1 = X/QC 225400
N2 = Y/QC 225500
N3 = (Z + RE)/QC 225600
RETURN 225700
END 225800
```

```

SUBROUTINE TRUPAT(WR,PHI,ATTRU)
225900
226000
226100
C'''' TRUPOSPHERIC ATTENUATION MODEL.
226200
C'''' FREQUENCY RANGE OF MODEL IS 100MHZ TO 10GHZ.
226300
226400
226500
DIMENSION A(5),B(5),C(5),D(5,5)
226600
226700
226800
226900
DATA
227000
$ D/
227100
$ 0.2, 0.16, 0.13, 0.0, 0.0,
227200
$ 1.2, 0.67, 0.56, 0.3, 0.16,
227300
$ 3.0, 1.85, 1.3, 0.65, 0.34,
227400
$ 3.9, 2.3, 1.6, 0.89, 0.4,
227500
$ 5.7, 3.2, 2.1, 1.0, 0.52
227600
227700
227800
227900
PI = 3.141592654
228000
F = WR/(2.*PI)
228100
EL = (PI/2.) - PHI
228200
EL = EL * 180./PI
228300
228400
228500
C'''' INTERPOLATION IN FREQUENCY - ONCE.
228600
10 CONTINUE
228700
JSTEP = JSTEP + 1
228800
A(1) = 100.
228900
A(2) = 300.
229000
A(3) = 1000.
229100
A(4) = 3000.
229200
A(5) = 10000.
229300
C
229400
C(1) = 0.
229500
C(2) = 1.
229600
C(3) = 2.
229700
C(4) = 5.
229800
C(5) = 10.
229900
IF(F.LT.A(1))GO TO 22
230000
JA = 2
230100
IF(F.LE.A(2))GO TO 25
230200
JA = 3
230300
IF(F.LE.A(3))GO TO 25
230400
JA = 4
230500
IF(F.LE.A(4))GO TO 25
230600
JA = 5
230700
IF(F.LE.A(5))GO TO 25
230800
22 PRINT 13, F
230900
13 FORMAT( ' FREQUENCY IS ',F10.2, 'MHZ AND LIES OUTSIDE RANGE OF MODE
231000
$L' )
231100
24 ATTRU = 0.
231200
RETURN
231300
25 DO 30 KA=1,5
231400
30 B(KA) = (F - A(JA-1))*(D(KA,JA)-D(KA,JA-1)) / (A(JA) - A(JA-1) )
231500
$ + D(KA,JA-1)
231600
100 CONTINUE
231700
231800
231900
C'''' INTERPOLATION IN ELEVATION ANGLE - ONCE PER RAY.

```

IF(EL.LT.0) GO TO 40	232000
KB = 1	232100
IF(EL.LT.1.)GO TO 50	232200
KB= 2	232300
IF(EL.LT.2.) GO TO 50	232400
KB =3	232500
IF(EL.LT.5.) GO TO 50	232600
KB =4	232700
IF(EL.LE.10.) GO TU 50	232800
ATTRU = 0.	232900
RETURN	233000
40 PRINT 41	233100
41 FORMAT(' MALFUNCTION - ELEVATION ANGLE LESS THAN ZERU DEGREES.')	233200
ATTRU =0.	233300
RETURN	233400
50 ATTRU = B(KB) + (EL -C(KB))*(B(KB) - B(KB+1))/(C(KB) - C(KB+1))	233500
RETURN	233600
END	233700
	233800


```
//Z.FT51F001 DD SYSOUT=A,DCB=(RECFM=FBA,LRECL=133,BLKSIZE=3458),
//      SPACE=(3200,(100,50),RLSE)
```

```
//FT50F001 DD *
*****
```

The above card is used only when edit cards are inserted here.

```
// EXEC FORTHCLG,PARM.FORTHCLG,PARM.FORT='NOXREF'
//      PARM.LINK='MAP',TIME=30,REGION.GO=300K,PARM.GO='EU=-1,EO=200'
```

```
//FORT.SYSIN DD DSN=&CARFI,DISP=(OLD,DELETE)
```

```
//GO.FT09F001 DD DSN=NVRL.HUSER.P10,
*****
```

```
//      UNIT=TAPE9,LABEL=(,NL),
*****
```

```
// DCB=(RECFM=VBS,BLKSIZE=8912,DISP=(OLD,KEEP),
//      VOLUME=SER=5642
*****
```

The above 4 cards are used when data for PRELDA is on tape.

```
//FTS1F001 DD SYSOUT=A,DCB=(RECFM=FBA,LRECL=133,BLKSIZE=3458),
//      SPACE=(TRK,(800,200),RLSE)
```

```
//GO.FT50F001 DD *
Data deck follows.
```

DATA DECK

Explanation, read statement, and format of the data deck follows. All angles are read in degrees.

Card 1

```
READ 27, ELAB(41), ELAB(31), ELAB(21), ELAB(11), ELAB(1)
FØRMAT(5A3)
```

Used to annotate the Y axis of the contour plot. The first number is ELMIN, second is ELMIN+10*INC, third is ELMIN+20*INC, fourth is ELMIN+30*INC, and fifth is ELMIN+40*INC, where INC is the scan increment (elevation and azimuth) of the experiment.

Card 2

```
READ 21, TITLE
FØRMAT (10A8)
```

Used as a title for the sky maps and can contain absolutely anything you wish for a title up to 80 characters, including spaces.

Card 3

READ 15, DEL1, DEL2, ITER1, ITER2
FØRMAT(2F10,2I10)

DEL1 determines the maximum ray path step size in a non-refracting environment.
DEL2 determines the maximum ray path step size in a refracting environment.
ITER1 determines the minimum ray path step size in a non-refracting environment.
ITER2 determines the minimum ray path step size in a refracting environment.

Card 4

READ 15, LMU, LABS, ISEMIE
FØRMAT(2F10,I10)

LMU is the granularity limit on refractive index for determining slab width.
LABS is the granularity limit on incremental absorption for determining slab width.
ISEMIE is a flag to determine if the semi-essential print-out is desired. (ISEMIE = 0 means do not print) (ISEMIE \neq 0 means print) (See program running options.)

Card 5

READ 25, RAMAX, RANGE, THETA, CØLATI
FØRMAT(4F5)

RAMAX is the maximum distance to which a ray is traced.
RANGE is the distance from the radar to ground zero.
THETA is the azimuth of ground zero, measured from the radar.
CØLATI is the colatitude of the radar.

Card 6

READ 1, (R(I), I = 1, 10)
FØRMAT(10F8)

R is an array which allows up to 10 reference ranges to be read in. One more than what is read in is computed to insure that the last reference range is greater than RAMAX.

Card 7

READ 2, ABSL, RFRCL, GRPL, MISL, RTRGET, PATHL, IFLAG, DEVL
FØRMAT(6F8,I8,F8)

The following are program variables and an option flag (for choosing between path loss or absorption in output sky maps):

ABSL is the signal absorption limit.
RFRCL is the radar direction angle-error limit.
GRPL is the radar range error limit.
MISL is the radar miss distance limit
RTRGET is the target engagement range.

PATHL is the signal path loss limit.
IFLAG = 0 means do the absorption sky map
 = 1 means do the path-loss sky map.
DEVL is the ray deviation limit.

Card 8

READ 3, FR
FORMAT(E10.4)

FR is the radar frequency in megahertz.

Card 9

READ 4, NREC
FORMAT(I5)

NREC is the number of the phenomenology time step. It determines the input data tape block to be read from the Plasma Physics phenomenology tape.

Card 10

READ 5, THETMN, THETMX, THETAØ, ELMIN, ELMAX, ELEØ, INC, AZERØ
FORMAT(8F10)

The following is the angle information needed for scan and display control of ray tracing:

THETMN is the smallest angle in the azimuth scan loop.
THETMX is the largest angle in the azimuth scan loop.
THETAØ is the azimuthal angle for the engagement computation.
ELMIN is the smallest angle in the zenith scan loop.
ELMAX is the largest angle in the zenith scan loop.
ELEØ is the zenith angle for the engagement computation.
INC is the angular resolution of the calculation (scan increment).
AZERØ is the azimuthal angle that will be centered on the sky map plot. It is also used to redefine THETMN and/or THETMX in the event that the selected ones do not fit onto the contour plots.

Card 11

READ 1, TSKY
FORMAT(F8)

TSKY is the average background-sky temperature.